

1 **A systematic review of climate change science relevant to**

2 **Australian design flood estimation**

3 Conrad Wasko¹, Seth Westra², Rory Nathan¹, Acacia Pepler^{3,4}, Timothy H. Raupach^{4,5,6}, Andrew
4 Dowdy^{3,4,5}, Fiona Johnson^{7,8}, Michelle Ho¹, Kathleen L. McInnes⁹, Doerte Jakob¹⁰, Jason
5 Evans^{4,5,6}, Gabriele Villarini^{11,12}, Hayley J. Fowler¹³

6 ¹Department of Infrastructure Engineering, The University of Melbourne, Parkville, Victoria, Australia

7 ²School of Architectural and Civil Engineering, University of Adelaide, Adelaide, Australia

8 ³Australian Bureau of Meteorology, Sydney, Australia

9 ⁴National Environmental Science Program Climate System Hub, Australia

10 ⁵Climate Change Research Centre, University of New South Wales, Sydney, New South Wales, Australia

11 ⁶ARC Centre of Excellence for Climate Extremes, University of New South Wales, Kensington, New South Wales,
12 Australia

13 ⁷Water Research Centre, School of Civil and Environmental Engineering, University of New South Wales,
14 Kensington, New South Wales, Australia

15 ⁸Australia Research Council Training Centre in Data Analytics for Resources and Environments

16 ⁹CSIRO Environment, Aspendale, Australia

17 ¹⁰Australian Bureau of Meteorology, Melbourne, Australia

18 ¹¹Department of Civil and Environmental Engineering, Princeton University, New Jersey, USA

19 ¹²High Meadows Environmental Institute, Princeton University, New Jersey, USA

20 ¹³School of Engineering, Newcastle University, Newcastle upon Tyne, UK

21

22 *Correspondence to:* Conrad Wasko (conrad.wasko@unimelb.edu.au)

23

24 **Abstract**

25 In response to flood risk, design flood estimation is a cornerstone of planning, infrastructure design, setting of
26 insurance premiums and emergency response planning. Under stationary assumptions, flood guidance and the methods
27 used in design flood estimation are firmly established in practice and mature in their theoretical foundations, but under
28 climate change, guidance is still in its infancy. Human-caused climate change is influencing factors that contribute to
29 flood risk such as rainfall extremes and soil moisture, and there is a need for updated flood guidance. However, a
30 barrier to updating flood guidance is the translation of the science into practical application. For example, most science
31 pertaining to historical changes to flood risk focuses on examining trends in annual maximum flood events, or the
32 application of non-stationary flood frequency analysis. Although this science is valuable, in practice design flood
33 estimation focuses on exceedance probabilities much rarer than annual maximum events, such as the 1% annual
34 exceedance probability event or even rarer, using rainfall-based procedures, at locations where there are little to no

35 observations of streamflow. Here, we perform a systematic review to summarise the state-of-the-art understanding of
36 the impact of climate change on design flood estimation in the Australian context, while also drawing on international
37 literature. In addition, a meta-analysis, whereby results from multiple studies are combined, is conducted for extreme
38 rainfall to provide quantitative estimates of possible future changes. This information is described in the context of
39 contemporary design flood estimation practice, to facilitate the inclusion of climate science into design flood
40 estimation practice.

41 **1. Introduction**

42 Flood assessment provides critical information to evaluate the tolerability or acceptability of flood risks, and to support
43 the development of risk management strategies. Flood risk reduction measures can be exercised through the
44 construction of flood mitigation structures, zoning and development controls, and non-structural measures to better
45 respond to floods when they do occur, for example through flood warning systems and emergency management
46 planning. Here we adopt the term ‘risk’ to mean flood risk. Across the world, the associated hypothetical flood adopted
47 for design and planning purposes for management of risk is termed the *design flood* (Jain and Singh, 2003). In
48 Australia, the design flood is characterised in terms of an annual exceedance probability (AEP) rather than an annual
49 recurrence interval (ARI) with the aim of better highlighting the annual risks that the community is exposed to. There
50 are many different methods of estimating the design flood applicable for different AEPs, ranging from *flood frequency*
51 *analysis* which use streamflow observations, to *continuous simulation* which use long sequences of rainfall
52 observations, to those that use rainfall in *event-based modelling* through Intensity-Duration-Frequency (IDF) curves
53 (in Australia termed Intensity-Frequency-Duration, or IFD curves) and/or Probable Maximum Precipitation (PMP) as
54 inputs. Methods of design flood estimation are commonly stipulated by guiding documents; for example, The
55 Guidelines of Determining Flood Flow Frequency – Bulletin 17C (England et al., 2019) in the U.S.A., the Flood
56 Estimation Handbook (Institute of Hydrology, 1999) in the UK, and Australian Rainfall and Runoff (Ball et al., 2019a)
57 in Australia. Such guidance documents, though not necessarily legally binding, are seen as representing best practice.

58 Traditionally, the AEP, or flood quantile to which it corresponds, has been assumed to be static; however, with climate
59 change, it is now recognised that the flood hazard is changing (Milly et al., 2008). The primary driver of this change
60 in AEP to rainfall-induced flooding is the thermodynamic increase in extreme rainfall due to a 6-7%/°C increase in
61 the saturation vapor pressure of the atmosphere, as dictated by the Clausius-Clapeyron (CC) relationship (Trenberth
62 et al., 2003). Factors beyond the thermodynamic impact have been discussed in various reviews and commentaries
63 (Fowler et al., 2021; Allen and Ingram, 2002; Pendergrass, 2018). The vertical lapse rate (i.e., atmospheric stability)
64 increases as temperatures increase and rates of rainfall can decrease as the cloud base is lifted assuming moisture is
65 unchanging. But if the moisture increases, then the opposite is true, with rain more easily triggered. In addition, there
66 can be an increase in buoyancy creating stronger updrafts and deeper convection (referred to as super-CC scaling).
67 Finally, dynamical drivers related to changes in the global circulation can act to change the occurrence of rainfall
68 extremes by changing storm tracks and speeds, amplifying and dampening the thermodynamic influence on rainfall
69 extremes depending on location and time of year (Emori and Brown, 2005; Pfahl et al., 2017; Chan et al., 2023).

70

71 A recent review of climate change guidance has found that several jurisdictions around the world are already
72 incorporating climate change into their design flood guidance (Wasko et al., 2021b). For example, Belgium, Denmark,
73 England, New Zealand, Scotland, Sweden, the UK, and Wales are all recommending the use of climate change
74 adjustment factors for IFD rainfall intensities. Many countries also recommend higher climate change adjustment
75 factors for rarer precipitation events, consistent with findings from various modelling studies that rarer events will
76 intensify more with climate change (Gründemann et al., 2022; Pendergrass and Hartmann, 2014). Shorter duration
77 storms are likely to intensify at a greater rate than longer duration storms (Fowler et al., 2021) and subsequently, some
78 guidance, such as that from New Zealand and the UK, also accounts for storm duration in their climate change
79 adjustment factors (Wasko et al., 2021b).

80 Although substantial advances have been made in adjusting design flood estimation guidance to include climate
81 change, there remains a disconnect between climate science and existing guidance. For example, although there are
82 climate change adjustment techniques available for generating altered precipitation inputs, none of the guidance
83 reviewed provided recommendations for adjusting rainfall sequences used in continuous simulation. Also, current
84 guidelines for estimation of the PMP assume a stationary climate (Salas et al., 2020) despite evidence to the contrary
85 (Kunkel et al., 2013; Visser et al., 2022). Finally, while research has been undertaken into non-stationary flood
86 frequency analysis, and the underlying statistical theory is relatively mature (Salas et al., 2018; Stedinger and Griffis,
87 2011), these have not been adopted in guidance. For example, Bulletin 17C assumes time-invariance (England et al.,
88 2019).

89 There are multiple reasons for the disconnect between the science and flood estimation practice. Although widely
90 accepted in the scientific literature, the “chain-of-models” approach – whereby General Circulation Model (GCM)
91 outputs are bias corrected and downscaled to create inputs for hazard modelling (Hakala et al., 2019) – has large
92 uncertainties (Kundzewicz and Stakhiv, 2010; Lee et al., 2020), with the uncertainties often seen as a barrier for
93 adoption (Wasko et al., 2021b). Further, while much research has been undertaken on understanding the non-
94 stationarity of flooding, the research is not often directly comparable or translatable to the approaches and methods
95 used in design flood estimation, for example in the case of temporal and spatial patterns of rainfall or the influence of
96 antecedent conditions on rainfall losses (Quintero et al., 2022). Finally, most climate science focuses on the annual
97 maximum daily precipitation, often referred to as the ‘RX1 day index’ or Rx1D (Zhang et al., 2011), to measure
98 changes in extremes, with standard climate models not adequately resolving the processes that govern sub-daily
99 rainfall extremes. In contrast, design flood estimation generally requires consideration of sub-daily rainfall totals and
100 events much rarer than annual maxima.

101 With a literature search finding no existing synthesis of climate science relevant to the specific needs of design flood
102 estimation, here we undertake a systematic review of the latest science directly relevant to the inputs used in design
103 flood estimation. Although we focus on science relevant to Australia, international literature is incorporated, as design
104 flood estimation methods are used around the world. Finally, we combine the results from individual studies using the
105 process of meta-analysis to assess the level of consensus of different sources of evidence relating specifically to the
106 design flood estimation input of extreme rainfall under climate change. This review represents a critical step in

107 updating flood guidance and translating scientific knowledge into design flood practice. This review aims to (a) serve
108 as a template for scientific reviews as they relate to design flood estimation guidance updates, and (b) identify
109 knowledge gaps in the scientific literature that are required by engineers who perform design flood estimation.

110 **2. Design flood estimation practice**

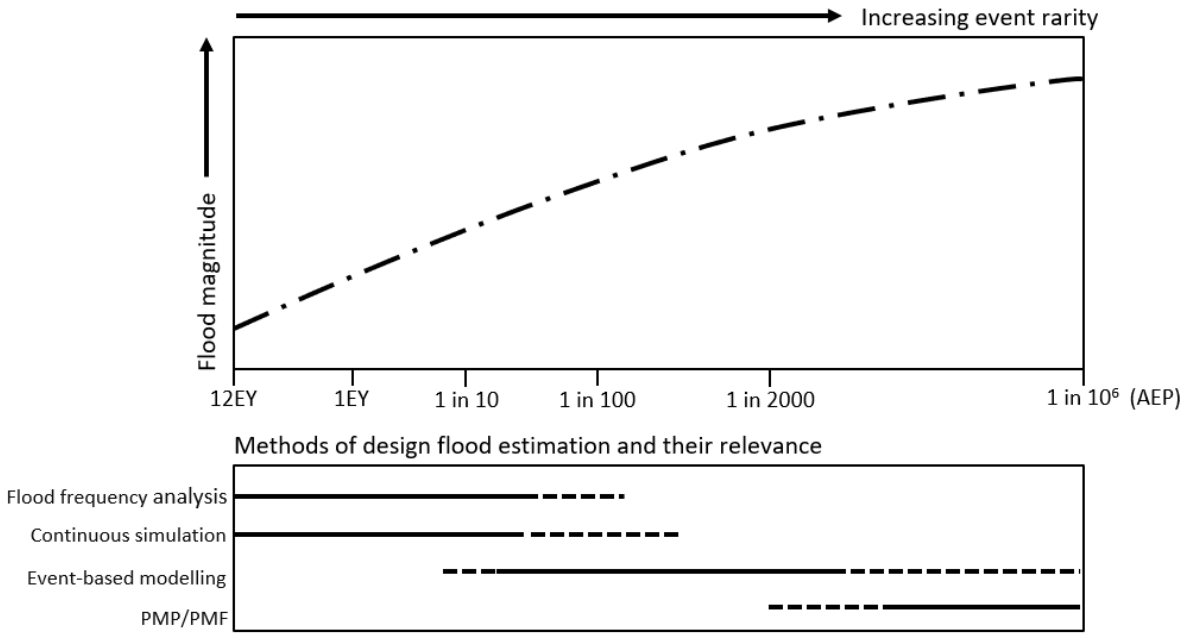
111 To contextualise the systematic review and meta-analysis that follows in later sections, this section briefly introduces
112 the primary design flood estimation approaches, with Figure 1 showing the typical AEP range that each method applies
113 to.

114 **1. Flood frequency analysis (FFA):** A flood frequency curve is derived by fitting a probability distribution such as
115 an extreme value distribution to streamflow data, which is then subsequently used to estimate the design flood
116 quantiles (Stedinger et al., 1993). This method is limited to catchments where streamflow data is available unless data
117 can be transposed or corrected. As flood records are typically in the order of decades, AEPs rarer than approximately
118 1 in 50 are generally subject to considerable uncertainty. Hence, flood frequency analysis is often not used by
119 practitioners as either at-site data is unavailable, the record is too short to estimate the target quantile, or there have
120 been significant changes to the catchment over the period of record. Regional flood frequency analysis is an extension
121 of flood frequency analysis where space is traded for time by pooling regional data to extend the applicability of this
122 method to rarer events (Hosking and Wallis, 1997).

123 **2. Continuous simulation:** A hydrologic model is used to simulate the streamflow of a catchment with flood maxima
124 then extracted from the modelled output to derive flood quantiles using an appropriate probability model (Boughton
125 and Droop, 2003). Where rainfall records of sufficient length are not available to drive the hydrologic model, the
126 modelling can be forced by stochastically generated data (e.g. Wilks, 1998). This approach is very useful in joint
127 probability assessments where system performance varies over multiple temporal and spatial scales (e.g., multiple
128 sewer overflows or the design of linear infrastructure), or in more volume-dependent systems comprised of compound
129 storages. Due to its reliance on long rainfall sequences, continuous simulation, like flood frequency analysis, is usually
130 only used to estimate more frequent flood events, with a further limitation being the difficulty in stochastically
131 generating reliable sequences of rainfall data (Woldemeskel et al., 2016).

132 **3. Event-based (IFD) modelling:** This is the most common method used for design flood estimation. A rainfall depth
133 or intensity of given AEP and duration is sampled from an IFD curve and combined with rainfall temporal patterns to
134 create a design rainfall event (or “burst”) of a given duration (see Chapter 14 of Chow et al., 1988). In some
135 applications, it is preferable to consider design events based on complete storms, and thus it is necessary to augment
136 the rainfall bursts derived from IFD curves with rainfalls that might be expected to occur prior (or subsequent) to the
137 burst period. As the design storm rainfall is generally a point rainfall but applied over a catchment, an Areal Reduction
138 Factor (ARF) is applied before the design rainfall event is used as an input to a model to estimate the runoff
139 hydrograph. Rainfall that does not contribute to the flood hydrograph as it enters depressions in the catchment, is
140 intercepted, or is infiltrated into the soil, is removed through a “loss” model. Finally, the hydrograph response may be
141 modulated by the tail water conditions, where the sea level will modulate the catchment outflow.

142 Due to the severe consequences of failures, critical infrastructure, such as dams or nuclear facilities, often need to be
 143 designed to withstand the largest event that is physically plausible, termed the Probable Maximum Flood (PMF). Like
 144 the above event-based modelling description, the PMF is derived from a rainfall event, but in this case the rainfall is
 145 the PMP. Most local jurisdictions follow the World Meteorological Organisation guidelines for estimating the PMP
 146 (WMO, 2009). The PMP is derived using observed “high efficiency” storms matched to a representative dew point
 147 temperature. The moisture (i.e., rainfall) in the storm is then maximised by assuming the same storm could occur with
 148 moisture equivalent to the maximum (persisting) dew point observed at that site.



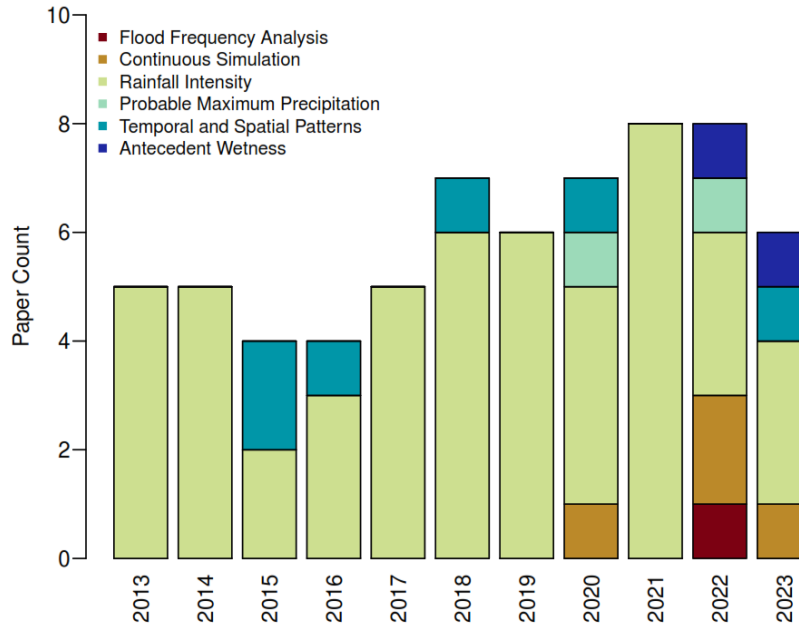
149
 150 **Figure 1.** The relevance of different flood estimation approaches as a function of AEP. The top panel presents a
 151 typical flood frequency curve where the flood magnitude increases with event rarity (AEP), with frequent events
 152 presented as events per year (EY). The bottom panel shows the range of event rarities for which various flood
 153 estimation approaches show utility. Dashed lines represent lower utility while solid lines represent higher utility.
 154 Figure adapted from James Ball et al. (2019). The PMP is used as an input in event-based models to derive the PMF.

155 The method adopted for design flood estimation depends on the problem being solved, the level of risk being designed
 156 for, and the available data. Flood frequency analysis is an important source of information when data are available
 157 and key assumptions (e.g. historical and future climatic and hydrological stationarity) are met, due to the implicit
 158 consideration of flood causing factors without a need for assumptions about joint interactions. However, most
 159 commonly, approaches based on event-based modelling are applied because flood data rarely exists at the location of
 160 interest, and if it does, it is often confounded by catchment non-stationary (e.g., urbanization, deforestation), or the
 161 record lengths are much shorter than the design AEP required.

162 3. Methodology

163 Systematic reviews represent a reproducible methodology for appraising the literature in the context of a specific topic
164 or issue (Page et al., 2021). Reviews were undertaken for each of the three key flood estimation methods (flood
165 frequency analysis, continuous simulation, and event-based modelling). Each review section was assigned a lead
166 author who was tasked with collecting scholarly articles from Scopus, with a secondary author tasked with reviewing
167 the results of the systematic review to reduce selection bias. Articles were selected targeting the last decade to ensure
168 a broad coverage of evidence while ensuring that evidence is relatively contemporary. The literature search for each
169 method of (or input to) design flood estimation contained different relevant keywords (see Supplementary Information
170 for key words for each section). To limit the scope of the review geographically, searches were made for literature
171 where either the title, abstract, or keywords contained “Australia.” To constrain the review only to climate change,
172 literature was also required to contain “change” in either the title, abstract, or keywords (it was deemed that using
173 “climate change” would be too restrictive). These criteria represent the foundation of the review, and the publication
174 base was further supplemented by other sources of information, particularly in cases where specific terminology was
175 used (e.g., the term “Clausius-Clapeyron” in the context of extreme rainfall) or where knowledge existed of additional
176 publications or international research not identified through the keyword searches. We note that the impact of factors
177 related to sea level (Section 4.3.6), although included in the review, was excluded from the requirements of the
178 systematic review as it is not explicitly part of Australia’s flood guidance as it relates to climate change (Bates et al.,
179 2019). Similarly, the introductory section on the processes affecting changes in extreme rainfall in Australia (Section
180 4.3.1) was excluded from the stricter systematic review requirements.

181 To select relevant literature from the search results, articles were first filtered to remove duplicates. Following this,
182 irrelevant articles based on a review of the abstracts, and then of the manuscript itself, were excluded. While the search
183 terms aided inclusion in the systematic review, many studies were not relevant to the assessment of flood risk and
184 were omitted. Finally, some additional studies (in particular, syntheses) were included based on the author’s
185 knowledge of the literature. Details of the searches (Table S1) and the full list of articles reviewed (Table S2) are
186 provided in the Supplementary Information with a summary of the articles found by publication year as they relate to
187 each of the systematic review topics provided in Figure 2.



188

189 **Figure 2.** Papers identified in the systematic review by publication year and review topic. Full details are provided
 190 in Table S2.

191 Recognising the importance of IFD estimates in design flood estimation, and the large volume of available literature
 192 providing quantitative estimates of changes in extreme rainfall, an analysis was performed to understand the average
 193 magnitude of extreme rainfall change and associated uncertainty. The analysis borrows from meta-analysis techniques
 194 which quantitatively combine results from multiple studies (Field and Gillett, 2010) and uses structured expert-
 195 elicitation methods consistent with those used by the IPCC (Zommers et al., 2020) as follows:

- 196 1. Where possible extreme rainfall change was quantified per degree of global temperature change (i.e., the
 197 global mean, including ocean and land regions). Additionally, variation with storm duration, severity
 198 (i.e., AEP), and location were considered. Global mean temperature was chosen to ensure consistency
 199 with the IPCC projections and to be representative of the climatic drivers of changes in moisture sources.
 200 The exception to this was rainfall-temperature scaling studies, which use local temperature differences
 201 as a proxy for anthropogenic climate change.
- 202 2. Assessment was made, through consensus between authors, whether there was enough evidence to
 203 calculate the magnitude of extreme rainfall change with varying storm duration, severity, and location –
 204 and what, if any, distinction was to be made for these factors.
- 205 3. Co-authors independently used the collected evidence to determine their best estimate of the change in
 206 extreme rainfall as well as a likely range. Typically, each study was weighted by how confident each
 207 author was in the evidence presented in the study. This included consideration of the study methodology
 208 (e.g., observation-based studies, model-based studies) and various statistical considerations (e.g., sample
 209 size and/or representativeness over the spatial domain).

210 4. The best estimates from each author were then compared, and through a consensus process, a single
211 central estimate was derived together with a likely (66%) range to represent assessment uncertainty.

212 **4. Synthesis of the literature and systematic review**

213 In this section, the literature is reviewed for each of the three key flood estimation methods (flood frequency analysis,
214 continuous simulation, and event-based modelling). An overview of the implications of climate change on each
215 method is first presented, followed by a systematic review using the keywords provided in the Supplementary
216 Information. In the context of event-based (IFD) modelling, each of the inputs to the design flood estimate are
217 reviewed. For extreme rainfalls, the systematic review is followed by the results of the meta-analysis.

218 **4.1 Flood frequency analysis**

219 **4.1.1 Impact of climate change**

220 Flood frequency (or regional flood frequency) analysis generally uses annual maxima or threshold excess values of
221 instantaneous flood data to derive a frequency curve by fitting an appropriate statistical model (Stedinger et al., 1993).
222 Changes in flood maxima due to climate change are generally related back to changes in extreme precipitation. As
223 temperature increases, so does the saturation water vapour of the atmosphere, leading to, all other things being equal,
224 greater extreme precipitation, and hence pluvial flooding. However, flooding is dependent on the flood generating
225 mechanism (Villarini and Wasko, 2021). In the absence of snowmelt, changes in antecedent conditions related to soil
226 moisture and baseflow have been shown to modulate flood events (Berghuijs and Slater, 2023), with changes in soil
227 moisture having a lesser impact on rarer floods (Ivancic and Shaw, 2015; Wasko and Nathan, 2019; Neri et al., 2019;
228 Bennett et al., 2018). Where snow is present, warmer temperatures cause a reduction in the frequency of rain-on-snow
229 flood events at lower elevations due to snowpack declines, whereas at higher elevations rain-on-snow events become
230 more frequent due to a shift from snowfall to rain (Musselman et al., 2018).

231 Across Australia, for frequent flood events in the order of annual maxima, more streamflow gauges show decreases
232 in annual maxima than increases (Ishak et al., 2013; Zhang et al., 2016). There is a clear regional pattern, with
233 decreases more likely in the extra-tropics, and increases more likely in the tropics. These changes have a strong
234 correlation to changes in antecedent soil moisture and mean rainfall due to the expansion of the tropics (Wasko et al.,
235 2021c; Wasko and Nathan, 2019). However, there is a statistically significant increasing trend in the frequency of
236 rarer floods since the late 19th century (Power and Callaghan, 2016) due to increases in extreme rainfall (Wasko and
237 Nathan, 2019; Guerreiro et al., 2018). Where research examines changes in flood frequency for Australia, it is often
238 related to changes in catchment conditions (Kemp et al., 2020) or interannual variability (McMahon and Kiem, 2018;
239 Franks and Kuczera, 2002). Specifically related to climate change, most studies for Australia argue trends in annual
240 maxima have implications for non-stationary flood frequency analysis (Ishak et al., 2014), but often fail to detect
241 statistically significant trends (Ishak et al., 2013; Zhang et al., 2016) due to natural variability (Villarini and Wasko,
242 2021).

243 In a review of the projection of flooding with warmer temperatures, Wasko (2021) summarised the global literature
244 on non-stationary flood frequency analysis. It was noted that non-stationary flood frequency analysis for climate
245 change is typically performed using time-dependent parameters (e.g. Salas et al., 2018). Wasko (2021) also noted that

246 one of the shortcomings of non-stationary flood frequency analysis using a time covariate is the inability to project
247 with confidence for climate change due to the lack of a causal relationship (see for example Faulkner et al. 2020).
248 Hence it is argued that any non-stationary flood frequency analysis should ensure that the statistical model structure
249 is representative of the processes controlling flooding (Schlef et al., 2018; Trambly et al., 2014; Kim and Villarini,
250 2023; Villarini and Wasko, 2021; Faulkner et al., 2020), with a framework for model construction provided in Schlef
251 et al. (2018). Examples of physically motivated non-stationary frequency analysis from the global literature include
252 using combinations of rainfall, potential evaporation, soil moisture, temperature, and large-scale drivers of moisture
253 transport as covariates (Guo et al., 2023; Han et al., 2022; Trambly et al., 2014; Schlef et al., 2018; Condon et al.,
254 2015; Kim and Villarini, 2023; Towler et al., 2010). In principle, this is similar to studies performed in the United
255 States, which have used precipitation and temperature as covariates for non-stationary flood frequency analysis
256 (Condon et al., 2015; Towler et al., 2010; Kim and Villarini, 2023). But even the use of physically-based covariates
257 is problematic as the covariates may not capture the differing processes that affect rainfall and therefore flood changes,
258 for example thermodynamic versus dynamical changes to extreme rainfall which vary with storm duration (Schlef et
259 al., 2018). A final complication is that even if the changes in flood drivers are captured by the covariates there is no
260 guarantee that these flood drivers will be those governing flooding in the future due to changes in the dominant flood
261 mechanism (Chegwidden, Oriana et al., 2020; Zhang et al., 2022; Wasko, 2022). Possibly for the above reasons, there
262 is little formal guidance for how to perform non-stationary flood frequency analysis. One of the most well-developed
263 guidance documents on flood frequency analysis – Bulletin 17C (England et al., 2019) – while acknowledging the
264 potential impacts of climate change on flood risk, does not explicitly give guidance for climate change, but instead
265 refers the user to published literature for non-stationary flood frequency (Salas and Obeysekera, 2014; Stedinger and
266 Griffis, 2011), leaving the door open for a variety of analyses based on “time-varying parameters or other appropriate
267 techniques”. Indeed Ahmed et al. (2023) note there is a dearth of guidance on how to consider non-stationarity in
268 regional flood quantile estimation, arguing alongside other reviews (Zalnezhad et al., 2022) that further research is
269 needed on the impacts of climate change on flood frequency analysis.

270 **4.1.2 Systematic review**

271 For Australia, the systematic review only yielded one manuscript. Using 105 catchments across the east coast of
272 Australia, Han et al. (2022) fit a non-stationary regional flood frequency model using the covariates of catchment area,
273 mean annual rainfall, mean annual potential evaporation, and rainfall intensity with a duration of 24 hours for a target
274 return period/exceedance probability. The proposed method was found to be effective in capturing the differing trends
275 with differing recurrence intervals, and projections were derived, with more sites having increases projected for rarer
276 events (1 in 20 AEP) than for frequent events (1 in 2 AEP).

277 **4.2 Continuous simulation**

278 **4.2.1. Impact of climate change**

279 Where streamflow data is not available, flood frequency curves can be derived from simulated streamflow using a
280 rainfall-runoff model driven by long sequences of rainfall and evapotranspiration. The process of deriving flood
281 frequency curves through continuous simulation often necessitates the use of a weather generator to stochastically
282 generate the model inputs due to the long record lengths required for flood frequency estimation. For future climate

283 conditions, these model input time series are generally derived through downscaling methods (Fowler et al., 2007;
284 Teutschbein and Seibert, 2012) where GCM outputs are bias corrected and downscaled to create realistic inputs for
285 hydrologic (rainfall-runoff) models to simulate streamflow and consequently to derive flood frequency estimates.
286 Examples of this include Norway’s flood guidance (Lawrence and Hisdal, 2011) and eFLaG in the UK (Hannaford et
287 al., 2023), where the magnitude of a flow of a given exceedance probability is compared to a reference period to
288 provide climate adjustment factors.

289 While changes in the hydrologic cycle and mean rainfall are largely constrained by the availability of energy, extreme
290 rainfall changes are constrained by moisture availability (Allen and Ingram, 2002). For Australia, increases in pan
291 evaporation have been observed (Stephens et al., 2018b). For rainfall, longer dry spells between weather events are
292 projected (Grose et al., 2020), with a shift from frontal rainfall to convective rainfall, particularly in the southern parts
293 of the continent (Pepler et al., 2021). Rainfall events are expected to have, on average, a shorter storm duration (Wasko
294 et al., 2021a) with greater peak rainfall (Visser et al., 2023), and slower movement (Kossin, 2018; Kahraman et al.,
295 2021). As a result, although the frequency of extreme rainfall events may decline, when they do occur, the extreme
296 rainfall from the event is projected to increase (Grose et al., 2020) – with greater increases expected for more extreme
297 events (Wasko et al., 2023). Hence, just accounting for mean or extreme rainfall changes in isolation is not sufficient
298 and changes to the entire rainfall time series are required to study responses to climate change.

299 **4.2.2. Systematic review**

300 In climate literature the term “downscaling” is an umbrella term describing the conversion of coarse-resolution climate
301 model outputs to catchment-scale relevant outputs. The systematic review focused on “downscaling” yielded three
302 relevant manuscripts. In addition to these, one set of reports from the Australian Bureau of Meteorology was included
303 (Assessment Reports). Using five GCMs from the Coupled Model Intercomparison Project Phase 5 (CMIP5) and eight
304 global hydrologic models, Gu et al. (2020) projected changes up to the 1 in 50 AEP flood using the ISI-MIP trend-
305 preserving bias correction method (Hempel et al., 2013). Frequent floods were projected to decrease across large parts
306 of Australia, with some increases in the tropics. These patterns were amplified for rarer events, with decreases (or no
307 change) projected for rarer floods across the southern part of the country. The Australian Bureau of Meteorology has
308 published a dataset consisting of four CMIP5 GCMs and four downscaling methods gridded across the entire continent
309 (Wilson et al., 2022; Peter et al., 2023). Using this data (Wilson et al., 2022; Peter et al., 2023) as an input to the
310 AWRA-L daily water balance model (Frost et al., 2018) the annual maxima and 1 in 20 AEP flood events were
311 projected to increase across most of the continent (Assessment Reports).

312 Wasko et al. (2023) used the MRNBC and QME downscaling methods that were found to perform best for hydrologic
313 variables (Vogel et al., 2023) in 301 locally calibrated catchment rainfall-runoff models across the continent.
314 Decreases in frequent flooding up to the 1 in 5 AEP were projected across large parts of the continent, while for rarer
315 events, the flood magnitude was projected to increase across the northern and eastern coasts. Differences in the results
316 in this study and those above were attributed to (1) the use of rainfall-runoff models that were calibrated locally (i.e.,
317 different parameter set for each catchment) to flood frequency quantiles, whereas AWRA-L is calibrated to match
318 dynamics of daily streamflow and satellite soil moisture and evapotranspiration across Australia simultaneously using

319 a single set of parameters (Frost et al., 2018), and (2) due to the different downscaling methods adopted (Wasko et al.,
320 2023). Recent research has shown that, for hydrological applications, multi-variate bias correction that considers
321 cross-correlations among variables, temporal auto-correlations, and biases at multiple time scales (daily to annual)
322 performs the best (Vogel et al., 2023; Zhan et al., 2022; Robertson et al., 2023). Further, both the bias correction and
323 rainfall-runoff model calibration should be evaluated for the target statistics of interest (flood frequency in this case),
324 while also ensuring they are representative of the flood processes to guarantee robustness under change (Krysanova
325 et al., 2018). Finally, Zhan et al. (2022) and Sharma et al. (2021), among others, note that the uncertainty and variability
326 in climate projections, complexity in selecting data, as well as data processing, all hamper the adoption of climate data
327 in continuous simulation. Indeed, Dale (2021) argues that one of the primary requirements for design flood estimation
328 moving forward is “a standard, accepted approach for deriving time series rainfall that is representative of future
329 climatic conditions for continuous simulation modelling”.

330 **4.3 Event-based (IFD) modelling**

331 **4.3.1 Processes affecting changes in Australian extreme rainfall**

332 Before performing a systematic review of the complementary sources of knowledge that provide insight into how
333 climate change could influence rainfall extremes, we first provide a background to the changes in Australian extreme
334 rainfall, with this section excluded from the requirements of the systematic review. In Australia, extreme rainfall is
335 typically associated with thunderstorms, cyclones, troughs or fronts (Dowdy and Catto, 2017; Pepler et al., 2021;
336 Warren et al., 2021), including tropical cyclones (TCs) in northern Australia (Dare et al., 2012; Lavender and Abbs,
337 2013; Villarini and Denniston, 2016; Bell et al., 2019), east coast lows (ECLs) in the east and southeast of Australia
338 (Pepler and Dowdy, 2022; Dowdy et al., 2019) and thunderstorms (convective systems) throughout Australia (Dowdy,
339 2020). Other physical processes leading to extreme rainfall occurrence include enhanced advection of moisture to a
340 region, such as from atmospheric rivers – large narrow bands of water vapor (Wu et al., 2020; Reid et al., 2021; Black
341 et al., 2021) – and the temporal compounding of hazards such as heatwaves impacting heavy rainfall occurrence
342 (Sauter et al., 2023).

343 Tropical cyclones (TCs) can impact on northern regions of Australia, particularly in near-coastal locations, with their
344 occurrence generally from November to April (Chand et al., 2019). Although there is considerable interannual
345 variability in the number of TCs that occur near Australia, including influences of large-scale drivers such as the El
346 Niño-Southern Oscillation (ENSO), a significant downward trend in the frequency of observed Australian TCs has
347 occurred in recent decades (Dowdy, 2014; Chand et al., 2019, 2022). Climate models also indicate that TC numbers
348 in the Australian region are likely to continue decreasing in coming decades due to anthropogenic climate change
349 (Walsh et al., 2016; Bell et al., 2019; Bhatia et al., 2018; CSIRO and Bureau of Meteorology, 2015). However,
350 although fewer TCs are likely in a warmer world in general, this is more likely for non-severe TCs than severe TCs,
351 with extreme rainfall from TCs likely to increase in intensity at rates that could exceed 6-7%/°C of warming (Walsh
352 et al., 2016; Bhatia et al., 2018; Lighthill et al., 1993; Holland and Bruyère, 2014; Sobel et al., 2016; Emanuel, 2017;
353 Parker et al., 2018; Patricola and Wehner, 2018; Wehner et al., 2018; Knutson et al., 2020, 2019; Vecchi et al., 2019;
354 Kossin et al., 2020; Seneviratne et al., 2023). In addition to the frequency and severity, some studies have indicated a
355 potential poleward shift of TCs (Kossin et al., 2014), but there are considerable uncertainties around whether or not

356 this is occurring (Knutson et al., 2019; Bell et al., 2019; Chand et al., 2019; Tauvale and Tsuboki, 2019). Finally, some
357 studies have suggested a potential trend in the translational speed of TCs in a warming world (Kossin, 2018), while
358 others have suggested this might not be a significant change (Lanzante, 2019; Moon et al., 2019; Yamaguchi et al.,
359 2020).

360 East coast lows (ECLs) are cyclones near southeastern Australia that can be caused by both mid-latitude and tropical
361 influences over a range of levels in the atmosphere. Fewer ECLs are likely to occur due to anthropogenic climate
362 change, at a rate of about -10%/°C of global warming, with this change more likely for cooler months (Dowdy et al.,
363 2019; Pepler and Dowdy, 2022; Cavicchia et al., 2020). A recent study using RCM projections reported that the
364 number of cyclones exceeding the current 95th percentile for maximum rain rate is expected to increase by more than
365 25%/K in Australia's eastern seaboard and Tasmania under a high emissions pathway (RCP8.5) by 2070–2099. Both
366 the eastern seaboard and Tasmania are projected to have twice as many cyclones with heavy localised rain as in 1980–
367 2009 (Pepler and Dowdy, 2022). That study also found that about 90% of model simulations had at least one ECL in
368 the period 2070–2099 with a higher maximum rain rate than any in the period 1980–2009 for southeast Australia and
369 similarly for Tasmania. It is noted here that RCM projections are not at fine-enough scales to be convection-permitting
370 and so may not necessarily capture some changes in rainfall efficiency associated with enhanced convective processes
371 from increased atmospheric moisture capacity.

372 Convective storms, such as severe thunderstorms, can cause relatively localised storms as well as mesoscale
373 convective and linear systems (Hitchcock et al., 2021). As climate models have a limited ability to simulate fine-scale
374 aspects associated with thunderstorms (e.g., Bergemann et al. 2022), projections are typically based on environmental
375 conditions conducive to thunderstorm formation, such as convective available potential energy or other related
376 atmospheric metrics associated with deep and moist convection. Projections using environmental conditions such as
377 these have indicated a broad range of plausible changes in the frequency of thunderstorm environments for regions
378 throughout Australia, including potential increases or decreases depending on the metric or model selections used
379 (Allen et al., 2014; Brown and Dowdy, 2021). Some of the latest set of GCMs indicate an increase in convection-
380 related extreme rainfall over Australia relating to the Madden-Julian Oscillation (Liang et al., 2022).

381 Using lightning observations as a proxy for convective storm occurrence, a decline in the number of thunderstorms
382 during the cooler months of the year has been observed in parts of southern Australia (Bates et al., 2015). Another
383 study based on rainfall observations and reanalysis data reported a trend since 1979 towards fewer thunderstorms for
384 most regions of Australia, with the strongest and most significant trends in northern and central Australia during the
385 spring and summer, in addition to increasing trends in thunderstorm frequency on the eastern seaboard (Dowdy, 2020).
386 However, the total rainfall associated with thunderstorms increased in most regions over the same time period, such
387 that the intensity of rainfall per thunderstorm increased at about 2-3 times the Clausius-Clapeyron rate (Dowdy, 2020).
388 Importantly, most of southern Australia saw an increase in the frequency of thunderstorms associated with rainfall of
389 at least 10 mm over the same period, particularly during the warm months (Pepler et al., 2021). That increase in rainfall
390 intensity exceeding the Clausius-Clapeyron rate is broadly similar to some other studies based on observations and

391 modelling for Australia, including those focussed on short-duration extremes (Westra and Sisson, 2011; Bao et al.,
392 2017; Guerreiro et al., 2018; Ayat et al., 2022), with the larger increases tending to be in northern rather than in
393 southern regions. These high rates of change in rainfall intensity can occur from changes in rainfall efficiency, which
394 increases due to additional moisture capacity in a warmer atmosphere providing additional latent heat from
395 condensation as energy in the convective processes – so-called super-CC scaling. This process is relevant for
396 thunderstorms and TCs given the convective processes that provide energy for their formation and intensification, as
397 well as ECLs that sometimes have mesoscale convective features embedded within their broader synoptic structure
398 (Holland et al., 1987; Mills et al., 2010; Dowdy et al., 2019).

399 Extratropical cyclones and fronts can also sometimes cause extreme rainfall in southern Australia. Recent studies have
400 reported a trend towards fewer of these events, particularly during the cooler months of the year, including a reduction
401 in the frequency of events that generate at least 10 mm of rainfall (Pepler et al., 2021). Projections of extratropical
402 cyclones and fronts in this storm-track region of the Southern Hemisphere are broadly similar to the observed trends,
403 with studies indicating a general reduction in frequency for this region, particularly during the cooler months of the
404 year (Seneviratne et al., 2023; CSIRO and Bureau of Meteorology, 2015). The projections are also consistent with
405 observed reductions in multi-day rainfall events (Fu et al., 2023; Dey et al., 2019), which tend to be associated with
406 long-lived synoptic systems (i.e., at least 24 hours) such as extratropical cyclones.

407 Finally, the frequency of atmospheric rivers in Australia increased over the 1979-2019 period in one study (Reid et
408 al., 2022), and may increase in frequency in a warming climate, including near eastern Australia (Wang et al., 2023).
409 For example, a recent study demonstrated how an atmospheric river contributed to extreme multiday rainfall and
410 flooding in Sydney in March 2021, finding that, depending on the emission scenario, this type of atmospheric river
411 could increase in frequency by about 50-100% around the end of this century (Reid et al., 2021), but projections have
412 not been assessed in detail for elsewhere in Australia.

413 In summary, more intense rainfall extremes associated with TCs are likely to occur for northern Australia during the
414 warmer months of the year. For eastern Australia, fewer ECLs are likely to occur, but with an increase in the
415 occurrence of ECLs that cause extreme precipitation. For southern Australia, fewer extratropical cyclones and fronts
416 are likely to occur during the cooler months of the year, leading to a potential reduction in rainfall extremes during
417 these months. Increases in moisture transport by atmospheric rivers has also been reported, with the frequency of
418 strong atmospheric rivers potentially increasing by 50-100% in eastern Australia towards the end of this century. The
419 increased water vapour capacity of the atmosphere in a warming world can increase rainfall efficiency in some cases,
420 such as through enhanced latent heat from condensation contributing energy to the convective processes. This can
421 lead to increases in the intensity of extreme rainfall that are notably larger in magnitude than the 6-7%/°C increase
422 associated with the Clausius-Clapeyron relation. Studies have indicated that increased rainfall efficiency in the order
423 of two or more times the Clausius-Clapeyron relationship rate are plausible for short-duration rainfall extremes in
424 general for Australia (Guerreiro et al., 2018; Dowdy, 2020; Ayat et al., 2022).

425 **4.3.2 Rainfall intensity**

426 **4.3.1.1 Impact of climate change**

427 IFD curves are typically derived using statistical models, such as the Generalized Extreme Value (GEV) distribution,
428 fitted to annual maximum rainfall across a range of durations and severities (AEPs). Anthropogenic changes in
429 extreme rainfall, both in their intensity and frequency, will therefore lead to changes in IFDs (Milly et al., 2008). In
430 the scientific literature, changes in extreme rainfalls are generally modelled using non-stationary frequency analysis
431 with appropriate covariates. While this is an active area of research (Schlef et al., 2023; Wasko, 2021) it has the same
432 shortcomings as non-stationary flood frequency analysis. Most studies use a time covariate to impart a temporal trend
433 (Schlef et al., 2023). However, there is evidence that accounting for the different drivers of extreme rainfall, for
434 example temperature for short duration rainfall, and climate modes such as the El Niño-Southern Oscillation (ENSO)
435 and the Indian Ocean Dipole (IOD) for long duration rainfall, can improve model performance (Agilan and
436 Umamahesh, 2015, 2017). This is consistent with the arguments put forward by Schlef et al. (2018) that covariates
437 should capture the thermodynamic and dynamic processes that affect rainfall changes. For non-stationary frequency
438 analysis, there is evidence emerging that GEV models should consider changes in both location and scale parameters
439 (Prosdocimi and Kjeldsen, 2021; Jayaweera et al., 2023). Finally, Schlef et al. (2023) summarised that for non-
440 stationary IFD analysis “the majority of covariate-based studies focus on the historical period, effectively reducing
441 the study to a sophisticated check for non-stationarity, rather than a framework for projection of non-stationary IDF
442 curves” and hence their predictive ability remains untested (Schlef et al., 2023).

443 Likely due to the difficulties in fitting non-stationary IFDs, the majority of climate change guidance for practitioners
444 is to scale the IFD rainfall depth or intensity using a climate adjustment (or uplift) factor derived from an assessment
445 of how extreme rainfalls are likely to change under climate change (Wasko et al., 2021b). Studies that assess potential
446 changes in extreme rainfall can be roughly separated into three categories: (1) studies that assess historical trends; (2)
447 studies that investigate the association of extreme rainfalls and temperature; and (3) studies that directly project
448 changes in extreme rainfall using model experiments.

449 **4.3.1.2 Systematic review**

450 Our systematic review identified 40 manuscripts that quantified the relationship between temperature changes and
451 rainfall intensity, with the manuscripts roughly evenly split between the above three approaches. Model-based
452 projections were almost always focussed on daily to multi-day rainfall extremes, with the exception of two studies
453 that employed regional models over small regions of Australia to provide projections of sub-daily rainfall (Mantegna
454 et al., 2017; Herath et al., 2016). In contrast, scaling studies were more likely to assess sub-daily rainfall, and about
455 half the papers assessing historical trends included sub-daily (usually hourly) rainfall.

456 Historical analysis of trends in high daily rainfall totals, such as the wettest day per year (Rx1D) or the 99th percentile
457 of the daily rainfall distribution, find a range of trends depending on the region and years used (Dey et al., 2019; Du
458 et al., 2019; Alexander and Arblaster, 2017; Sun et al., 2021; Liu et al., 2022a). Many older studies detected no
459 significant trend or a decreasing trend in Rx1D (e.g., Hajani and Rahman, 2018), including some large negative trends
460 when calculated for individual stations (Yilmaz and Perera, 2014; Chen et al., 2013). However, more recent studies
461 that draw on larger volumes of stations or gridded data more commonly detect increasing trends in Rx1D, many of

462 which are close to 7%/K (Wasko and Nathan, 2019; Dey et al., 2019; Guerreiro et al., 2018). Increases are most
463 apparent in the annual maximum intensity of events of no more than two days duration, which increased by between
464 13% and 30% over the period 1911-2016 for different regions of Australia (Dey et al., 2019). Changes in rainfall
465 intensity are less robust for longer duration rainfall events, with studies finding little change or even a decrease in the
466 intensity of the wettest five-day rainfall (Rx5D) in southeast and southwestern Australia over the period since 1950
467 (Du et al., 2019; Fu et al., 2023), although this result may be influenced by multidecadal variability including very
468 high rainfall totals in the 1950 and 1970s. Decreases in long-duration rainfall events are most evident during the
469 autumn and winter (Zheng et al., 2015), associated with extratropical weather systems (Pepler et al., 2020). While
470 total rain days have decreased in many parts of Australia, the intensity of rainfall on wet days may have increased
471 (Contractor et al., 2018), as has the average intensity of rainfall on days with thunderstorm activity (Dowdy, 2020).

472 There is increasingly strong evidence suggesting that an increase in the intensity of sub-daily rainfall has already
473 occurred. Guerreiro et al. (2018) found an average increase of 2.8 mm or 9.4% in the average wettest hour of the year
474 between 1966–1989 and 1990–2013 across Australia, equivalent to 19.5%/K, with increases observed at most stations
475 analysed. When divided into northern and southern Australia, trends were greater than 21%/K in the north, which has
476 seen a large increase in total rain over the same period (Dey et al., 2019); however, even in southern Australia,
477 increases were larger than those expected based on Clausius-Clapeyron for frequencies up to the seven wettest hours
478 per year (7EY), and close to 14%/K for the wettest four hours per year (4EY). In Victoria, studies have found an 89%
479 increase in the frequency of hourly rainfall > 18 mm/h (Osburn et al., 2021) between 1958-1985 and 1987-2014, as
480 well as increases in hourly totals > 40 mm/h (Tolhurst et al., 2023). Yilmaz and Perera (2014) also found increasing
481 trends in Melbourne rainfall intensities for durations of three hours or less between 1925-2010, with 1 in 2 AEP values
482 5-7% higher when calculated using data from 1967-2010 versus 1925-1966 (~13-17%/K), though not all differences
483 were statistically significant. In southeast Queensland and northeast New South Wales, increasing trends for annual
484 maxima for events with a duration of less than 12 hours have been reported (Laz et al., 2014), while Chen et al. (2013)
485 reported that the heaviest rainfalls at timescales of six minutes to six hours increased between the earlier and later 20th
486 century by more than 20% in Melbourne, Sydney and Brisbane. Very large increases of ~20%/decade in sub-hourly
487 rainfall have also been identified in Sydney using both radar and rain gauge data based on the short period of 1999-
488 2017 (Ayat et al., 2022). Trends tend to be strongest for convective rainfall, which has its largest contribution to short
489 duration events and during the warm half of the year. For instance, heavy rainfall in Greater Sydney during the summer
490 months increased by more than 6%/decade for all durations from six minutes to 48 h over 1966-2012 (Zheng et al.,
491 2015).

492 Scaling studies typically use quantile regression on rainfall-temperature pairs or linear regression on extreme rainfall
493 percentiles after grouping records by temperature classes to calculate the relationship between day-to-day temperature
494 variability and the upper tail of the rainfall distribution, as represented by the 90th or 99th percentile of rainfall for a
495 given temperature range (Wasko and Sharma, 2014). While early scaling studies used dry bulb air temperature, such
496 approaches were sensitive to the cooling influence of rainfall on air temperature as well as the temporal and spatial
497 scales of rainfall (Bao et al., 2017; Barbero et al., 2017) and often found negative scaling in the northern tropics

498 (Wasko et al., 2018). Recent studies have found more homogenous results by scaling against moisture availability,
499 most commonly represented by the dewpoint temperature, as well as by accounting for intermittency in precipitation
500 events (Visser et al., 2021; Schleiss, 2018). Studies typically find a median scaling over Australia of 7-8%/K for daily
501 rainfall (Magan et al., 2020; Roderick et al., 2020; Bui et al., 2019; Wasko et al., 2018; Ali et al., 2021b; Visser et al.,
502 2020). This regional convergence to Clausius-Clapeyron scaling hides larger variability in the scaling at local station
503 scales, ranging typically between 5-10%/K, although in the northern tropics many stations exhibit scaling greater than
504 14%/K between rainfall and dewpoint temperature (Magan et al., 2020; Wasko et al., 2018).

505 Scaling is typically stronger for sub-daily rainfall, with median scaling over Australia typically 8-10%/K and scaling
506 in tropical regions frequently exceeding 14%/K (Wasko et al., 2018; Ali et al., 2021b; Visser et al., 2021). For rarer
507 events, Wasko and Sharma (2017) used a stochastic weather generator conditioned on temperature and found hourly
508 rainfall scaling for Sydney and Brisbane increased from 6-9%/K for an AEP of 1 in 2 to 10-12%/K for a 1 in 10 AEP
509 and 18%/K for a 1 in 100 AEP, although the uncertainty ranges were large. Scaling rates exceeding 15%/K between
510 dewpoint temperature and daily rainfall over Australia have also been calculated using a global $0.25^\circ \times 0.25^\circ$
511 latitude/longitude resolution model (Zhang et al., 2019), although scaling in the Sydney region was $\sim 4\%/K$ for hourly
512 rainfall using a 2 km convection permitting model (Li et al., 2018).

513 GCMs are not expected to accurately simulate rainfall extremes due to deficiencies in representing the key phenomena
514 responsible for extreme rainfall including convection and thunderstorms or tropical cyclones. This is particularly true
515 of short-lived or sub-daily extremes, with GCMs better at simulating daily or longer extremes such as extratropical
516 lows, which cause widespread and prolonged heavy rainfall (Kendon et al., 2017). Projections from CMIP5 models
517 between 1986-2005 and the late 21st century ($\sim 2081-2100$) indicate an increase in RX1D under a high emissions
518 scenario (Alexander and Arblaster, 2017), with regional mean increases in RX1D ranging from 13% in Eastern
519 Australia to 19% in Northern Australia ($\sim 4-6\%/K$) (Climate Change in Australia). A $4\%/K$ increase in RX1D was also
520 found by Chevuturi et al. (2018) when comparing a 2-degree warmer world with historical simulations, while Ju et al.
521 (2021) found an 11% increase in RX1D in a 2-degree warmer world ($5.5\%/K$). Models in the Coupled Model
522 Intercomparison Project Phase 6 (CMIP6) simulate a slightly smaller change in RX1D, with a 6.2-7.3% increase in
523 Rx1D for Australia between the preindustrial climate and the 2-degree warming level and a 10.3-11.2% increase by 3
524 degrees ($3-4\%/K$, Gutiérrez et al., 2021) and a 9.4% ($\sim 3\%/K$) increase in Rx1D by the end of the century (Grose et
525 al., 2020).

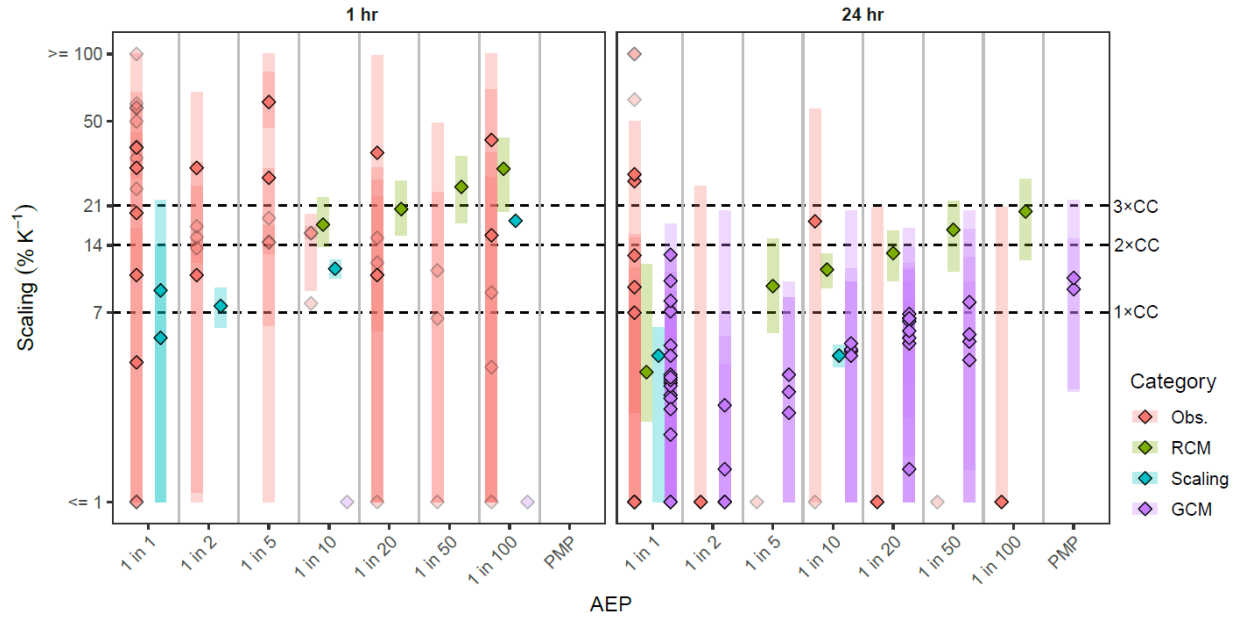
526 Results from regional climate models are broadly consistent with GCMs for daily rainfall, including a projected
527 regional mean increase of $5.7\%/K$ in the 99th percentile of wet days using the NARClIM ensemble (Bao et al., 2017)
528 and larger increases in the 99.5th ($6.5\%/K$) and 99.9th ($9.2\%/K$) percentiles. Pepler and Dowdy (2022) also found a
529 $4\%/K$ increase in the frequency of days exceeding the 99.7th percentile using a CMIP5-based RCM ensemble, with
530 the largest increases projected in Tasmania ($12\%/K$), while Herold et al. (2021) reported a doubling in the frequency
531 of current 1 in 20 AEP events by 2060-2079. Projected increases are smaller for multi-day rainfall, with a median
532 increase in Rx5D of 10% ($\sim 3\%/K$) reported in Sillmann et al. (2013), $4\%/K$ in Ju et al. (2021), and no significant
533 change in Chen et al. (2014). While fewer studies have assessed changes to less frequent rainfall extremes, these are

534 typically larger than the increases projected for annual maxima. For instance, CMIP5 models simulate a 22-26%
535 increase (7-8%/K) in the 1 in 20 AEP daily rainfall by the end of the 21st century (Climate Change in Australia), and
536 statistically downscaled climate data project a similar 20% increase in the 1 in 50 AEP by the end of the century
537 (6%/K; Wasko et al., 2023). Slightly smaller increases for the 1 in 10 AEP of 15.5% by the end of the century were
538 found using CMIP6 models (~5%/K, Grose et al., 2020).

539 Studies investigating the projection of sub-daily rainfall extremes are rare for Australia, but regional modelling for the
540 Tasmanian region indicated increases of greater than 40% in AEP of 1 in 10 and rarer in a 2.9-degree warmer world;
541 more than 14%/K (Mantegna et al., 2017). This is consistent with the stronger observed trends and scaling rates
542 reported for rainfall of short durations. Projected increases are likely to be larger for convective extremes, which
543 dominate sub-daily rainfall and are poorly simulated even in regional climate models. For example, Shields et al.,
544 (2016) projected a 12.5% increase in convective rain rates above the 95th percentile in the Australasian region using a
545 $0.5^\circ \times 0.5^\circ$ latitude/longitude global model by the late 21st century (~4%/K) but no change in large-scale rainfall.
546 Finally, regional model experiments also indicate increases of 15% in tropical cyclone rain rates per degree of SST
547 increase (Bruyère et al., 2019).

548 **4.3.1.2 Meta-analysis**

549 Where possible, observed and projected changes were extracted from each paper or dataset. Absolute changes were
550 converted to changes as a percent per degree of warming, with the global mean warming over the appropriate time
551 period extracted either from the Berkeley Earth Surface Temperature dataset (Rohde and Hausfather, 2020), or the
552 ensemble mean for the corresponding CMIP generation and emissions scenario. These quantitative results are
553 summarised in Figure 3, with extended details provided in the Supplementary Data Table. The centre changes are
554 central estimates of the change in extreme rainfall amount converted to %/K. The type of central estimate (median or
555 mean) is indicated in the Supplementary Data Table. Minimum and maximum changes are the largest range of changes
556 reported by each study; these are usually minima and maxima (for example across stations). It is noted that some
557 papers are included in Figure 3 multiple times for different durations and exceedance percentiles.



558

559 **Figure 3.** Summary of extreme rainfall change standardised, where possible, in per degrees of global temperature
 560 change. Note that rainfall-temperature scaling studies use local temperatures. Dashed lines indicate Clausius-
 561 Clapeyron (1×CC), 2×CC, and 3×CC scaling respectively. Diamonds indicate the central estimate of scaling and
 562 shaded bars indicate the range (where possible, the minimum to maximum) of scaling estimates. Diamonds are
 563 opaque for results in which there was higher confidence and transparent for estimates in which authors found
 564 “disqualifying features” that significantly lowered weighting in the meta-analysis. The few studies with AEPs
 565 between the values shown here were included in the nearest AEP for this plot.

566 By consensus it was deemed that the results for the meta-analysis would focus on daily and hourly rainfall durations
 567 as the majority of studies focus on these two durations with studies and the mechanisms that cause extreme rainfall at
 568 the two durations are often distinct (albeit short duration extremes are often embedded in longer duration extremes).
 569 Studies investigating storm durations of 6 hours or less were grouped into the hourly rainfall duration, with studies
 570 with durations of greater than 6 hours grouped with the daily rainfall duration. The potential for rates of change to
 571 vary both by location and exceedance probability was also explored. In relation to changes by location, there is
 572 significant heterogeneity in the rainfall-generating mechanisms across the Australian landmass (Linacre and Geerts,
 573 1997). However, when comparing the published scaling rates across the different geographies, there was insufficient
 574 evidence to quantify the differences between regions, with a relative scarcity of studies in regions outside of the
 575 populated areas of eastern Australia, and few consistent methodologies applied to all of Australia. Similarly, although
 576 there is some evidence that rarer extremes are likely increasing more than frequent extremes, it was deemed there was
 577 not enough evidence to quantify this difference through the meta-analysis (see Figure 3). This was because of (1) the
 578 large variability of extreme rainfall changes between studies relative to the variability with AEP, and (2) where there
 579 appears to be a trend with AEP this is generally a result of a single study analysing multiple AEPs. Hence the
 580 uncertainty intervals in the meta-analysis were developed with the aim of encompassing much of the variability in the
 581 extreme rainfall changes across space and exceedance probability.

582 Multiple co-authors independently used the available evidence to determine their best estimates of a central scaling
 583 rate and the likely range of extreme rainfall change, for events rarer than the annual maxima up to the PMP. For both
 584 daily and hourly durations, each relevant study was assessed based on the type of evidence (i.e., trend, association, or
 585 projection), the study methodology, the number of sites analysed, the age of the study, its spatial extent, and theoretical
 586 considerations. The results of each co-author's independent assessment are presented in Table S3. Following the
 587 independent analysis by the co-authors, a consensus was drawn between the participating co-authors with regard to
 588 the central (median) estimate and the likely range (66%) of extreme rainfall change. The consensus scaling rates and
 589 ranges are shown in Table 1.

590 **Table 1.** Results of a meta-analysis presenting extreme rainfall change, using a multiple-lines-of-evidence approach
 591 that draws on the studies in the Supplementary Data Table. This synthesis is based on a review of all studies
 592 covering extremes from the annual maxima through to the probable maximum precipitation (PMP) event (see
 593 Section 4.3.3 for further information on the PMP). The estimates are presented per degree global temperature
 594 change.

	<=1 hr	>1 hr and <24 hr	>=24 hr
Central (median) estimate	15%/K	Interpolation zone	8%/K
'Likely' range (corresponding to ~66% range)	7%-28%/K	Interpolation zone	2%-15%/K

595
 596 Weightings given by individual authors reflected the following findings. At daily timescales, RCM projections and
 597 scaling approaches typically had higher scaling rates than GCM projections, likely due to deficiencies in GCMs
 598 representing key extreme rainfall generation processes. Moreover, many observational studies used few sites with
 599 limited spatial coverage. In most studies using historical data across larger extents and recent periods, results were
 600 between 4-10%/K, with a central estimate of 8%/K for rarer events (e.g., 1 in 100 AEP), noting also that a greater
 601 weight was given to those global and Australia-wide studies. The likely range encompasses small but non-negative
 602 changes, which are most likely due to changes relevant to more frequent, multi-day events of 72+ hour duration. The
 603 likely range also encompasses potential scaling of at least twice the Clausius-Clapeyron rate, most likely for rarer
 604 events such as 1 in 100 AEP and for locations in northern Australia.

605 For sub-daily timescales, estimates of change are predominantly based on historical observations (trends), due to a
 606 relative paucity of projection information. These studies suggest that changes below the Clausius-Clapeyron rate of
 607 7%/K are unlikely, with potential changes in excess of 15%/K observed for rarer events. This is broadly consistent
 608 with the single available regional model study (Mantegna et al., 2017), which had projected increases of 16%/K for a
 609 1 in 10 AEP and 29%/K for 1 in 100 AEP. Slightly weaker changes are found in scaling studies compared to the other
 610 lines of evidence, with the tropics again showing evidence of greater increases compared to the south. The likely range
 611 hence incorporates this spatial inhomogeneity noting that greater uncertainty exists on the upper estimate of change
 612 than the lower estimate. While the meta-analysis central estimate of 15%/K is based on the best available information,

613 there is an urgent need for more detailed assessment of changes in sub-daily rainfall in a changing climate using
614 convection-permitting models.

615 **4.3.3 Probable maximum precipitation**

616 **4.3.3.1 Impact of climate change**

617 The PMP is defined as the greatest depth of precipitation meteorologically possible under modern meteorological
618 conditions for a given duration occurring over a catchment area or a storm area of a given size, at a certain time of the
619 year (WMO, 2009). It needs to be recognised that this theoretical definition differs from its “operational estimate,”
620 which is based on a set of simplifying assumptions and calculated from an observational sample of
621 hydrometeorological extremes (Schaefer, 1994). Hence, in Australia and elsewhere, successive estimates of the PMP
622 adopted for design purposes have increased over time as methods and data sets change (Bureau of Meteorology, 2003).
623 As a result, PMP estimates for climate change are heavily dependent on the operational methods employed.

624 The methods used to derive operational PMP estimates can be broadly divided into statistical methods and
625 hydrometeorological methods. Statistical methods are commonly used in engineering studies as they can be applied
626 with little effort and do not require hydrometeorological expertise. The most widely used statistical approach was
627 developed by Hershfield (1965) and is based on enveloping the observations obtained from a large number of rainfall
628 gauges to extrapolate a simple 2-parameter (Gumbel) distribution. Hydrometeorological methods used to derive
629 operational estimates include approaches based on the maximisation of local storm data, referred to as in-situ
630 maximisation, the transposition of extreme storms nearby to the catchment with similar topography, known as storm
631 transposition, and the enveloping of storm data over a large region after adjusting for differing moisture availability
632 and topography, known as generalised methods. Generalised methods differ from the in-situ and transposition methods
633 in that they use all available data over a large region and include adjustments for moisture availability and differing
634 topographic effects on rainfall depth. Generalised PMP methods are employed in Australia as well as a number of
635 other countries, including New Zealand (Thompson and Tomlinson, 1995), India (Rakhecha and Kennedy, 1985),
636 China (Gu et al., 2022), and the USA (England et al., 2020). For Australia, the storm transposition zone varies with
637 climate region as the mechanisms driving extreme rainfall vary.

638 In generalised hydrometeorological methods, the PMP event is assumed to originate from the simultaneous occurrence
639 of a maximum amount of moisture (moisture maximisation) and a maximum conversion rate of moisture to
640 precipitation (storm efficiency). Moisture maximisation involves multiplying observed storm precipitation depths by
641 the ratio of the seasonal maximum precipitable water for the storm location to the representative precipitable water
642 for the storm, with the precipitable water estimated from surface dewpoint data assuming saturation and pseudo
643 adiabatic conditions. This assumes that in a large sample of storms recorded over a long period at least one storm
644 operates near maximum efficiency.

645 Potential increases in future daily PMP estimates are predominantly founded on projected increases in atmospheric
646 water vapor, which have been found to closely follow temperature changes with an approximate Clausius-Clapeyron
647 relationship of 7% per 1°C warming (noting that this does not consider potential changes in rainfall efficiency). While
648 the WMO manual (WMO, 2009) makes no allowance for long-term climatic trends, one of the most comprehensive

649 studies that examined changes in maximum water vapour concentrations across the globe found increases in
650 atmospheric water vapor of 20%–30% by the end of the century (Kunkel et al., 2013), approximately consistent with
651 the Clausius-Clapeyron relationship. Kunkel et al. (2013) adopted a “hybrid” approach that merged traditional
652 hydrometeorological PMP methods with outputs from an ensemble of seven GCMs, an approach that is seen as an
653 advance on traditional PMP estimates as it incorporates simulated historical and future climate model data (Salas et
654 al., 2020). They found that the PMP will change by an amount comparable to the mean water vapour changes, with
655 little evidence for changes in storm efficiency (Kunkel et al., 2013); however it is noted that GCMs do not simulate
656 many of the key process that could lead to changes in storm efficiency. The relatively minor importance of changes
657 in storm efficiency compared to precipitable water under climate change was also found by Ben Alaya et al. (2020),
658 who based their conclusions on an analysis of non-stationarity in a bivariate model of precipitable water and storm
659 efficiency using temperature as a covariate.

660 Since Kunkel et al. (2013), many other hybrid approaches have been applied using either global or regional climate
661 models, and similar results have been found for catchment- or region-specific studies in northern America (Beauchamp
662 et al., 2013; Chen et al., 2017; Cyphers et al., 2022; Clavet-Gaumont et al., 2017; Rousseau et al., 2014; Rouhani and
663 Leconte, 2020; Labonté-Raymond et al., 2020), Chile (Lagos-Zúñiga and Vargas M., 2014), and Korea (Lee et al.,
664 2016). While one study projected decreases in the PMP using a hybrid modelling approach, it was based on a single
665 GCM model (CanESM2) and the projections were for a region in the southeast of the Caspian Sea (Afzali-Gorouh et
666 al., 2022). Other region-specific studies have applied physically-based approaches using regional atmospheric models
667 and found results that are consistent with the Clausius-Clapeyron relationship in north America (Ishida et al., 2018;
668 Gangrade et al., 2018; Rastogi et al., 2017), China (Liu et al., 2022b), and Chile (Lagos-Zúñiga and Vargas M., 2014).

669 Statistical methods based on Hershfield (1965) have also been used to assess the non-stationarity of PMP estimates,
670 where a recent study (Sarkar and Maity, 2020) used a global reanalysis data set to conclude that global PMP estimates
671 have increased by an average of 25% over the world between the periods of 1948-1977 and 1978-2012. These changes
672 are appreciably larger (e.g., about quadruple) than what would be expected from the Clausius-Clapeyron relationship,
673 though differences between statistical and hydrometeorological methods are evident in other studies in Canada
674 (Labonté-Raymond et al., 2020), India (Sarkar and Maity, 2020), Vietnam (Kawagoe and Sarukkalige, 2019) and the
675 USA (Lee and Singh, 2020). The degree of conservatism associated with the statistical method (i.e., the tendency to
676 produce high estimates) is heavily dependent on the robustness of the envelope curves. Given the lack of physical
677 reasoning in the statistical method, it is difficult to reconcile differences with estimates derived using
678 hydrometeorological concepts. This is also true of generalised methods, which in principle do not vary with storm
679 duration, with research into changes in the PMP with climate change largely using daily rainfall data.

680 **4.3.3.2 Systematic review**

681 A systematic search yielded one recent paper relevant to projected changes in operational PMP estimates for Australia
682 (Visser et al., 2022), with Salas et al. (2020) summarising existing methods and findings. Visser et al. (2022) undertook
683 an analysis of moisture availability, comprising dewpoint data from 30 synoptic stations across Australia covering the
684 period from 1960 to 2018 and 3-hourly ERA5 reanalysis data covering the period from 1979 to the present (Hersbach

685 et al., 2020). It was found that the annual maximum persisting dewpoints have increased leading to increased PMP
686 estimates. Projections of dewpoint temperature were used to derive future PMP estimates across Australia using the
687 ACCESS-CM2 model. The projected results showed increases of 4%-29% (average of 13%) by 2100 for SSP1-2.6
688 and 12-55% (average of 33%) for SPP5-8.5 (Visser et al., 2022). If global temperature increases are used, these
689 changes translate to average increases slightly greater than the Clausius-Clapeyron relationship (e.g., 8.9%/K for
690 SSP5-8.5).

691 Jakob et al. (2009) investigated how the local moisture availability, storm type, depth-duration-area curves and relative
692 storm efficiency used in deriving operational PMP estimates might be changing over time, and how the identified
693 changes have impacted the PMP estimates. The analysis was based on data from 38 locations across Australia from a
694 combination of upper-air (radiosonde) and surface dewpoint observations. No large-scale significant changes in
695 moisture availability were found, though significant increases were found along parts of the east coast, as well as a
696 region in south-eastern Australia with summer decreases. When comparing moisture availability for a historical
697 climate period (1981-2000) and the next few decades using outputs from a single global climate model, they found
698 the 90th percentile values increased from the 2020s to the 2050s and the 2090s, however they also found some evidence
699 for lower extreme moisture availability in some regions. Similar to the above studies, they found little evidence for
700 significant changes in storm efficiency, depth-duration-area curves, or storm types, and no significant changes were
701 found in generalised rainfall depths (again noting that such global models are not expected to simulate some of the
702 key rainfall generation processes). The results obtained by Jakob et al. (2009) are not inconsistent with those of Visser
703 et al. (2022), but the difference in conclusions may be explained by the longer and more extensive data sets used by
704 Visser et al. (2022) and the updated global climate model outputs used to project the dewpoint temperatures.

705 Despite this compelling evidence, there is no formal recommendation for increases in PMP estimates with the Manual
706 on Estimation of Probable Maximum Precipitation (WMO, 2009) in their chapter on “PMP and Climate Change”
707 summarising the results of Jakob et al. (2009). To the best of the authors’ knowledge, no agency responsible for
708 providing operational PMP estimates for design purposes anywhere in the world has yet provided uplift factors to
709 ensure that the PMP estimates based on historic observations are relevant to future conditions, despite the majority of
710 studies into impact of climate change on the PMP finding the PMP is likely to be increasing at the CC rate for daily
711 rainfall.

712 **4.3.4 Temporal and spatial patterns**

713 **4.3.4.1 Impact of climate change**

714 The temporal and spatial patterns of extreme rainfall have long been recognised as important factors in determining
715 the magnitude of a flood event (Herrera et al., 2023). Conceptually, as weather systems change and storms intensify
716 due to increases in temperature, changes in both the temporal and spatial pattern of rainfall are expected with
717 anthropogenic climate change. Given that sub-daily rainfalls are expected to intensify more than daily rainfalls
718 (Section 4.2.1) this implies that storm temporal patterns will also intensify. In the design flood paradigm, once a
719 rainfall depth has been estimated from the appropriate IFD relationship, a temporal profile is used to distribute the
720 total rainfall across the storm duration. When the rainfall distribution across the storm duration is less uniform, higher

721 flood peaks will generally occur (Ball, 1994). For example, front or rear loaded storms, where more than 50% of the
722 total rainfall falls in either the first half or the second half of the storm respectively (Visser et al., 2023), can have
723 differing impacts on flood peaks through their interactions with any storage (natural or constructed) in the catchment.

724 In the context of design flood estimation, as the underlying data for the IFD relationships is point rainfall, the influence
725 of spatial scale on average rainfall intensities is considered through ARFs. For small catchments the point rainfall
726 provides a reasonable approximation of the catchment average rainfall. However, for larger catchments, it is less likely
727 that the most intense rainfall in a storm will occur over the whole catchment and the catchment average rainfall for
728 any particular event will be lower than the point rainfall represented by the IFD relationship. ARFs represent this
729 expected rainfall reduction, with the reduction dependent on the catchment area, storm duration, and frequency.

730 **4.3.4.2 Systematic review**

731 Some limited research has been undertaken with respect to changes to temporal patterns and spatial patterns of design
732 rainfalls, primarily using scaling relationships calculated from observed data, while there exists some limited
733 modelling via dynamic downscaling for the Sydney region. A total of seven papers were found as part of the systematic
734 review. The findings to date suggest that temporal patterns are becoming more front-loaded (greater percentage of
735 precipitation falling earlier in the storm) with higher temperatures. There is also an increase in the proportion of rain
736 falling in the wettest period of the storm, leading to increased peakiness (less uniformity) of the temporal patterns.

737 Temporal pattern changes have been analysed in two main ways. The first is broadly based on the average variability
738 method, whereby the changes in the proportion of rainfall within a period are calculated. For example, Wasko and
739 Sharma (2015a) found for 1 hour storm bursts, the highest 12-minute period had a median scaling of 2.1% per degree
740 temperature increase for Australia. The scaling rate was dependent on the duration of the storm and the latitude of the
741 station. Wasko and Sharma (2015b) identified 500 one-hour bursts for five stations, stratified them into five
742 temperature bins and calculated the temporal pattern using the average variability method for each bin. In general, the
743 highest temperature bin had peakier (i.e., less uniform) temporal patterns than the lowest temperature bin. Wasko and
744 Sharma (2017) also used the average variability method to calculate the scaling of temporal patterns. These later
745 analyses were based on first fitting a stochastic rainfall generation model to historical observations, and then using
746 regression models to explore the relationships between the rainfall generation model parameters and temperature. For
747 simulations representing the end of the 21st century under RCP8.5, the peak rainfall fraction in the temporal patterns
748 increased from 40% to 50% for two models that were fitted separately for Brisbane and Sydney.

749 Australia's flood guidance (Ball et al., 2019a) has moved away from using the average variability method for temporal
750 patterns, and instead now provides an ensemble of temporal patterns for design rainfall analyses. Consistent with this
751 approach, Visser et al. (2023) provide the most comprehensive analyses of scaling relationships for temporal patterns
752 for Australia. From an original database of 1489 rainfall gauges 151 stations had sufficient data for scaling analysis,
753 and trends could be calculated for 55 locations from 1960-2016, with 28 stations having coincident temperature and
754 precipitation data. It was found that storms have historically become more front-loaded, with storms also becoming
755 more front-loaded when the coincident temperature was higher. There is a strong regional pattern in the proportion of
756 front-loaded events, ranging from 50% of events in the south of Australia to close to 70% of events in the tropics.

757 Scaling relationships for the temporal patterns were found to be stronger when related to temperature rather than dew
758 point temperature.

759 The only study to directly calculate ARFs in the context of climate change is Li et al. (2015). In this work, ARFs were
760 calculated for the Sydney region using a high-resolution RCM. It was found that for 1hr storms ARFs would increase
761 (i.e., larger future storms) whilst for longer durations (6 to 72 hr) ARFs would decrease, with the largest decreases for
762 large catchment areas and the rarest events. But as this analysis was based on a single climate model applied over a
763 limited geographical domain it is not possible to generalise these results. Calculating ARFs from the RCM also
764 assumed that the point rainfall to 4 km² ARF would not change in the future (as 4 km² was the resolution of the RCM
765 so smaller area ARFs could not be calculated).

766 Other studies have analysed changes to spatial patterns of storms, but further work will be required to relate their
767 findings to methods such as ARFs used with design rainfalls. Wasko et al. (2016) found that the effective radius of
768 storms decreased with temperature at over 80% of the stations analysed in Australia using quantile regression for
769 storms above the 90th percentile. For stations classified as temperate, this decrease in effective radius was despite an
770 increase in peak precipitation, which suggested that moisture was being redistributed from the edge of the storms to
771 the centre. Li et al. (2018) reproduced these results for the Sydney region using RCM simulations. However, in both
772 studies the storms were limited to radii of 50 km and were assumed to be circular. Li et al. (2018) pointed out that
773 there were good opportunities to use RCM simulations to analyse changes in storm advection and not limiting the
774 analyses to circular storms.

775 Finally, Han et al. (2020) used copulas to analyse the spatial dependence of monthly maximum rainfalls. They found
776 that around 40% of the stations had decreasing trends in connectivity and that the overall average connectivity was
777 lower for storms associated with higher dewpoint temperatures, particularly in southern Australia. However, the
778 analyses were not seasonally stratified and therefore it is not clear if the findings could also be explained by the
779 seasonally different rainfall mechanisms. Although evidence is emerging for temporal and spatial clustering of storm
780 events both in Australia and globally (e.g., Chan et al., 2023; Chang et al., 2016; Ghanghas et al., 2023; Kahraman et
781 al., 2021; Tan and Shao, 2017), the evidence for changes in the spatial pattern of precipitation, compared to changes
782 in the temporal pattern of precipitation, remains weaker.

783 **4.3.5 Antecedent wetness**

784 **4.3.5.1 Impact of climate change**

785 When rainfall falls on a catchment, there is a range of different runoff processes that lead to catchment runoff and
786 subsequent streamflow. These runoff processes include infiltration excess or Hortonian overland flow, saturation
787 excess runoff, variable source area, partial area runoff, subsurface storm flow, and impervious area runoff. In
788 modelling these runoff processes in design flood estimation, the rainfall is partitioned into direct flow or runoff, which,
789 along with baseflow, contributes to the observed flood hydrograph, and rainfall losses that do not influence the flood
790 event's hydrograph. Rainfall losses primarily result from: 1) interception by vegetation and man-made surfaces which
791 are eventually evaporated 2) depression storage on the land surface ranging in size from soil-particle-sized depressions

792 to lakes; and 3) infiltrated water stored in the soil, which may later contribute to baseflow (Hill and Thomson, 2019;
793 Pilgrim and Cordery, 1993; O’Shea et al., 2021).

794 Physically, rainfall losses are largely influenced by antecedent soil moisture and soil properties, which govern the
795 hydraulic gradient of the soil and thus affect the rate of infiltration (Liu et al., 2011; Bennett et al., 2018). Antecedent
796 soil moisture is a strong modulator of the flood response (Tramblay et al., 2010; Pathiraja et al., 2012; Woldemeskel
797 and Sharma, 2016; Wasko et al., 2020; Brocca et al., 2009; Quintero et al., 2022) and is influenced by variability at
798 multi-annual and multi-decadal time scales (Kiem and Verdon-Kidd, 2013). Incorporating information regarding
799 antecedent soil moisture into loss models (refer Section 2) has also been shown to improve flood estimates (Cordery,
800 1970; Tramblay et al., 2010; Sunwoo and Choi, 2017; Bahramian et al., 2023); these loss models have been
801 incorporated into the Australia’s flood guidance (Hill et al., 2016).

802 To model the flood response in event-based flood routing models, it is necessary to conceptualise rainfall losses and
803 employ a mathematically explicit representation. More complex loss models, such as Horton’s method, conceptualise
804 the infiltration as decreasing exponentially as the soil saturates, whereas the Green-Ampt method assumes a sharp
805 wetting front exists in the soil column, separating a saturated upper soil layer from the underlying soil layer that
806 contains some initial moisture content (Rossman, 2010). Research has also explored the merits of hybrid methods
807 where continuous simulation is used to condition the initial state of the catchment before modelling the discrete flood
808 event using an event-based flood model (Heneker et al., 2003; Sheikh et al., 2009; Li et al., 2014; Yu et al., 2019;
809 Stephens et al., 2018a). Despite authors arguing that loss models should involve modelling physical representations
810 of the runoff process (Kemp and Daniell, 2016), there has been limited adoption in practice of more complex
811 approaches to loss modelling (Paquet et al., 2013). This is because the benefits of estimating rainfall losses relevant
812 to floods using physical process-based models are limited due to their complexity and incomplete understanding of
813 runoff generation processes as well as the inadequate availability of hydrological data (Pilgrim and Cordery, 1993).
814 For example, complex fully-distributed models often seek to resolve processes at spatial and temporal scales for which
815 data is limited or unavailable, and consequently such models are more liable to overfitting, leading to poor predictive
816 capabilities. As a result, parsimonious lumped models of rainfall loss are commonly employed.

817 Amongst the most used parsimonious lumped models of rainfall loss are the initial loss continuing loss model (ILCL),
818 the Probability Distributed Model (PDM), the Soil Conservation Service Curve Number (SCS-CN) and the initial loss
819 proportional loss (ILPL) model (Pilgrim and Cordery, 1993; O’Shea et al., 2021; US Army Corps of Engineers, 2000).
820 Broadly, these models divide losses into an initial loss, whereby all rainfall is infiltrated into the soil, up to a point at
821 which the hydrograph rises and the rainfall begins contributing to the runoff response and the loss becomes a fractional
822 amount of the rainfall. The parameters of these models are typically calibrated using historical rainfall and streamflow
823 data (e.g., Brown et al., 2022; Clayton, 2012; Gamage et al., 2015) with either a central tendency value (i.e., mean or
824 median), or a probabilistic distribution of loss parameters adopted for deterministic design flood estimation approaches
825 (Rahman et al., 2002; Zhang et al., 2023; Nathan et al., 2003; Gamage et al., 2013; Loveridge and Rahman, 2021;
826 Ishak and Rahman, 2006).

827 Under climate change, it has been shown that antecedent soil moisture is changing (Berg et al., 2017; Seneviratne et
 828 al., 2010; Wasko et al., 2021a) and will likely continue to change due to a range of factors. These factors include
 829 increased temperatures, increased rainfall variability, changes in drought duration and frequency (Ukkola et al., 2020),
 830 and changes to the persistence of large-scale ocean-atmospheric mechanisms such as increased persistence of La Niña
 831 (Geng et al., 2023). Any changes in the antecedent soil moisture due to climate change will impact on the resultant
 832 design flood estimate (Ivancic and Shaw, 2015; O’Shea et al., 2021; Quintero et al., 2022).

833 4.3.5.2 Systematic review

834 While there is ample evidence that climate change will alter antecedent soil moisture conditions, which in turn
 835 modulate flood responses and hence rainfall losses, there have been few studies quantifying how climate change will
 836 affect rainfall loss parameter values. A systematic review found several studies that have assessed the impact of trends
 837 in antecedent moisture conditions and rainfall losses on floods (Earl et al., 2023; Loveridge and Rahman, 2013).
 838 However, we found only two studies projecting rainfall losses, where overall rainfall losses (Ho et al., 2022) and
 839 rainfall loss parameters (Ho et al., 2023, 2022) were projected under climate change. These studies examined the
 840 relationships between total rainfall losses and the parameters of the ILCL rainfall loss model in relation to antecedent
 841 soil moisture in largely unregulated catchments across Australia. These studies focused on the ILCL model as it was
 842 found to be unbiased in modelling rarer events than those used in calibration, a common practice in design flood
 843 estimation (O’Shea et al., 2021). Ho et al. (2023) found a consistent negative linear relationship between the loss
 844 parameters and antecedent soil moisture, where increased antecedent soil moisture was associated with decreased
 845 losses. For locations where the relationships between the loss parameters and antecedent moisture conditions were
 846 statistically significant, projections of the loss parameter values were made using projections of antecedent soil
 847 moisture developed by the Australian Bureau of Meteorology (Srikanthan et al., 2022; Wilson et al., 2022; Vogel et
 848 al., 2023). On average, by the end of the century and under RCP 8.5, initial losses were projected to increase by
 849 5.0 mm (9%) with the interquartile range of the change from 3.3 to 6.3 mm (6%-12%). Continuing losses were
 850 projected to increase on average by 0.45 mm/hr (13%), with an interquartile range of the change of 0.18 to 0.6 mm/hr
 851 (8%-23%). To remain consistent with the meta-analysis methodology the above changes, on a per catchment basis,
 852 were standardised using global mean temperature and pooled across Natural Resource Management Regions (Figure
 853 S1, Figure S2). Following this, the scaling factors were pooled across RCP to produce the scaling rates shown in
 854 Table 2. Here it was deemed that the variability between regions (refer to Figure 2 from Ho et al. (2023)) was sufficient
 855 to respect regional differences, with events greater or equal to an annual maxima partial duration series adopted for
 856 the development of soil moisture-loss relationships.

857 **Table 2.** Median scaling factors for loss parameters together presented per degree global temperature change for
 858 clusters of Natural Resource Management Regions (CSIRO and Bureau of Meteorology, 2015), adapted from Ho et
 859 al. (2023). The ‘likely’ range (corresponding to ~66% range) is presented in parenthesis.

Natural Resource Management Region	IL (%/°C)	CL (%/°C)
Southern and South-Western Flatlands	4.5 (2.0-7.1)	5.6 (2.5-8.7)
Murray Basin	3.1 (1.0-5.7)	6.7 (1.5-12.1)
Southern Slopes	3.9 (1.5-7.2)	8.5 (2.9-15.7)

East Coast	2.0 (0.6-4.3)	3.8 (1.1-8.0)
Central Slopes	1.1 (0.4-2.2)	2.0 (-0.5-7.5)
Wet Tropics	0.8 (-0.4-2.0)	1.4 (-0.1-4.8)
Monsoonal North	2.4 (1.0-5.4)	4.4 (3.1-9.5)

860

861 **4.3.6 Sea level factors**

862 At the coastal terminus of a catchment, sea levels can modulate flooding, and hence incorporating the appropriate sea
863 level variations in the tail water boundary conditions is an important consideration for coastal and estuarine flood
864 modelling. Moreover, research has shown that extreme rainfall and storm surge processes are statistically dependent,
865 and therefore their interaction needs to be taken into account (Zheng et al., 2013). Here, the literature related to the
866 impact of climate change on factors related to sea level rise are briefly reviewed, but as changes in the sea level are
867 not covered in Australia’s flood estimation guidance (Bates et al., 2019), a systemic review was not performed.

868 Coastal sea levels vary due to multiple processes that operate on different time and space scales, ranging from
869 astronomical tides and storm surges to long-term sea-level rise due to global warming (McInnes et al., 2016).
870 Astronomical tides occur on a predictable and recurring basis, with relatively consistent frequency. Storm surges, on
871 the other hand, are less frequent and, because they occur in conjunction with severe weather events with low
872 atmospheric pressure, storm surge intensity is related to the strength of the storm. For coastal flooding, the same
873 weather systems that cause storm surges can also produce high rainfall totals and the potential for compound flooding
874 along the coast (Bevacqua et al., 2019; Collins et al., 2019; Zheng et al., 2013).

875 Both observed and modelled results (Wu et al., 2018; Zheng et al., 2013; Bevacqua et al., 2020) indicate that the
876 dependence between storm surges and extreme rainfalls is strongest in the north and northwest of Australia, followed
877 by the west and northeast of Australia. It is weak and/or statistically not significant on the northeastern tip of
878 Queensland, along the southeast coast of Western Australia, along small parts of the South Australian coastline, and
879 along the eastern part of the Victorian coast near Bass Strait. As the co-occurrence of extreme rainfall with extreme
880 storm surge is similar to the co-occurrence of runoff with storm surge (Bevacqua et al., 2020), methods for
881 incorporating this dependence are included in Australia’s flood guidance (Westra et al., 2019) – despite sea level
882 rise not being included. In the northern part of the continent, coincident extremes are most likely due to the occurrence
883 of tropical cyclones. Along the southwest and southern coastline, coincident extremes are most likely due to
884 extratropical lows and associated cold frontal systems during the winter half year. Along the southeast coast,
885 coincident events are most likely due to cut-off lows or frontal systems (Wu et al., 2018).

886 While studies have focussed on the coincidence of rainfall or runoff events with storm surges or storm tides, other
887 factors can also affect regional sea level variability on differing time scales. For example, coastally-trapped waves
888 (CTWs) can cause sea level variability along Australia’s extratropical coastline on timescales from weeks to months,
889 with amplitudes correlating with continental shelf width and ranging from 0.7 m along the south coast to 0.05–0.10 m
890 along the east coast (Eliot and Pattiaratchi, 2010; Woodham et al., 2013). In some locations, seasonal-scale sea level

891 variations are an important consideration. For example, the Gulf of Carpentaria experiences a significant annual sea
 892 level range of about 0.8 m, which is driven mainly by the seasonal reversal of the prevailing winds. On interannual
 893 time scales the El Niño-Southern Oscillation causes sea level variations with higher (lower) than average sea levels
 894 during La Niña's (El Niño's), which have a maximum range in the Gulf of Carpentaria and decrease in magnitude
 895 with distance anticlockwise around the coastline (White et al., 2014; McInnes et al., 2016).

896 Sea-level rise (SLR) is increasing the frequency of coastal flooding (Hague et al., 2023). Over the period from 2007
 897 to 2018 sea levels rose at an average rate of 3.6 ± 1.7 mm/yr based on a global network of tide gauge records, and
 898 3.8 ± 0.3 mm/yr based on satellite altimeters (Wang et al., 2021). Over the period 1993-2018 in the same two datasets,
 899 the rates of SLR were 0.063 ± 0.120 and 0.053 ± 0.026 mm/yr², respectively, indicating that SLR is accelerating
 900 (Wang et al., 2021). In Australia, the rate of SLR based on Australian gauges from the ANCHORS dataset, with at
 901 least 50 years of data over 1966 to 2019, was 1.94 mm/yr, and over 1993 to 2019 was 3.74 mm/yr (Hague et al., 2022).
 902 With the increase in the flood frequency over the observational record, mainly because SLR is increasing the height
 903 of the tides with ongoing SLR, flooding events will become increasingly predictable (Hague et al., 2023).

904 **Table 3.** Sea-level rise (m) relative to 1995-2014 for CMIP6 and associated likely (66%) confidence intervals
 905 (Source: Table 9.9 in Fox-Kemper et al. (2021)).

Scenario	2050	2100	2150
SSP1-1.9	0.18 (0.15-0.23)	0.38 (0.28–0.55)	0.57 (0.37–0.86)
SSP1-2.6	0.19 (0.16-0.25)	0.44 (0.32–0.62)	0.68 (0.46–0.99)
SSP2-4.5	0.20 (0.17-0.26)	0.56 (0.44–0.76)	0.92 (0.66–1.33)
SSP3-7.0	0.22 (0.18-0.27)	0.68 (0.55–0.90)	0.92 (0.66–1.33)
SSP5-8.5	0.23 (0.20-0.29)	0.77 (0.63–1.01)	1.98 (0.98–4.82)
SSP5-8.5*	0.24 (0.20-0.40)	0.88 (0.63–1.60)	1.98 (0.98–4.82)

906 *includes additional 'low confidence' processes

907 Projections of future SLR provided by the IPCC in its Sixth Assessment (AR6) report for a set of future greenhouse
 908 gas emission pathways termed SSPs (Fox-Kemper et al., 2021) are summarised for the years 2050, 2100 and 2150 in
 909 Table 3, along with their associated uncertainties. Note this only refers to mean sea level changes; processes associated
 910 with extreme sea levels such as storm surge and wave set-up that may be used in design flood estimation are not
 911 included. The processes included in the projections are assessed by the IPCC to be of '*medium confidence*' and include
 912 changes due to thermal expansion, the mass balance of glaciers and ice sheets, and terrestrial water storage. The IPCC
 913 also provide scenarios they assess with '*low confidence*' of occurring on the time scales considered, such as dynamical
 914 processes that could lead to more rapid disintegration of the ice sheets (DeConto and Pollard, 2016; Fox-Kemper et
 915 al., 2021).

916 Changes to weather and circulation patterns will also potentially change storm surge and wave patterns, altering
 917 compound flooding. For example, Colberg et al. (2019) investigated changes in extreme sea levels around Australia
 918 by forcing a hydrodynamic model with winds and surface pressure from four GCMs run with an RCP 8.5 emission
 919 scenario over the periods 1981-1991 and 2081–2099. The largest positive extreme sea-level changes were found over
 920 the Gulf of Carpentaria due to changes in the northwest monsoon, while mainly negative changes in seasonal

921 maximum sea levels up to -5.0 cm were found along Australia’s southern coastline due to the projected southward
922 movement of the subtropical ridge and associated cold frontal systems, with these results broadly consistent with other
923 studies (Colberg and McInnes, 2012; Vousdoukas et al., 2018). Extreme coastal sea levels are also affected by wave
924 breaking processes that cause wave setup (O’Grady et al., 2019), with the 1 in 100 AEP wave height projected to
925 increase by 5 to 15% over the Southern Ocean by the end of the 21st century (2081-2100), compared to the 1979–2005
926 period (Meucci et al., 2020). Finally, coastal erosion of sandy shorelines and estuaries under SLR will also contribute
927 to changes in coastal flooding patterns. Historical coastline movement around the Australian coast has been evaluated
928 through analysis of satellite images using a technique to filter satellite pixels to a consistent tide datum (Bishop-Taylor
929 et al., 2019, 2021). Over 22% of Australia’s non-rocky coastline shows trends of significant coastal retreat or growth
930 since 1988, with most change (15.8%) occurring at rates greater than 0.5 m/yr.

931 **5. Discussion**

932 From this systematic review on climate change science relevant to design flood estimation in Australia, it emerged
933 that most published research relates to changes in extreme rainfall intensity, and hence the IFDs and PMPs that are
934 used in event-based modelling. Here we aim to resolve the understanding of changes in extreme rainfall with
935 methodologies applied for design flood estimation. Following this, our methods are discussed, and finally factors that
936 were beyond the scope of this review are acknowledged and a summary of future research priorities is presented.

937 **5.1 Alignment of evidence for changes in extreme rainfall with design flood estimation**

938 Although we were unable to quantify the increases in extreme rainfall across a range of frequencies, studies using
939 rainfall-temperature scaling (Wasko and Sharma, 2017b), historical trends (Wasko and Nathan, 2019; Jayaweera et
940 al., 2023), and climate change projections (Pendergrass and Hartmann, 2014; Pendergrass, 2018; Carey-Smith et al.,
941 2018), all show that the rate of rainfall increase becomes greater with increasing rarity. Operational methods employed
942 to estimate PMPs are restricted to the consideration of thermodynamic increases in the moisture holding capacity
943 through changes in the moisture adjustment factor (Visser et al., 2022). However, short duration extremes (sub-daily)
944 have been shown to increase at rates greater than CC scaling both for Australia (presented herein) and globally (Fowler
945 et al., 2021). There is no obvious physical explanation for why changes to sub-daily PMP estimates should differ from
946 other studies on sub-daily extreme precipitation. Synthesising the evidence, it appears that (1) increases in rare long
947 duration rainfalls should plateau to a rate of increase commensurate with the PMP, which is likely to be increasing at
948 the CC rate for daily rainfall; and (2) increases in short duration PMPs, in the absence of research into changes in PMP
949 for sub-daily durations, should increase at the rate of short duration rainfall extremes. It is plausible that PMPs will
950 increase in line with short duration rainfall extremes due to an increase in storm efficiency, which is a well-established
951 mechanism in short duration rainfall due to latent heat release increasing buoyancy (Lenderink et al., 2019). Further,
952 increases in rainfall intensities above those simply owing to thermodynamics are also possible due to reductions in the
953 speed of lateral storm movement.

954 It is clear that increases in the order of 2-3 times the CC rate are a possibility for design rainfalls throughout Australia,
955 with greater potential increases in the north than in the south. This is generally related to the occurrence of convective
956 storms, such as severe thunderstorms that can cause short duration (e.g., less than about 6 hours) localised extreme

957 rainfall. Although current Australian climate modelling studies are generally not able to simulate the processes
958 relevant to these convective rainfall extremes, as they are not run at convection-permitting scales, the observation-
959 based increases are broadly consistent with theoretical expectations based on increased rainfall efficiency from
960 increased condensation for enhanced convection. Changes greater than the CC rate due to more efficient convective
961 processes can also be relevant for annual maxima longer than that of typical thunderstorms. For example, the highest
962 recorded daily rainfall at Adelaide occurred over a period of only two hours due to a thunderstorm (Ashcroft et al.
963 2019). This means that increases greater than the CC rate may also be plausible for more widespread and longer
964 duration rainfall extremes, such as multiday-duration events associated with TCs in near-coastal northern regions and
965 ECLs in eastern and south-eastern regions that sometimes contain deep moist convection (Callaghan and Power,
966 2014).

967 **5.2 Systematic review and meta-analysis considerations**

968 We have attempted to minimise biases where possible. Consistent with the IPCC methodologies, a multiple-lines-of-
969 evidence approach was adopted considering historical changes, future projections, and physical argumentation. As
970 such, inherent methodological biases, such as issues associated with hypothesis testing favouring the null hypothesis,
971 would only apply to a proportion of the evidence. Next, analyses to inform assessment reports such as the IPCC often
972 present projections separately from any claims of significance and are not required to demonstrate originality of
973 contribution; therefore, these studies are less likely to be affected by both the hypothesis testing and publication biases
974 - noting that hypothesis testing bias and publication bias would be expected to act in opposing ways. Finally, researcher
975 biases were addressed by having two researchers independently evaluate each reference for their area, and by adopting
976 a systematic review framework so that publications are not just chosen on the basis of a researcher's prior knowledge
977 or expectation. This was also addressed in the meta-analysis by sensitivity testing the results through multiple
978 researchers independently weighting evidence. The outcomes of the per-researcher analyses were consistently similar
979 (Table S3).

980 In addition to the review biases, the limitations of each line of empirical evidence need to be acknowledged. It can be
981 difficult to identify a climate change signal in observational records, firstly due to the small signal to noise ratio, but
982 secondly due to the difficulty of obtaining high quality instrumental data (Hall et al., 2014). For example, it is difficult
983 to detect a statistically significant change resulting from Clausius-Clapeyron scaling at a single rain gauge based on
984 observed warming rates and typical record lengths (Westra et al., 2013), such that the absence of a statistically
985 significant result does not necessarily imply the absence of a trend. Single site studies were hence given low weighting
986 in the meta-analysis. Further, it needs to be acknowledged that a historical trend can only be extrapolated to the future
987 by assuming the causal relationship remains unchanged, which may not be true (Wasko, 2022; Zhang et al., 2022).
988 The second line of evidence was the empirical relationship between day-to-day variability in rainfall and surface air
989 or dew-point temperature for high quantiles of the distribution. Although robust relationships have now been
990 established globally (Ali et al., 2018, 2021a, b), debate remains over the use of these scaling relationships for
991 projection as near-surface conditions may not reflect key factors in rainfall production, such as potential future changes
992 in the vertical temperature profile of the atmosphere or changes to rainfall efficiency. The limitations of the above two

993 sources of evidence can be somewhat overcome by the third line of evidence, that is, climate modelling which
994 explicitly models atmospheric conditions; however, it needs to be acknowledged that not all processes related to
995 rainfall are resolved (François et al., 2019). Global as well as many regional climate models have large spatial scales
996 compared to some of the physical processes associated with rainfall (e.g., localised convection) and struggle to
997 represent some aspects of rainfall occurrence (e.g., short-duration convective rainfall extremes, such as produced by
998 thunderstorms). Hence, recommendations here are based on an expert evaluation that has combined all the key lines
999 of evidence, recognising the known limitations of any single line of evidence.

1000 Many jurisdictions rely on the best and most up to date climate change estimates for their climate change flood
1001 guidance which may come from a single line of evidence such as climate modelling (Chan et al., 2023b; Wasko et al.,
1002 2021b). Using a single line of evidence such as climate modelling has the advantage of maintaining consistency in the
1003 evidence used for deriving uplift factors between storm durations, rarities, and across diverse climatic regions. Without
1004 consensus in Australia on the best line of evidence, the aim of the systematic review and meta-analysis was to translate
1005 existing scientific knowledge from multiple lines of evidence to practical flood guidance under climate change. Meta-
1006 analyses are common place in the medical sciences (Field and Gillett, 2010), but to date we are unaware of applications
1007 of meta-analyses in the assessment of changes to extreme rainfall due to climate change. The lack of standardised
1008 practices to reporting quantitative results including consistent approaches to reporting standard errors in the physical
1009 sciences (as opposed to medical sciences) represents a burden to performing meta-analyses. Here this was overcome
1010 by standardising individual lines of evidence on global temperature. However, combining individual studies relies on
1011 subjectivity of the experts involved in synthesising the available information. The authors involved in the meta-
1012 analysis represented a wide range of backgrounds including hydrology, climate science, and meteorology, with each
1013 individual adopting an independent method of synthesis. The similarity of the final best estimates of change between
1014 the individual authors gives credence to the robustness of the results (Table S3). This suggests the methods here could
1015 be used to synthesise available evidence for similar studies to transfer scientific knowledge to engineering guidance.

1016 **5.3 Factors omitted and recommendations for future work**

1017 This review focussed on a set of salient factors relevant to design flood estimation, and hence there are some aspects
1018 that are not covered. Australia has three small regions located in the south-east of the country that currently sustain
1019 snowpacks over the winter period: the Snowy Mountains region in southern New South Wales, the Victorian Alps,
1020 and the Tasmania highlands. Studies of the contribution of rain-on-snow events to flood risks have been undertaken
1021 using simple water budget approaches (Stephens et al., 2016; Nathan and Bowles, 1997). While rain-on-snow events
1022 dominated the generation of more frequent floods (≥ 1 in 50 AEP), they were less important for more extreme events.
1023 The key engineering design focus in these regions is related to the overtopping risks of hydroelectric dams; and as
1024 such, snowmelt floods are considered a localised issue for Australia and are not covered in the national flood guidelines
1025 (Ball et al., 2019a).

1026 Design flood practice in Australia, as elsewhere in the world, generally adopts areal lumped temporal patterns in
1027 combination with a fixed spatial pattern. The information available to characterise this variability is very limited and
1028 this dearth of evidence poses problems for design flood estimation under stationarity assumptions and limits our ability

1029 to estimate the impacts of climate change on flood risks. With climate change, it is important to correctly reflect
1030 changes in spatial and temporal correlation structures and transition probabilities, particularly for large catchments,
1031 which are sensitive to spatial variability in rainfalls, or for such applications as the design of linear infrastructure such
1032 as railways and major highways (Le et al., 2019). It can be expected that the only way the impacts of climate change
1033 can be considered on the spatio-temporal patterns of extreme rainfall is through a combination of physical modelling
1034 (e.g., Chang et al. 2016) and careful regional pooling (e.g., Visser et al. 2023). Finally, it is also worth noting that no
1035 attention is given to the impact of climate change on factors exogenous to storm climatic drivers. An example of this
1036 is the assessment of water levels in dams, or surcharge flooding from sewer networks. Climate change impacts for
1037 such assessments are the result of a complex mix of water demands and water management strategies (not to mention
1038 longer-term climatic conditions) that are not a function of storm events, with such analyses requiring tailored
1039 approaches for which it is difficult to provide general guidance.

1040 There is a need for guidance on how to perform flood frequency analysis and continuous simulation under climate
1041 change, but a lack of consensus remains on how best to perform these (Schlef et al., 2023). While non-stationary flood
1042 frequency analysis is an attractive prospect due to its use of observed flood data, extrapolating historical trends into
1043 the future is not justifiable. Rather, Faulkner et al. (2020) advise the use of non-stationary flood frequency analysis as
1044 a means for obtaining current day estimates. In the case of continuous simulation, stochastically generating reliable
1045 rainfall sequences remains challenging (Woldemeskel et al., 2016), and under climate change a standard approach for
1046 deriving rainfall time series remains a research priority (Dale, 2021). Recent research has shown that bias-correcting
1047 for changes to long-term persistence (interannual variability) is critical for climate change impact studies (Vogel et
1048 al., 2023; Robertson et al., 2023) and this should be considered moving forward. While event-based methods allow
1049 the adjustment of the primary flood drivers for climate change, a gap remains to understand under climate change
1050 which drivers the design flood estimate is most sensitive to, and hence which should be factored for climate change.
1051 Identifying the drivers with the strongest effects could be addressed by sensitivity/stress testing (Hannaford et al.,
1052 2023) or applying a storyline approach in flood estimation (de Bruijn et al., 2016; Shepherd et al., 2018; Hazeleger et
1053 al., 2015). This would require an understanding of the causal mechanisms of flood events which remains limited in
1054 Australia (Wasko and Guo, 2022).

1055 Finally, the development of climate models with the ability to resolve convection processes in other parts of the world
1056 (Chan et al., 2020, 2016) suggests the potential for improved simulations and projections of short duration rainfall
1057 extremes in Australia. Improved projections of short duration extreme rainfalls would be particularly valuable given
1058 the understanding that these events are increasing at a greater rate than long duration rainfalls. However, a substantial
1059 constraint to modelling convection processes are the computationally intensive modelling efforts required to cover the
1060 geographic expanse of Australia.

1061 **6. Summary and conclusions**

1062 This paper describes a review of the scientific literature as it relates to the impact of climate change on design flood
1063 estimation for Australia. To ensure the review is reproducible and to minimise the potential for bias, we adopted the

1064 framework of a systematic review. To be included, studies needed to pertain to either flood risk drivers or a measure
1065 of the flood hazard itself; how these are impacted on by climate change; and be relevant to Australia. As design flood
1066 estimation is undertaken using similar methods across the world, knowledge from relevant international research was
1067 included in addition to the systematic review, particularly in instances where local evidence was limited. The
1068 conclusions of this systematic review, as they relate to the methods for design flood estimation, are described below
1069 and summarised in Table 4:

- 1070 1. There is a general absence of a scientifically defensible methodology for performing flood frequency analysis
1071 in the context of projections for a future climate. The extrapolation of a historical temporal trend is not
1072 recommended, with many studies arguing that any non-stationary flood frequency analysis should ensure
1073 that the statistical model structure is representative of the processes controlling flooding. But as flood
1074 processes change with climate change, and with historical data likely to be influenced by other drivers such
1075 as land-use change, extrapolating historical trends into the future is not considered a viable method for
1076 developing future estimates of flood risk.
- 1077 2. The use of continuous simulation for flood frequency projections requires downscaling and bias-correction
1078 of GCM outputs to derive hydrologic inputs such as rainfall that represent a future climate. Due to the
1079 complexity in extracting GCM data and appropriately transforming the GCM data to the local scale,
1080 approaches of projecting flood frequency through continuous simulation are likely to, at least in the near
1081 term, remain limited to research applications. Dale (2021) notes that a standard approach for deriving time
1082 series rainfalls under climate change remains a research priority. If continuous simulation is to be applied,
1083 careful attention needs to be paid to ensuring downscaling and bias-correction methodologies accurately
1084 correct both extreme rainfall and long-term variability (persistence) characteristics that are important to
1085 hydrological applications (Vogel et al., 2023; Robertson et al., 2023).
- 1086 3. The primary input into event-based modelling is the IFD rainfall. The IPCC states that the frequency and
1087 intensity of heavy precipitation events have likely increased due to climate change (Seneviratne et al., 2023).
1088 Here we find that both daily and sub-daily rainfall are increasing with warming, with the rate of increase
1089 greater for shorter durations. Moreover, there is emerging evidence that the rarer the rainfall, the greater
1090 increase, and that increases in sub-daily rainfall extremes are greater in the tropics. However, there is
1091 currently not enough quantitative evidence across different exceedance probabilities or geographic zones to
1092 quantify projections of extreme rainfall across different regions of Australia.
- 1093 4. Both literature from Australia and across the world provides a consensus view that the PMP is likely
1094 increasing at the CC rate for daily rainfall. Despite no research on changes in the PMP at the sub-daily scale,
1095 it appears extreme rainfall increases plateau with increasing severity (Pendergrass, 2018). Hence, as storms
1096 intensify with climate change due to latent heat release, it can be assumed that changes above the CC scaling
1097 rate for the rarest of extreme rainfalls at the sub-daily scale can be taken as representative of changes to the
1098 PMP for similar durations.
- 1099 5. Evidence exists to suggest that temporal patterns will become more front loaded and intense with climate
1100 change, but evidence for changes in spatial patterns is not conclusive, with changes likely to vary with

1101 weather system. Currently, there is no adopted methodology for how to incorporate these changes into design
 1102 flood estimation, or assessment of the impact incorporating such changes will have on the design flood
 1103 estimate.

1104 6. With climate change, across Australia, catchment soil moisture conditions prior to an extreme rainfall event
 1105 are largely becoming drier and hence losses are projected to increase (Ho et al., 2023). These changes in
 1106 antecedent moisture conditions have been shown to modulate both historical and future frequent floods with
 1107 a lesser impact on rarer floods (Wasko and Nathan, 2019; Wasko et al., 2023).

1108 7. Sea levels have risen across Australia, impacting estuarine flooding, and resulting in much of Australia's
 1109 coastline retreating. With future increases in sea level projected with global warming, estuarine flooding
 1110 events will become increasingly predictable. However, the changes to the interaction between coastal sea
 1111 levels and pluvial riverine flooding remain poorly understood.

1112
 1113 **Table 4.** Conclusions of systematic review of climate change science relevant to Australian design flood
 1114 estimation.

Method	Quantity	Findings
Flood frequency analysis	Streamflow	No defensible methods were identified for factoring in climate change into flood frequency estimates.
Continuous simulation	Rainfall and evaporation	At present, there are limited studies that describe how to generate realistic time series of weather suitable for flood risk estimation. Further research is required before there is a continuous simulation method suitable for standard practice in design flood estimation.
Event-based estimation	Extreme rainfall (up to and including the PMP)	Heavy precipitation events have increased and will continue to increase due to climate change, with the highest rates of increase associated with short-duration rainfall. Australia-wide estimates (including a central estimate and 'likely' range) are provided in Table 1, varying by duration. Whilst there is reason to believe that scaling rates will vary both geographically (with higher rates in the north of Australia) and by exceedance probability (with higher rates for rarer events), insufficient evidence was available to quantify the differences in projected changes with location and AEP. It is, however, likely that these changes are within the uncertainty intervals provided in Table 1.
	Temporal patterns	Temporal patterns may become more front-loaded, with increases in peak intensities with climate change, but research on the impact of these changes on design flood estimation is lacking.
	Areal reduction factors	Evidence for changes in spatial patterns with climate change is not conclusive.
	Antecedent conditions	For Australia there is evidence of drying antecedent conditions, meaning increased losses in design flood estimation.
	Sea level interaction	Whilst there is significant evidence that sea levels are increasing and will continue to increase due to climate change, the changes to the interaction between high ocean levels (due to the combination of high astronomic tides and storm surges) and heavy rainfall events remains poorly understood.

1115

1116 To synthesise findings for changes in rainfall intensity quantitatively, a meta-analysis was performed. The uncertainty
1117 presented in the meta-analysis serves to demonstrate that a single line of evidence is not sufficient for deciding on the
1118 impact of climate change. As studies vary widely in the approaches and assumptions, multiple lines of evidence should
1119 be considered in decision making related to climate change, and the latest climate science reviewed in decision making.
1120 Although Australia is not a climatically homogenous nation, there does not exist enough information to distinguish
1121 extreme rainfall changes regionally, highlighting the need for continental-scale, high-resolution (convection-
1122 permitting) modelling efforts to help understand the impact of climate change on extreme rainfalls. Nevertheless, there
1123 is now a large body of work on changes to flood drivers as a result of climate change, and whilst significant uncertainty
1124 remains, this work can be used to form the basis for producing improved methods for defensible estimates of future
1125 flood risk.

1126 **Code availability**

1127 Code used to calculate warming levels can be found at https://github.com/traupach/warming_levels.

1128 **Author contribution**

1129 **CW** Conceptualization, Writing – original draft preparation. **SW** Conceptualization, Methodology, Writing –
1130 original draft preparation, Writing – review & editing. **RN** Conceptualization, Writing – original draft preparation.
1131 **AP** Writing – original draft preparation, Formal analysis. **TR** Writing – original draft preparation, Formal analysis.
1132 **AD** Writing – original draft preparation. **FJ** Writing – original draft preparation. **MH** Writing – original draft
1133 preparation. **KLM** Writing – original draft preparation. **DJ** Writing – review & editing. **JE** Writing – review &
1134 editing. **GV** Writing – review & editing. **HJF** Writing – review & editing.

1135 **Competing interests**

1136 The authors declare that they have no conflict of interest.

1137 **Acknowledgments**

1138 This work was supported by Department of Climate Change, Energy, the Environment and Water. Conrad Wasko
1139 acknowledges support from the Australian Research Council (DE210100479). Acacia Pepler, Andrew Dowdy, Jason
1140 Evans, Kathleen McInnes, and Timothy Raupach acknowledge funding from the Climate System Hub of the
1141 Australian National Environmental Science Program. Fiona Johnson is supported by the ARC Training Centre in Data
1142 Analytics for Resources and Environments (IC190100031).

1143 **References**

1144 Afzali-Gorouh, Z., Faridhosseini, A., Bakhtiari, B., Mosaedi, A., and Salehnia, N.: Monitoring and projection of
1145 climate change impact on 24-h probable maximum precipitation in the Southeast of Caspian Sea, *Nat. Hazards*, 114,
1146 77–99, <https://doi.org/10.1007/s11069-022-05380-1>, 2022.
1147 Agilan, V. and Umamahesh, N. V.: Detection and attribution of non-stationarity in intensity and frequency of daily
1148 and 4-h extreme rainfall of Hyderabad, India, *J. Hydrol.*, 530, 677–697,
1149 <https://doi.org/10.1016/j.jhydrol.2015.10.028>, 2015.
1150 Agilan, V. and Umamahesh, N. V.: What are the best covariates for developing non-stationary rainfall Intensity-
1151 Duration-Frequency relationship?, *Adv. Water Resour.*, 101, 11–22,
1152 <https://doi.org/10.1016/j.advwatres.2016.12.016>, 2017.
1153 Ahmed, A., Yildirim, G., Haddad, K., and Rahman, A.: Regional Flood Frequency Analysis: A Bibliometric
1154 Overview, *Water (Switzerland)*, 15, <https://doi.org/10.3390/w15091658>, 2023.

1155 Ben Alaya, M. A., Zwiers, F. W., and Zhang, X.: Probable maximum precipitation in a warming climate over North
1156 America in CanRCM4 and CRCM5, *Clim. Change*, 158, 611–629, <https://doi.org/10.1007/s10584-019-02591-7>,
1157 2020.

1158 Alexander, L. V. and Arblaster, J. M.: Historical and projected trends in temperature and precipitation extremes in
1159 Australia in observations and CMIP5, *Weather Clim. Extrem.*, 15, 34–56,
1160 <https://doi.org/10.1016/j.wace.2017.02.001>, 2017.

1161 Ali, H., Fowler, H. J., and Mishra, V.: Global Observational Evidence of Strong Linkage Between Dew Point
1162 Temperature and Precipitation Extremes, *Geophys. Res. Lett.*, 45, 320–330, <https://doi.org/10.1029/2018GL080557>,
1163 2018.

1164 Ali, H., Fowler, H. J., Lenderink, G., Lewis, E., and Pritchard, D.: Consistent Large-Scale Response of Hourly
1165 Extreme Precipitation to Temperature Variation Over Land, *Geophys. Res. Lett.*, 48, GRL61841,
1166 <https://doi.org/10.1029/2020GL090317>, 2021a.

1167 Ali, H., Peleg, N., and Fowler, H. J.: Global Scaling of Rainfall With Dewpoint Temperature Reveals Considerable
1168 Ocean-Land Difference, *Geophys. Res. Lett.*, 48, e2021GL093798, <https://doi.org/10.1029/2021GL093798>, 2021b.

1169 Allen, J. T., Karoly, D. J., and Walsh, K. J.: Future Australian Severe Thunderstorm Environments. Part II: The
1170 Influence of a Strongly Warming Climate on Convective Environments, *J. Clim.*, 27, 3848–3868,
1171 <https://doi.org/10.1175/JCLI-D-13-00426.1>, 2014.

1172 Allen, M. R. and Ingram, W. J.: Constraints on future changes in climate and the hydrologic cycle, *Nature*, 419,
1173 224–232, <https://doi.org/10.1038/nature01092>, 2002.

1174 Ayat, H., Evans, J. P., Sherwood, S. C., and Soderholm, J.: Intensification of subhourly heavy rainfall, *Science* (80-
1175), 378, 655–659, <https://doi.org/10.1126/science.abn8657>, 2022.

1176 Bahramian, K., Nathan, R., Western, A. W., and Ryu, D.: Probabilistic Conditioning and Recalibration of an Event-
1177 Based Flood Forecasting Model Using Real-Time Streamflow Observations, *J. Hydrol. Eng.*, 28, 04023003,
1178 [https://doi.org/10.1061/\(ASCE\)HE.1943-5584.0002236](https://doi.org/10.1061/(ASCE)HE.1943-5584.0002236), 2023.

1179 Ball, J., Babister, M., Nathan, R., Weeks, W., Wienmann, R., Retallick, M., and Testoni, I. (Eds.): Australian
1180 Rainfall and Runoff: A Guide to Flood Estimation, Commonwealth of Australia, 2019a.

1181 Ball, J., Babister, M., Retallick, M., and Weinmann, E.: Chapter 1. Introduction, Book 1: Scope and philosophy, in:
1182 Australian Rainfall and Runoff - A Guide to Flood Estimation, edited by: Ball, J., Babister, M., Nathan, R., Weeks,
1183 W., Weinmann, E., Retallick, M., and Testoni, I., Commonwealth of Australia, 2019b.

1184 Ball, J. E.: The influence of storm temporal patterns on catchment response, *J. Hydrol.*, 158, 285–303,
1185 [https://doi.org/10.1016/0022-1694\(94\)90058-2](https://doi.org/10.1016/0022-1694(94)90058-2), 1994.

1186 Bao, J., Sherwood, S. C., Alexander, L. V., and Evans, J. P.: Future increases in extreme precipitation exceed
1187 observed scaling rates, *Nat. Clim. Chang.*, 7, 128–132, <https://doi.org/10.1038/nclimate3201>, 2017.

1188 Barbero, R., Westra, S., Lenderink, G., and Fowler, H. J.: Temperature-extreme precipitation scaling: a two-way
1189 causality?, *Int. J. Climatol.*, 38, e1274–e1279, <https://doi.org/10.1002/joc.5370>, 2017.

1190 Bates, B., McLuckie, D., Westra, S., Johnson, F., Green, J., Mummery, J., and Abbs, D.: Chapter 6. Climate Change
1191 Considerations, Book 1: Scope and Philosophy, in: Australian Rainfall and Runoff - A Guide to Flood Estimation,
1192 edited by: Ball, J., Babister, M., Nathan, R., Weinmann, E., Retallick, M., and Testoni, I., Commonwealth of
1193 Australia, 2019.

1194 Bates, B. C., Chandler, R. E., and Dowdy, A. J.: Estimating trends and seasonality in Australian monthly lightning
1195 flash counts, *J. Geophys. Res. Atmos.*, 120, 3973–3983, <https://doi.org/10.1002/2014JD023011>, 2015.

1196 Beauchamp, J., Leconte, R., Trudel, M., and Brissette, F.: Estimation of the summer-fall PMP and PMF of a
1197 northern watershed under a changed climate, *Water Resour. Res.*, 49, 3852–3862,
1198 <https://doi.org/10.1002/wrcr.20336>, 2013.

1199 Bell, S. S., Chand, S. S., Tory, K. J., Dowdy, A. J., Turville, C., and Ye, H.: Projections of southern hemisphere
1200 tropical cyclone track density using CMIP5 models, *Clim. Dyn.*, 52, 6065–6079, [https://doi.org/10.1007/s00382-](https://doi.org/10.1007/s00382-018-4497-4)
1201 018-4497-4, 2019.

1202 Bennett, B., Leonard, M., Deng, Y., and Westra, S.: An empirical investigation into the effect of antecedent
1203 precipitation on flood volume, *J. Hydrol.*, 567, 435–445, <https://doi.org/10.1016/j.jhydrol.2018.10.025>, 2018.

1204 Berg, A., Sheffield, J., and Milly, P. C. D.: Divergent surface and total soil moisture projections under global
1205 warming, *Geophys. Res. Lett.*, 44, 236–244, <https://doi.org/10.1002/2016GL071921>, 2017.

1206 Bergemann, M., Lane, T. P., Wales, S., Narsey, S., and Louf, V.: High-resolution simulations of tropical island
1207 thunderstorms: Does an increase in resolution improve the representation of extreme rainfall?, *Q. J. R. Meteorol.*
1208 *Soc.*, 148, 3303–3318, <https://doi.org/10.1002/qj.4360>, 2022.

1209 Berghuijs, W. R. and Slater, L. J.: Groundwater shapes North American river floods, *Environ. Res. Lett.*, 18,
1210 034043, <https://doi.org/10.1088/1748-9326/acbecc>, 2023.

1211 Bevacqua, E., Maraun, D., Vousdoukas, M. I., Voukouvalas, E., Vrac, M., Mentaschi, L., and Widmann, M.: Higher
1212 probability of compound flooding from precipitation and storm surge in Europe under anthropogenic climate
1213 change, *Sci. Adv.*, 5, eaaw5531, <https://doi.org/10.1126/sciadv.aaw5531>, 2019.

1214 Bevacqua, E., Vousdoukas, M. I., Shepherd, T. G., and Vrac, M.: Brief communication: The role of using
1215 precipitation or river discharge data when assessing global coastal compound flooding, *Nat. Hazards Earth Syst.*
1216 *Sci.*, 20, 1765–1782, <https://doi.org/10.5194/nhess-20-1765-2020>, 2020.

1217 Bhatia, K., Vecchi, G., Murakami, H., Underwood, S., and Kossin, J.: Projected Response of Tropical Cyclone
1218 Intensity and Intensification in a Global Climate Model, *J. Clim.*, 31, 8281–8303, <https://doi.org/10.1175/JCLI-D-17-0898.1>, 2018.

1220 Bishop-Taylor, R., Sagar, S., Lymburner, L., and Beaman, R. J.: Between the tides: Modelling the elevation of
1221 Australia’s exposed intertidal zone at continental scale, *Estuar. Coast. Shelf Sci.*, 223, 115–128,
1222 <https://doi.org/10.1016/j.ecss.2019.03.006>, 2019.

1223 Bishop-Taylor, R., Nanson, R., Sagar, S., and Lymburner, L.: Mapping Australia’s dynamic coastline at mean sea
1224 level using three decades of Landsat imagery, *Remote Sens. Environ.*, 267, 112734,
1225 <https://doi.org/10.1016/j.rse.2021.112734>, 2021.

1226 Black, A. S., Risbey, J. S., Chapman, C. C., Monselesan, D. P., Moore II, T. S., Pook, M. J., Richardson, D., Sloyan,
1227 B. M., Squire, D. T., and Tozer, C. R.: Australian Northwest Cloudbands and Their Relationship to Atmospheric
1228 Rivers and Precipitation, *Mon. Weather Rev.*, 149, 1125–1139, <https://doi.org/10.1175/MWR-D-20-0308.1>, 2021.

1229 Climate Change in Australia: <https://www.climatechangeinaustralia.gov.au/en/communication-resources/reports/>.

1230 Boughton, W. and Droop, O.: Continuous simulation for design flood estimation—a review, *Environ. Model.*
1231 *Softw.*, 18, 309–318, [https://doi.org/10.1016/S1364-8152\(03\)00004-5](https://doi.org/10.1016/S1364-8152(03)00004-5), 2003.

1232 Brocca, L., Melone, F., Moramarco, T., and Singh, V. P.: Assimilation of Observed Soil Moisture Data in Storm
1233 Rainfall-Runoff Modeling, *J. Hydrol. Eng.*, 14, 153–165, [https://doi.org/10.1061/\(ASCE\)1084-0699\(2009\)14:2\(153\)](https://doi.org/10.1061/(ASCE)1084-0699(2009)14:2(153)), 2009.

1234

1235 Brown, A. and Dowdy, A.: Severe Convective Wind Environments and Future Projected Changes in Australia, *J.*
1236 *Geophys. Res. Atmos.*, 126, e2021JD034633, <https://doi.org/10.1029/2021JD034633>, 2021.

1237 Brown, I. W., McDougall, K., Alam, M. J., Chowdhury, R., and Chadalavada, S.: Calibration of a continuous
1238 hydrologic simulation model in the urban Gowrie Creek catchment in Toowoomba, Australia, *J. Hydrol. Reg. Stud.*,
1239 40, 101021, <https://doi.org/10.1016/j.ejrh.2022.101021>, 2022.

1240 de Bruijn, K. M., Lips, N., Gersonius, B., and Middelkoop, H.: The storyline approach: a new way to analyse and
1241 improve flood event management, *Nat. Hazards*, 81, 99–121, <https://doi.org/10.1007/s11069-015-2074-2>, 2016.

1242 Bruyère, C. L., Done, J. M., Jaye, A. B., Holland, G. J., Buckley, B., Henderson, D. J., Leplastrier, M., and Chan, P.:
1243 Physically-based landfalling tropical cyclone scenarios in support of risk assessment, *Weather Clim. Extrem.*, 26,
1244 100229, <https://doi.org/10.1016/j.wace.2019.100229>, 2019.

1245 Bui, A., Johnson, F., and Wasko, C.: The relationship of atmospheric air temperature and dew point temperature to
1246 extreme rainfall, *Environ. Res. Lett.*, 14, 074025, <https://doi.org/10.1088/1748-9326/ab2a26>, 2019.

1247 Bureau of Meteorology: Guidebook of the Estimation of Probable Maximum Precipitation: Generalised Tropical
1248 Storm Method, Hydrometeorological Advisory Service, 2003.

1249 Assessment Reports: <https://awo.bom.gov.au/about/overview/assessment-reports#regionsandreports>.

1250 Callaghan, J. and Power, S. B.: Major coastal flooding in southeastern Australia 1860–2012, associated deaths and
1251 weather systems, *Aust. Meteorol. Oceanogr. J.*, 64, 183–213, 2014.

1252 Carey-Smith, T., Henderson, R., and Singh, S.: High Intensity Rainfall Design System Version 4, NIWA Client Rep.
1253 2018022CH, 2018.

1254 Cavicchia, L., Pepler, A., Dowdy, A., Evans, J., Di Luca, A., and Walsh, K.: Future Changes in the Occurrence of
1255 Hybrid Cyclones: The Added Value of Cyclone Classification for the East Australian Low-Pressure Systems,
1256 *Geophys. Res. Lett.*, 47, e2019GL085751, <https://doi.org/10.1029/2019GL085751>, 2020.

1257 Chan, S. C., Kendon, E. J., Roberts, N. M., Fowler, H. J., and Blenkinsop, S.: The characteristics of summer sub-
1258 hourly rainfall over the southern UK in a high-resolution convective permitting model, *Environ. Res. Lett.*, 11,
1259 094024, <https://doi.org/10.1088/1748-9326/11/9/094024>, 2016.

1260 Chan, S. C., Kendon, E. J., Berthou, S., Fosser, G., Lewis, E., and Fowler, H. J.: Europe-wide precipitation
1261 projections at convection permitting scale with the Unified Model, *Clim. Dyn.*, 55, 409–428,
1262 <https://doi.org/10.1007/s00382-020-05192-8>, 2020.

1263 Chan, S. C., Kendon, E. J., Fowler, H. J., Kahraman, A., Crook, J., Ban, N., and Prein, A. F.: Large-scale dynamics
1264 moderate impact-relevant changes to organised convective storms, *Commun. Earth Environ.*, 4, 8,
1265 <https://doi.org/10.1038/s43247-022-00669-2>, 2023a.

1266 Chan, S. C., Kendon, E. J., Fowler, H. J., Youngman, B. D., Dale, M., and Short, C.: New extreme rainfall
1267 projections for improved climate resilience of urban drainage systems, *Clim. Serv.*, 30, 100375,
1268 <https://doi.org/10.1016/j.cliser.2023.100375>, 2023b.

1269 Chand, S. S., Dowdy, A. J., Ramsay, H. A., Walsh, K. J. E., Tory, K. J., Power, S. B., Bell, S. S., Lavender, S. L.,
1270 Ye, H., and Kuleshov, Y.: Review of tropical cyclones in the Australian region: Climatology, variability,
1271 predictability, and trends, *WIREs Clim. Chang.*, 10, e602, <https://doi.org/10.1002/wcc.602>, 2019.

1272 Chand, S. S., Walsh, K. J. E., Camargo, S. J., Kossin, J. P., Tory, K. J., Wehner, M. F., Chan, J. C. L., Klotzbach, P.
1273 J., Dowdy, A. J., Bell, S. S., Ramsay, H. A., and Murakami, H.: Declining tropical cyclone frequency under global
1274 warming, *Nat. Clim. Chang.*, 12, 655–661, <https://doi.org/10.1038/s41558-022-01388-4>, 2022.

1275 Chang, W., Stein, M. L., Wang, J., Kotamarthi, V. R., and Moyer, E. J.: Changes in spatiotemporal precipitation
1276 patterns in changing climate conditions, *J. Clim.*, 29, 8355–8376, <https://doi.org/10.1175/JCLI-D-15-0844.1>, 2016.

1277 Chegwiddden, Oriana, S., Rupp, D. E., and Nijssen, B.: Climate change alters flood magnitudes and mechanisms in
1278 climatically-diverse headwaters across the northwestern United States, *Environ. Res. Lett.*, 15, 094048,
1279 <https://doi.org/10.1088/1748-9326/ab986f>, 2020.

1280 Chen, H., Sun, J., and Chen, X.: Projection and uncertainty analysis of global precipitation-related extremes using
1281 CMIP5 models, *Int. J. Climatol.*, 34, 2730–2748, <https://doi.org/10.1002/joc.3871>, 2014.

1282 Chen, X., Hossain, F., and Leung, L. R.: Probable Maximum Precipitation in the U.S. Pacific Northwest in a
1283 Changing Climate, *Water Resour. Res.*, 53, 9600–9622, <https://doi.org/10.1002/2017WR021094>, 2017.

1284 Chen, Y.-R., Yu, B., and Jenkins, G.: Secular variation in rainfall and intensity–frequency–duration curves in
1285 Eastern Australia, *J. Water Clim. Chang.*, 4, 244–251, <https://doi.org/10.2166/wcc.2013.138>, 2013.

1286 Chevuturi, A., Klingaman, N. P., Turner, A. G., and Hannah, S.: Projected Changes in the Asian-Australian
1287 Monsoon Region in 1.5°C and 2.0°C Global-Warming Scenarios, *Earth’s Futur.*, 6, 339–358,
1288 <https://doi.org/10.1002/2017EF000734>, 2018.

1289 Chow, V., Maidment, D., and Mays, L.: *Applied Hydrology*, McGraw-Hill, Singapore, 572 pp., 1988.

1290 Clavet-Gaumont, J., Huard, D., Frigon, A., Koenig, K., Slota, P., Rousseau, A., Klein, I., Thiémonge, N., Houdré,
1291 F., Perdikaris, J., Turcotte, R., Lafleur, J., and Larouche, B.: Probable maximum flood in a changing climate: An
1292 overview for Canadian basins, *J. Hydrol. Reg. Stud.*, 13, 11–25, <https://doi.org/10.1016/j.ejrh.2017.07.003>, 2017.

1293 Clayton, A.: Revision of hydrological design loss rates for the central and eastern Kimberley region of western
1294 Australia, in: 34th Hydrology and Water Resources Symposium, 947–953, 2012.

1295 Colberg, F. and McInnes, K. L.: The impact of future changes in weather patterns on extreme sea levels over
1296 southern Australia, *J. Geophys. Res. Ocean.*, 117, C08001, <https://doi.org/10.1029/2012JC007919>, 2012.

1297 Colberg, F., McInnes, K. L., O’Grady, J., and Hoeke, R.: Atmospheric circulation changes and their impact on
1298 extreme sea levels around Australia, *Nat. Hazards Earth Syst. Sci.*, 19, 1067–1086, <https://doi.org/10.5194/nhess-19-1067-2019>, 2019.

1300 Collins, M., Sutherland, M., Bouwer, L., Cheong, S.-M., Frölicher, T., Combes, H. J. Des, Roxy, M. K., Losada, I.,
1301 McInnes, K., Ratter, B., Rivera-Arriaga, E., Susanto, R. D., Swingedouw, D., and Tibig, L.: Extremes, Abrupt
1302 Changes and Managing Risk, in: IPCC Special Report on the Ocean and Cryosphere in a Changing Climate, edited
1303 by: Pörtner, H.-O., Roberts, D. C., Masson-Delmotte, V., Zhai, P., Tigno, M., Poloczanska, E., Mintenbeck, K.,
1304 Alegría, A., Nicolai, M., Okem, A., Petzold, J., Rama, B., and Weyer, N. M., [in press], 2019.

1305 Condon, L. E., Gangopadhyay, S., and Pruitt, T.: Climate change and non-stationary flood risk for the upper
1306 Truckee River basin, *Hydrol. Earth Syst. Sci.*, 19, 159–175, <https://doi.org/10.5194/hess-19-159-2015>, 2015.

1307 Contractor, S., Donat, M. G., and Alexander, L. V.: Intensification of the Daily Wet Day Rainfall Distribution
1308 Across Australia, *Geophys. Res. Lett.*, 45, 8568–8576, <https://doi.org/10.1029/2018GL078875>, 2018.

1309 Cordery, I.: Antecedent wetness for design flood estimation, *Civ. Eng. Trans. Inst. Eng. Aust.*, 12, 181–185, 1970.

1310 CSIRO and Bureau of Meteorology: Climate Change in Australia Projections for Australia’s Natural Resource
1311 Management Regions: Technical Report, 2015.

1312 Cyphers, L., Sutton, A., Hopkinson, L. C., and Quaranta, J. D.: Probable Maximum Precipitation Evaluation for a
1313 West Virginia Watershed, United States, *J. Hydrol. Eng.*, 27, 04022014, [https://doi.org/10.1061/\(ASCE\)HE.1943-5584.0002191](https://doi.org/10.1061/(ASCE)HE.1943-5584.0002191), 2022.

1315 Dale, M.: Managing the effects of extreme sub-daily rainfall and flash floods - A practitioner’s perspective, *Philos.*
1316 *Trans. R. Soc. A Math. Phys. Eng. Sci.*, 379, 20190550, <https://doi.org/10.1098/rsta.2019.0550>, 2021.

1317 Dare, R. A., Davidson, N. E., and McBride, J. L.: Tropical Cyclone Contribution to Rainfall over Australia, *Mon.*
1318 *Weather Rev.*, 140, 3606–3619, <https://doi.org/10.1175/MWR-D-11-00340.1>, 2012.

1319 DeConto, R. M. and Pollard, D.: Contribution of Antarctica to past and future sea-level rise, *Nature*, 531, 591–597,
1320 <https://doi.org/10.1038/nature17145>, 2016.

1321 Dey, R., Lewis, S. C., Arblaster, J. M., and Abram, N. J.: A review of past and projected changes in Australia’s
1322 rainfall, *Wiley Interdiscip. Rev. Clim. Chang.*, 10, e577, <https://doi.org/10.1002/wcc.577>, 2019.

1323 Dowdy, A. J.: Long-term changes in Australian tropical cyclone numbers, *Atmos. Sci. Lett.*, 15, 292–298,
1324 <https://doi.org/10.1002/asl2.502>, 2014.

1325 Dowdy, A. J.: Climatology of thunderstorms, convective rainfall and dry lightning environments in Australia, *Clim.*
1326 *Dyn.*, 54, 3041–3052, <https://doi.org/10.1007/s00382-020-05167-9>, 2020.

1327 Dowdy, A. J. and Catto, J. L.: Extreme weather caused by concurrent cyclone, front and thunderstorm occurrences,
1328 *Sci. Rep.*, 7, 40359, <https://doi.org/10.1038/srep40359>, 2017.

1329 Dowdy, A. J., Pepler, A., Di Luca, A., Cavicchia, L., Mills, G., Evans, J. P., Louis, S., McInnes, K. L., and Walsh,
1330 K.: Review of Australian east coast low pressure systems and associated extremes, *Clim. Dyn.*, 53, 4887–4910,
1331 <https://doi.org/10.1007/s00382-019-04836-8>, 2019.

1332 Du, H., Alexander, L. V., Donat, M. G., Lippmann, T., Srivastava, A., Salinger, J., Kruger, A., Choi, G., He, H. S.,
1333 Fujibe, F., Rusticucci, M., Nandintsetseg, B., Manzanas, R., Rehman, S., Abbas, F., Zhai, P., Yabi, I., Stambaugh,
1334 M. C., Wang, S., Batbold, A., Oliveira, P. T., Adrees, M., Hou, W., Zong, S., Santos e Silva, C. M., Lucio, P. S., and
1335 Wu, Z.: Precipitation From Persistent Extremes is Increasing in Most Regions and Globally, *Geophys. Res. Lett.*,
1336 46, 6041–6049, <https://doi.org/10.1029/2019GL081898>, 2019.

1337 Earl, N., Remenyi, T. A., King, A., Love, P. T., Rollins, D., and Harris, R. M. B.: Changing compound rainfall
1338 events in Tasmania, *Int. J. Climatol.*, 43, 538–557, <https://doi.org/10.1002/joc.7791>, 2023.

1339 Eliot, M. and Pattiaratchi, C.: Remote forcing of water levels by tropical cyclones in southwest Australia, *Cont.*
1340 *Shelf Res.*, 30, 1549–1561, <https://doi.org/10.1016/j.csr.2010.06.002>, 2010.

1341 Emanuel, K.: A fast intensity simulator for tropical cyclone risk analysis, *Nat. Hazards*, 88, 779–796,
1342 <https://doi.org/10.1007/s11069-017-2890-7>, 2017.

1343 England, J. F., Sankovich, V. L., and Caldwell, R. J.: Review of probable maximum precipitation procedures and
1344 databases used to develop hydrometeorological reports, 2020.

1345 England, J. F. J., Cohn, T. A., Faber, B. A., Stedinger, J. R., Thomas, W. O. J., Veilleux, A. G., Kiang, J. E., and
1346 Mason, R.R., J.: Guidelines for Determining Flood Flow Frequency Bulletin 17C, in: U.S. Geological Survey
1347 Techniques and Methods, 148, <https://doi.org/https://doi.org/10.3133/tm4B5>, 2019.

1348 Faulkner, D., Warren, S., Spencer, P., and Sharkey, P.: Can we still predict the future from the past? Implementing
1349 non-stationary flood frequency analysis in the UK, *J. Flood Risk Manag.*, 13, e12582,
1350 <https://doi.org/10.1111/jfr3.12582>, 2020.

1351 Field, A. P. and Gillett, R.: How to do a meta-analysis, *Br. J. Math. Stat. Psychol.*, 63, 665–694,
1352 <https://doi.org/10.1348/000711010X502733>, 2010.

1353 Fowler, H. J., Blenkinsop, S., and Tebaldi, C.: Linking climate change modelling to impacts studies: recent advances
1354 in downscaling techniques for hydrological modelling, *Int. J. Climatol.*, 27, 1547–1578,
1355 <https://doi.org/10.1002/joc.1556>, 2007.

1356 Fowler, H. J., Lenderink, G., Prein, A. F., Westra, S., Allan, R. P., Ban, N., Barbero, R., Berg, P., Blenkinsop, S.,
1357 Do, H. X., Guerreiro, S., Haerter, J. O., Kendon, E. J., Lewis, E., Schaer, C., Sharma, A., Villarini, G., Wasko, C.,
1358 and Zhang, X.: Anthropogenic intensification of short-duration rainfall extremes, *Nat. Rev. Earth Environ.*, 2, 107–
1359 122, <https://doi.org/10.1038/s43017-020-00128-6>, 2021.

1360 Fox-Kemper, B., Hewitt, H. T., Xiao, C., Aðalgeirsdóttir, G., Drijfhout, S. S., Edwards, T. L., Golledge, N. R.,
1361 Hemer, M., Kopp, R. E., Krinner, G., Mix, A., Notz, D., Nowicki, S., Nurhati, I. S., Ruiz, L., Sallée, J.-B., Slangen,
1362 A. B. A., and Yu, Y.: Ocean, Cryosphere and Sea Level Change, in: *Climate Change 2021: The Physical Science*
1363 *Basis. Contribution of Working Group I to the Sixth Assessment Report of the Intergovernmental Panel on Climate*
1364 *Change*, edited by: Masson-Delmotte, V., P.Zhai, Pirani, A., Connors, S. L., Péan, C., Berger, S., Caud, N., Chen,
1365 Y., Goldfarb, L., Gomis, M. I., Huang, M., Leitzell, K., Lonnoy, E., Matthews, J. B. R., Maycock, T. K., Waterfield,
1366 T., Yelekçi, O., Yu, R., and Zhou, B., Cambridge University Press, Cambridge, United Kingdom and New York,
1367 NY, USA, 1211–1362, <https://doi.org/10.1017/9781009157896.011>, 2021.

1368 François, B., Schlef, K. E., Wi, S., and Brown, C. M.: Design considerations for riverine floods in a changing
1369 climate – A review, *J. Hydrol.*, 574, 557–573, <https://doi.org/10.1016/j.jhydrol.2019.04.068>, 2019.

1370 Franks, S. and Kuczera, G.: Flood frequency analysis: Evidence and implications of secular climate variability, *New*

1371 South Wales, *Water Resour. Res.*, 38, 20-1-20–7, <https://doi.org/10.1029/2001WR000232>, 2002.

1372 Frost, A. J. ., Ramchurn, A. ., and Smith, A. .: The Australian landscape water balance model (AWRA-L v6).
1373 Technical Description of the Australian Water Resources Assessment Landscape model version 6., Melbourne,
1374 Australia, 50 pp., 2018.

1375 Fu, G., Chiew, F. H. S., and Post, D. A.: Trends and variability of rainfall characteristics influencing annual
1376 streamflow: A case study of southeast Australia, *Int. J. Climatol.*, 43, 1407–1430, <https://doi.org/10.1002/joc.7923>,
1377 2023.

1378 Gamage, S. H. P. W., Hewa, G. A., and Beecham, S.: Probability distributions for explaining hydrological losses in
1379 South Australian catchments, *Hydrol. Earth Syst. Sci.*, 17, 4541–4553, <https://doi.org/10.5194/hess-17-4541-2013>,
1380 2013.

1381 Gamage, S. H. P. W., Hewa, G. A., and Beecham, S.: Modelling hydrological losses for varying rainfall and
1382 moisture conditions in South Australian catchments, *J. Hydrol. Reg. Stud.*, 4, 1–21,
1383 <https://doi.org/10.1016/j.ejrh.2015.04.005>, 2015.

1384 Gangrade, S., Kao, S., Naz, B. S., Rastogi, D., Ashfaq, M., Singh, N., and Preston, B. L.: Sensitivity of Probable
1385 Maximum Flood in a Changing Environment, *Water Resour. Res.*, 54, 3913–3936,
1386 <https://doi.org/10.1029/2017WR021987>, 2018.

1387 Geng, T., Jia, F., Cai, W., Wu, L., Gan, B., Jing, Z., Li, S., and McPhaden, M. J.: Increased occurrences of
1388 consecutive La Niña events under global warming, *Nature*, 619, 774–781, <https://doi.org/10.1038/s41586-023-06236-9>, 2023.

1390 Ghanghas, A., Sharma, A., Dey, S., and Merwade, V.: How Is Spatial Homogeneity in Precipitation Extremes
1391 Changing Globally?, *Geophys. Res. Lett.*, 50, e2023GL103233, <https://doi.org/10.1029/2023GL103233>, 2023.

1392 Grose, M. R., Narsey, S., Delage, F. P., Dowdy, A. J., Bador, M., Boschat, G., Chung, C., Kajtar, J. B., Rauniyar, S.,
1393 Freund, M. B., Lyu, K., Rashid, H., Zhang, X., Wales, S., Trenham, C., Holbrook, N. J., Cowan, T., Alexander, L.,
1394 Arblaster, J. M., and Power, S.: Insights From CMIP6 for Australia’s Future Climate, *Earth’s Futur.*, 8,
1395 e2019EF001469, <https://doi.org/10.1029/2019EF001469>, 2020.

1396 Gründemann, G. J., van de Giesen, N., Brunner, L., and van der Ent, R.: Rarest rainfall events will see the greatest
1397 relative increase in magnitude under future climate change, *Commun. Earth Environ.*, 3,
1398 <https://doi.org/10.1038/s43247-022-00558-8>, 2022.

1399 Gu, X., Zhang, Q., Li, J., Liu, J., Xu, C. Y., and Sun, P.: The changing nature and projection of floods across
1400 Australia, *J. Hydrol.*, 584, 124703, <https://doi.org/10.1016/j.jhydrol.2020.124703>, 2020.

1401 Gu, X., Ye, L., Xin, Q., Zhang, C., Zeng, F., Nerantzaki, S. D., and Papalexiou, S. M.: Extreme Precipitation in
1402 China: A Review on Statistical Methods and Applications, *Adv. Water Resour.*, 163, 104144,
1403 <https://doi.org/10.1016/j.advwatres.2022.104144>, 2022.

1404 Guerreiro, S. B., Fowler, H. J., Barbero, R., Westra, S., Lenderink, G., Blenkinsop, S., Lewis, E., and Li, X.-F.:
1405 Detection of continental-scale intensification of hourly rainfall extremes, *Nat. Clim. Chang.*, 8, 803–807,
1406 <https://doi.org/10.1038/s41558-018-0245-3>, 2018.

1407 Guo, S., Xiong, L., Chen, J., Guo, S., Xia, J., Zeng, L., and Xu, C. Y.: Nonstationary Regional Flood Frequency
1408 Analysis Based on the Bayesian Method, *Water Resour. Manag.*, 37, 659–681, <https://doi.org/10.1007/s11269-022-03394-9>, 2023.

1410 Gutiérrez, J. M., Jones, R. G., Narisma, G. T., Alves, L. M., Amjad, M., Gorodetskaya, I. ., Grose, M., Klutse, N. A.
1411 B., Krakovska, S., Li, J., Martínez-Castro, D., Mearns, L. O., Mernild, S. H., Ngo-Duc, T., Hurk, B. van den, and
1412 Yoon, J.-H.: Atlas, in: *Climate Change 2021: The Physical Science Basis. Contribution of Working Group I to the*
1413 *Sixth Assessment Report of the Intergovernmental Panel on Climate Change*, edited by: Masson-Delmotte, V., Zhai,
1414 P., Pirani, A., Connors, S. L., Péan, C., Berger, S., Caud, N., Chen, Y., Goldfarb, L., Gomis, M. I., Huang, M.,
1415 Leitzell, K., Lonnoy, E., Matthews, J. B. R., T.K.Maycock, Waterfield, T., Yelekçi, O., Yu, R., and Zhou, B.,
1416 Cambridge University Press, 2021.

1417 Hague, B. S., Jones, D. A., Jakob, D., McGregor, S., and Reef, R.: Australian Coastal Flooding Trends and Forcing
1418 Factors, *Earth’s Futur.*, 10, e2021EF002483, <https://doi.org/10.1029/2021EF002483>, 2022.

1419 Hague, B. S., Grayson, R. B., Talke, S. A., Black, M. T., and Jakob, D.: The effect of tidal range and mean sea-level
1420 changes on coastal flood hazards at Lakes Entrance, south-east Australia, *J. South. Hemisph. Earth Syst. Sci.*,
1421 <https://doi.org/10.1071/ES22036>, 2023.

1422 Hajani, E. and Rahman, A.: Characterizing changes in rainfall: a case study for New South Wales, Australia, *Int. J.*
1423 *Climatol.*, 38, 1452–1462, <https://doi.org/10.1002/joc.5258>, 2018.

1424 Hakala, K., Addor, N., Teutschbein, C., Vis, M., Dakhlaoui, H., and Seibert, J.: Hydrological Modeling of Climate

1425 Change Impacts, in: *Encyclopedia of water: Science, technology, and society*, John Wiley & Sons, Inc,
1426 <https://doi.org/10.1002/9781119300762.wsts0062>, 2019.

1427 Hall, J., Arheimer, B., Borga, M., Brázdil, R., Claps, P., Kiss, A., Kjeldsen, T. R., Kriaučiūnienė, J., Kundzewicz, Z.
1428 W., Lang, M., Llasat, M. C., Macdonald, N., McIntyre, N., Mediero, L., Merz, B., Merz, R., Molnar, P., Montanari,
1429 A., Neuhold, C., Parajka, J., Perdigão, R. A. P., Plavcová, L., Rogger, M., Salinas, J. L., Sauquet, E., Schär, C.,
1430 Szolgay, J., Viglione, A., and Blöschl, G.: Understanding flood regime changes in Europe: a state-of-the-art
1431 assessment, *Hydrol. Earth Syst. Sci.*, 18, 2735–2772, <https://doi.org/10.5194/hess-18-2735-2014>, 2014.

1432 Han, X., Mehrotra, R., and Sharma, A.: Measuring the spatial connectivity of extreme rainfall, *J. Hydrol.*, 590,
1433 <https://doi.org/10.1016/j.jhydrol.2020.125510>, 2020.

1434 Han, X., Mehrotra, R., Sharma, A., and Rahman, A.: Incorporating nonstationarity in regional flood frequency
1435 analysis procedures to account for climate change impact, *J. Hydrol.*, 612, 128235,
1436 <https://doi.org/10.1016/j.jhydrol.2022.128235>, 2022.

1437 Hannaford, J., Mackay, J. D., Ascott, M., Bell, V. A., Chitson, T., Cole, S., Counsell, C., Durant, M., Jackson, C. R.,
1438 Kay, A. L., Lane, R. A., Mansour, M., Moore, R., Parry, S., Rudd, A. C., Simpson, M., Facer-Childs, K., Turner, S.,
1439 Wallbank, J. R., Wells, S., and Wilcox, A.: The enhanced future Flows and Groundwater dataset: development and
1440 evaluation of nationally consistent hydrological projections based on UKCP18, *Earth Syst. Sci. Data*, 15, 2391–
1441 2415, <https://doi.org/10.5194/essd-15-2391-2023>, 2023.

1442 Hazeleger, W., Van Den Hurk, B. J. J. M., Min, E., Van Oldenborgh, G. J., Petersen, A. C., Stainforth, D. A.,
1443 Vasileiadou, E., and Smith, L. A.: Tales of future weather, *Nat. Clim. Chang.*, 5, 107–113,
1444 <https://doi.org/10.1038/nclimate2450>, 2015.

1445 Hempel, S., Frieler, K., Warszawski, L., Schewe, J., and Piontek, F.: A trend-preserving bias correction – the ISI-
1446 MIP approach, *Earth Syst. Dyn.*, 4, 219–236, <https://doi.org/10.5194/esd-4-219-2013>, 2013.

1447 Heneker, T. M., Lambert, M. F., and Kuczera, G.: Overcoming the joint probability problem associated with initial
1448 loss estimation in design flood estimation, *Australas. J. Water Resour.*, 7, 101–109,
1449 <https://doi.org/10.1080/13241583.2003.11465233>, 2003.

1450 Herath, S. M., Sarukkalgige, P. R., and Nguyen, V. T. Van: A spatial temporal downscaling approach to development
1451 of IDF relations for Perth airport region in the context of climate change, *Hydrol. Sci. J.*, 61, 2061–2070,
1452 <https://doi.org/10.1080/02626667.2015.1083103>, 2016.

1453 Herold, N., Downes, S. M., Gross, M. H., Ji, F., Nishant, N., Macadam, I., Ridder, N. N., and Beyer, K.: Projected
1454 changes in the frequency of climate extremes over southeast Australia, *Environ. Res. Commun.*, 3, 011001,
1455 <https://doi.org/10.1088/2515-7620/abe6b1>, 2021.

1456 Herrera, R. V., Blenkinsop, S., Guerreiro, S. B., and Fowler, H. J.: The creation and climatology of a large
1457 independent rainfall event database for Great Britain, *Int. J. Climatol.*, 10.1002/joc.8187,
1458 <https://doi.org/10.1002/joc.8187>, 2023.

1459 Hersbach, H., Bell, B., Berrisford, P., Hirahara, S., Horányi, A., Muñoz-Sabater, J., Nicolas, J., Peubey, C., Radu,
1460 R., Schepers, D., Simmons, A., Soci, C., Abdalla, S., Abellan, X., Balsamo, G., Bechtold, P., Biavati, G., Bidlot, J.,
1461 Bonavita, M., Chiara, G., Dahlgren, P., Dee, D., Diamantakis, M., Dragani, R., Flemming, J., Forbes, R., Fuentes,
1462 M., Geer, A., Haimberger, L., Healy, S., Hogan, R. J., Hólm, E., Janisková, M., Keeley, S., Laloyaux, P., Lopez, P.,
1463 Lupu, C., Radnoti, G., Rosnay, P., Rozum, I., Vamborg, F., Villaume, S., and Thépaut, J.: The ERA5 global
1464 reanalysis, *Q. J. R. Meteorol. Soc.*, 146, 1999–2049, <https://doi.org/10.1002/qj.3803>, 2020.

1465 Hershfield, D. M.: Method for Estimating Probable Maximum Rainfall, *J. Am. Water Works Assoc.*, 57, 965–972,
1466 <https://doi.org/10.1002/j.1551-8833.1965.tb01486.x>, 1965.

1467 Hill, P. and Thomson, R.: Chapter 3. Losses, Book 5: Flood Hydrograph Estimation:, in: *Australian Rainfall and
1468 Runoff - A Guide to Flood Estimation*, edited by: Ball, J., Babister, M., Nathan, R., Weinmann, E., Retallick, M.,
1469 and Testoni, I., Commonwealth of Australia, 2019.

1470 Hill, P., Nathan, R., and Zhang, J.: Application of AWRA-L gridded soil moisture data for flood estimation, in: *37th
1471 Hydrology and Water Resources Symposium 2016: Water, Infrastructure and the Environment*, 179–186, 2016.

1472 Hitchcock, S. M., Lane, T. P., Warren, R. A., and Soderholm, J. S.: Linear Rainfall Features and Their Association
1473 with Rainfall Extremes near Melbourne, Australia, *Mon. Weather Rev.*, 149, 3401–3417,
1474 <https://doi.org/10.1175/MWR-D-21-0007.1>, 2021.

1475 Ho, M., Nathan, R., Wasko, C., Vogel, E., and Sharma, A.: Projecting changes in flood event runoff coefficients
1476 under climate change, *J. Hydrol.*, 615, 128689, <https://doi.org/10.1016/j.jhydrol.2022.128689>, 2022.

1477 Ho, M., Wasko, C., O’Shea, D., Nathan, R., Vogel, E., and Sharma, A.: Changes in flood-associated rainfall losses
1478 under climate change, *J. Hydrol.*, 625, 129950, <https://doi.org/10.1016/j.jhydrol.2023.129950>, 2023.

1479 Holland, G. and Bruyère, C. L.: Recent intense hurricane response to global climate change, *Clim. Dyn.*, 42, 617–
1480 627, <https://doi.org/10.1007/s00382-013-1713-0>, 2014.

1481 Holland, G. J., Lynch, A. H., and Leslie, L. M.: Australian East-Coast Cyclones. Part I: Synoptic Overview and
1482 Case Study, *Mon. Weather Rev.*, 115, 3024–3036, [https://doi.org/10.1175/1520-0493\(1987\)115<3024:AECCPI>2.0.CO;2](https://doi.org/10.1175/1520-0493(1987)115<3024:AECCPI>2.0.CO;2), 1987.

1484 Hosking, J. R. M. and Wallis, J. R.: *Regional Frequency Analysis*, Cambridge University Press,
1485 <https://doi.org/10.1017/CBO9780511529443>, 1997.

1486 Institute of Hydrology: *Flood Estimation Handbook* (five volumes), Centre for Ecology & Hydrology, 1999.

1487 Ishak, E. and Rahman, A.: Investigation into probabilistic nature of continuing loss in four catchments in Victoria,
1488 in: *30th Hydrology & Water Resources Symposium: Past, Present & Future*, 432–437, 2006.

1489 Ishak, E., Rahman, A., Westra, S., Sharma, A., and Kuczera, G.: Trend analysis of Australian annual maximum flood
1490 data: Exploring relationship with climate and catchment characteristics, *Hydrol. Water Resour. Symp. 2014*, HWRS
1491 2014 - Conf. Proc., 445–452, 2014.

1492 Ishak, E. H., Rahman, A., Westra, S., Sharma, A., and Kuczera, G.: Evaluating the non-stationarity of Australian
1493 annual maximum flood, *J. Hydrol.*, 494, 134–145, <https://doi.org/10.1016/j.jhydrol.2013.04.021>, 2013.

1494 Ishida, K., Ohara, N., Kavvas, M. L., Chen, Z. Q., and Anderson, M. L.: Impact of air temperature on physically-
1495 based maximum precipitation estimation through change in moisture holding capacity of air, *J. Hydrol.*, 556, 1050–
1496 1063, <https://doi.org/10.1016/j.jhydrol.2016.10.008>, 2018.

1497 Ivancic, T. J. and Shaw, S. B.: Examining why trends in very heavy precipitation should not be mistaken for trends
1498 in very high river discharge, *Clim. Change*, 133, 681–693, <https://doi.org/10.1007/s10584-015-1476-1>, 2015.

1499 Jain, S. K. and Singh, V. P.: *Water resources systems planning and management*, Elsevier, 2003.

1500 Jakob, D., Smalley, R., Meighen, J., Xuereb, K., and Taylor, B.: *Climate change and probable maximum
1501 precipitation*, Melbourne, 179 pp., 2009.

1502 Jayaweera, L., Wasko, C., Nathan, R., and Johnson, F.: Non-stationarity in extreme rainfalls across Australia, *J.
1503 Hydrol.*, 624, 129872, <https://doi.org/10.1016/j.jhydrol.2023.129872>, 2023.

1504 Ju, J., Wu, C., Yeh, P. J.-F., Dai, H., and Hu, B. X.: Global precipitation-related extremes at 1.5 °C and 2 °C of
1505 global warming targets: Projection and uncertainty assessment based on the CESM-LWR experiment, *Atmos. Res.*,
1506 264, 105868, <https://doi.org/10.1016/j.atmosres.2021.105868>, 2021.

1507 Kahraman, A., Kendon, E. J., Chan, S. C., and Fowler, H. J.: Quasi-Stationary Intense Rainstorms Spread Across
1508 Europe Under Climate Change, *Geophys. Res. Lett.*, 48, e2020GL092361, <https://doi.org/10.1029/2020GL092361>,
1509 2021.

1510 Kawagoe, S. and Sarukkalgige, R.: Estimation of probable maximum precipitation at three provinces in Northeast
1511 Vietnam using historical data and future climate change scenarios, *J. Hydrol. Reg. Stud.*, 23, 100599,
1512 <https://doi.org/10.1016/j.ejrh.2019.100599>, 2019.

1513 Kemp, D. and Daniell, T.: Stuck in the 1960s - the need for fundamental change in flood hydrology in Australia, in:
1514 *37th Hydrology & Water Resources Symposium 2016: Water, Infrastructure and the Environment*, 220–227, 2016.

1515 Kemp, D., Loffler, T., and Daniell, T.: The strange case of first creek - If the flood doesn't fit the curve should the
1516 curve fit the flood?, *30th Hydrol. Water Resour. Symp. HWRS 2006*, 2020.

1517 Kendon, E. J., Ban, N., Roberts, N. M., Fowler, H. J., Roberts, M. J., Chan, S. C., Evans, J. P., Fosser, G., and
1518 Wilkinson, J. M.: Do convection-permitting regional climate models improve projections of future precipitation
1519 change?, *Bull. Am. Meteorol. Soc.*, 98, 79–93, <https://doi.org/10.1175/BAMS-D-15-0004.1>, 2017.

1520 Kiem, A. S. and Verdon-Kidd, D. C.: The importance of understanding drivers of hydroclimatic variability for
1521 robust flood risk planning in the coastal zone, *Australas. J. Water Resour.*, 17, 126–134,
1522 <https://doi.org/10.7158/W13-015.2013.17.2>, 2013.

1523 Kim, H. and Villarini, G.: On the attribution of annual maximum discharge across the conterminous United States,
1524 *Adv. Water Resour.*, 171, 104360, <https://doi.org/10.1016/j.advwatres.2022.104360>, 2023.

1525 Knutson, T., Camargo, S. J., Chan, J. C. L., Emanuel, K., Ho, C.-H., Kossin, J., Mohapatra, M., Satoh, M., Sugi, M.,
1526 Walsh, K., and Wu, L.: *Tropical Cyclones and Climate Change Assessment: Part I: Detection and Attribution*, *Bull.
1527 Am. Meteorol. Soc.*, 100, 1987–2007, <https://doi.org/10.1175/BAMS-D-18-0189.1>, 2019.

1528 Knutson, T., Camargo, S. J., Chan, J. C. L., Emanuel, K., Ho, C.-H., Kossin, J., Mohapatra, M., Satoh, M., Sugi, M.,
1529 Walsh, K., and Wu, L.: *Tropical Cyclones and Climate Change Assessment: Part II: Projected Response to
1530 Anthropogenic Warming*, *Bull. Am. Meteorol. Soc.*, 101, E303–E322, <https://doi.org/10.1175/BAMS-D-18-0194.1>,
1531 2020.

1532 Kossin, J. P.: A global slowdown of tropical-cyclone translation speed, *Nature*, 558, 104–107,

1533 <https://doi.org/10.1038/s41586-018-0158-3>, 2018.

1534 Kossin, J. P., Emanuel, K. A., and Vecchi, G. A.: The poleward migration of the location of tropical cyclone
1535 maximum intensity, *Nature*, 509, 349–352, <https://doi.org/10.1038/nature13278>, 2014.

1536 Kossin, J. P., Knapp, K. R., Olander, T. L., and Velden, C. S.: Global increase in major tropical cyclone exceedance
1537 probability over the past four decades, *Proc. Natl. Acad. Sci.*, 117, 11975–11980,
1538 <https://doi.org/10.1073/pnas.1920849117>, 2020.

1539 Krysanova, V., Donnelly, C., Gelfan, A., Gerten, D., Arheimer, B., Hattermann, F., and Kundzewicz, Z. W.: How
1540 the performance of hydrological models relates to credibility of projections under climate change, *Hydrol. Sci. J.*,
1541 63, 696–720, <https://doi.org/10.1080/02626667.2018.1446214>, 2018.

1542 Kundzewicz, Z. W. and Stakhiv, E. Z.: Are climate models “ready for prime time” in water resources management
1543 applications, or is more research needed?, *Hydrol. Sci. J.*, 55, 1085–1089,
1544 <https://doi.org/10.1080/02626667.2010.513211>, 2010.

1545 Kunkel, K. E., Karl, T. R., Easterling, D. R., Redmond, K., Young, J., Yin, X., and Hennon, P.: Probable maximum
1546 precipitation and climate change, *Geophys. Res. Lett.*, 40, 1402–1408, <https://doi.org/10.1002/grl.50334>, 2013.

1547 Labonté-Raymond, P.-L., Pabst, T., Bussière, B., and Bresson, É.: Impact of climate change on extreme rainfall
1548 events and surface water management at mine waste storage facilities, *J. Hydrol.*, 590, 125383,
1549 <https://doi.org/10.1016/j.jhydrol.2020.125383>, 2020.

1550 Lagos-Zúñiga, M. A. and Vargas M., X.: PMP and PMF estimations in sparsely-gauged Andean basins and climate
1551 change projections, *Hydrol. Sci. J.*, 59, 2027–2042, <https://doi.org/10.1080/02626667.2013.877588>, 2014.

1552 Lanzante, J. R.: Uncertainties in tropical-cyclone translation speed, *Nature*, 570, E6–E15,
1553 <https://doi.org/10.1038/s41586-019-1223-2>, 2019.

1554 Lavender, S. L. and Abbs, D. J.: Trends in Australian rainfall: contribution of tropical cyclones and closed lows,
1555 *Clim. Dyn.*, 40, 317–326, <https://doi.org/10.1007/s00382-012-1566-y>, 2013.

1556 Lawrence, D. and Hisdal, H.: Hydrological projections for floods in Norway under a future climate, NVE Report,
1557 Middelthunsgate 29, 47 pp., 2011.

1558 Laz, O. U., Rahman, A., Yilmaz, A., and Haddad, K.: Trends in sub-hourly, sub-daily and daily extreme rainfall
1559 events in eastern Australia, *J. Water Clim. Chang.*, 5, 667–675, <https://doi.org/10.2166/wcc.2014.035>, 2014.

1560 Le, P. D., Leonard, M., and Westra, S.: Spatially dependent flood probabilities to support the design of civil
1561 infrastructure systems, *Hydrol. Earth Syst. Sci.*, 23, 4851–4867, <https://doi.org/10.5194/hess-23-4851-2019>, 2019.

1562 Lee, K. and Singh, V. P.: Analysis of uncertainty and non-stationarity in probable maximum precipitation in Brazos
1563 River basin, *J. Hydrol.*, 590, 125526, <https://doi.org/10.1016/j.jhydrol.2020.125526>, 2020.

1564 Lee, O., Park, Y., Kim, E. S., and Kim, S.: Projection of Korean Probable Maximum Precipitation under Future
1565 Climate Change Scenarios, *Adv. Meteorol.*, 2016, 3818236, <https://doi.org/10.1155/2016/3818236>, 2016.

1566 Lee, O., Sim, I., and Kim, S.: Application of the non-stationary peak-over-threshold methods for deriving rainfall
1567 extremes from temperature projections, *J. Hydrol.*, 585, 124318, <https://doi.org/10.1016/j.jhydrol.2019.124318>,
1568 2020.

1569 Lenderink, G., Belušić, D., Fowler, H. J., Kjellström, E., Lind, P., van Meijgaard, E., van Ulft, B., and de Vries, H.:
1570 Systematic increases in the thermodynamic response of hourly precipitation extremes in an idealized warming
1571 experiment with a convection-permitting climate model, *Environ. Res. Lett.*, 14, 074012,
1572 <https://doi.org/10.1088/1748-9326/ab214a>, 2019.

1573 Li, J., Thyer, M., Lambert, M., Kuczera, G., and Metcalfe, A.: An efficient causative event-based approach for
1574 deriving the annual flood frequency distribution, *J. Hydrol.*, 510, 412–423,
1575 <https://doi.org/10.1016/j.jhydrol.2013.12.035>, 2014.

1576 Li, J., Sharma, A., Johnson, F., and Evans, J.: Evaluating the effect of climate change on areal reduction factors
1577 using regional climate model projections, *J. Hydrol.*, 528, 419–434, <https://doi.org/10.1016/j.jhydrol.2015.06.067>,
1578 2015.

1579 Li, J., Wasko, C., Johnson, F., Evans, J. P., and Sharma, A.: Can Regional Climate Modeling Capture the Observed
1580 Changes in Spatial Organization of Extreme Storms at Higher Temperatures?, *Geophys. Res. Lett.*, 45, 4475–4484,
1581 <https://doi.org/10.1029/2018GL077716>, 2018.

1582 Liang, S., Wang, D., Ziegler, A. D., Li, L. Z. X., and Zeng, Z.: Madden–Julian Oscillation-induced extreme rainfalls
1583 constrained by global warming mitigation, *npj Clim. Atmos. Sci.*, 5, 67, [https://doi.org/10.1038/s41612-022-00291-](https://doi.org/10.1038/s41612-022-00291-1)
1584 1, 2022.

1585 Lighthill, J., Zheng, Z., Holland, G. J., and Emanuel, K. (Eds.): Tropical Cyclone Disasters, in: Proceedings of the
1586 ICSU/WMO International Symposium, 588, 1993.

1587 Linacre, E. and Geerts, B.: *Climates & Weather Explained*, Routledge, London; New York, 432 pp., 1997.

1588 Liu, H., Lei, T. W., Zhao, J., Yuan, C. P., Fan, Y. T., and Qu, L. Q.: Effects of rainfall intensity and antecedent soil
1589 water content on soil infiltrability under rainfall conditions using the run off-on-out method, *J. Hydrol.*, 396, 24–32,
1590 <https://doi.org/10.1016/j.jhydrol.2010.10.028>, 2011.

1591 Liu, J., Wu, D., Li, Y., Ren, H., Zhao, Y., Sun, X., Zhang, H., and Ji, M.: Spatiotemporal variation of precipitation
1592 on a global scale from 1960 to 2016 in a new normalized daily precipitation dataset, *Int. J. Climatol.*, 42, 3648–
1593 3665, <https://doi.org/10.1002/joc.7437>, 2022a.

1594 Liu, T., Li, B., Jin, L., Wang, S., Wen, J., and Wang, H.: Estimation of probable maximum precipitation of a high-
1595 mountain basin in a changing climate, *Hydrol. Res.*, 53, 221–240, <https://doi.org/10.2166/nh.2021.084>, 2022b.

1596 Loveridge, M. and Rahman, A.: Trend analysis of rainfall losses using an event-based hydrological model in eastern
1597 NSW, in: *20th International Congress on Modelling and Simulation*, 2013.

1598 Loveridge, M. and Rahman, A.: Effects of Probability-Distributed Losses on Flood Estimates Using Event-Based
1599 Rainfall-Runoff Models, *Water*, 13, 2049, <https://doi.org/10.3390/w13152049>, 2021.

1600 Magan, B., Kim, S., Wasko, C., Barbero, R., Moron, V., Nathan, R., and Sharma, A.: Impact of atmospheric
1601 circulation on the rainfall-temperature relationship in Australia, *Environ. Res. Lett.*, 15, 094098,
1602 <https://doi.org/10.1088/1748-9326/abab35>, 2020.

1603 Mantegna, G. A., White, C. J., Remenyi, T. A., Corney, S. P., and Fox-Hughes, P.: Simulating sub-daily Intensity-
1604 Frequency-Duration curves in Australia using a dynamical high-resolution regional climate model, *J. Hydrol.*, 554,
1605 277–291, <https://doi.org/10.1016/j.jhydrol.2017.09.025>, 2017.

1606 McInnes, K. L., White, C. J., Haigh, I. D., Hemer, M. A., Hoeke, R. K., Holbrook, N. J., Kiem, A. S., Oliver, E. C.
1607 J., Ranasinghe, R., Walsh, K. J. E., Westra, S., and Cox, R.: Natural hazards in Australia: sea level and coastal
1608 extremes, *Clim. Change*, 139, 69–83, <https://doi.org/10.1007/s10584-016-1647-8>, 2016.

1609 McMahon, G. M. and Kiem, A. S.: Large floods in South East Queensland, Australia: Is it valid to assume they
1610 occur randomly?, *Aust. J. Water Resour.*, 22, 4–14, <https://doi.org/10.1080/13241583.2018.1446677>, 2018.

1611 Meucci, A., Young, I. R., Hemer, M., Kirezci, E., and Ranasinghe, R.: Projected 21st century changes in extreme
1612 wind-wave events, *Sci. Adv.*, 6, eaaz7295, <https://doi.org/10.1126/sciadv.aaz7295>, 2020.

1613 Mills, G., Webb, R., Davidson, N. E., Kepert, J., Seed, A., and Abbs, D.: The Pasha Bulker east coast low of 8 June
1614 2007, 2010.

1615 Milly, P. C. D., Betancourt, J., Falkenmark, M., Hirsch, R. M., Kundzewicz, Z. W., Lettenmaier, D. P., and Stouffer,
1616 R. J.: CLIMATE CHANGE: Stationarity Is Dead: Whither Water Management?, *Science (80-.)*, 319, 573–574,
1617 <https://doi.org/10.1126/science.1151915>, 2008.

1618 Moon, I.-J., Kim, S.-H., and Chan, J. C. L.: Climate change and tropical cyclone trend, *Nature*, 570, E3–E5,
1619 <https://doi.org/10.1038/s41586-019-1222-3>, 2019.

1620 Musselman, K. N., Lehner, F., Ikeda, K., Clark, M. P., Prein, A. F., Liu, C., Barlage, M., and Rasmussen, R.:
1621 Projected increases and shifts in rain-on-snow flood risk over western North America, *Nat. Clim. Chang.*, 8, 808–
1622 812, <https://doi.org/10.1038/s41558-018-0236-4>, 2018.

1623 Nathan, R., Weinmann, E., and Hill, P.: Use of Monte Carlo Simulation to Estimate the Expected Probability of
1624 Large to Extreme Floods, in: *Hydrology and Water Resources Symposium*, 105–112, 2003.

1625 Nathan, R. J. and Bowles, D. S.: A Probability-Neutral Approach to the Estimation of Design Snowmelt Floods, in:
1626 *Hydrology and Water Resources Symposium: Wai-Whenua*, 125–130, 1997.

1627 Neri, A., Villarini, G., Slater, L. J., and Napolitano, F.: On the statistical attribution of the frequency of flood events
1628 across the U.S. Midwest, *Adv. Water Resour.*, 127, 225–236, <https://doi.org/10.1016/j.advwatres.2019.03.019>, 2019.

1629 O’Grady, J. G., McInnes, K. L., Hemer, M. A., Hoeke, R. K., Stephenson, A. G., and Colberg, F.: Extreme Water
1630 Levels for Australian Beaches Using Empirical Equations for Shoreline Wave Setup, *J. Geophys. Res. Ocean.*, 124,
1631 5468–5484, <https://doi.org/10.1029/2018JC014871>, 2019.

1632 O’Shea, D., Nathan, R., Wasko, C., and Hill, P.: Implications of event-based loss model structure on simulating
1633 large floods, *J. Hydrol.*, 595, 126008, <https://doi.org/10.1016/j.jhydrol.2021.126008>, 2021.

1634 Osburn, L., Hope, P., and Dowdy, A.: Changes in hourly extreme precipitation in victoria, Australia, from the
1635 observational record, *Weather Clim. Extrem.*, 31, 100294, <https://doi.org/10.1016/j.wace.2020.100294>, 2021.

1636 Page, M. J., McKenzie, J. E., Bossuyt, P. M., Boutron, I., Hoffmann, T. C., Mulrow, C. D., Shamseer, L., Tetzlaff, J.
1637 M., Akl, E. A., Brennan, S. E., Chou, R., Glanville, J., Grimshaw, J. M., Hróbjartsson, A., Lalu, M. M., Li, T.,
1638 Loder, E. W., Mayo-Wilson, E., McDonald, S., McGuinness, L. A., Stewart, L. A., Thomas, J., Tricco, A. C.,
1639 Welch, V. A., Whiting, P., and Moher, D.: The PRISMA 2020 statement: an updated guideline for reporting
1640 systematic reviews, *BMJ*, 372, n71, <https://doi.org/10.1136/bmj.n71>, 2021.

1641 Paquet, E., Garavaglia, F., Garçon, R., and Gailhard, J.: The SCHADEX method: A semi-continuous rainfall–runoff
1642 simulation for extreme flood estimation, *J. Hydrol.*, 495, 23–37, <https://doi.org/10.1016/j.jhydrol.2013.04.045>, 2013.

1643 Parker, C. L., Bruyère, C. L., Mooney, P. A., and Lynch, A. H.: The response of land-falling tropical cyclone
1644 characteristics to projected climate change in northeast Australia, *Clim. Dyn.*, 51, 3467–3485,
1645 <https://doi.org/10.1007/s00382-018-4091-9>, 2018.

1646 Pathiraja, S., Westra, S., and Sharma, A.: Why continuous simulation? The role of antecedent moisture in design
1647 flood estimation, *Water Resour. Res.*, 48, W06534, <https://doi.org/10.1029/2011WR010997>, 2012.

1648 Patricola, C. M. and Wehner, M. F.: Anthropogenic influences on major tropical cyclone events, *Nature*, 563, 339–
1649 346, <https://doi.org/10.1038/s41586-018-0673-2>, 2018.

1650 Pendergrass, A. G.: What precipitation is extreme?, *Science (80-.)*, 360, 1072–1073,
1651 <https://doi.org/10.1126/science.aat1871>, 2018.

1652 Pendergrass, A. G. and Hartmann, D. L.: Changes in the distribution of rain frequency and intensity in response to
1653 global warming, *J. Clim.*, 27, 8372–8383, <https://doi.org/10.1175/JCLI-D-14-00183.1>, 2014.

1654 Pepler, A. S. and Dowdy, A. J.: Australia’s Future Extratropical Cyclones, *J. Clim.*, 35, 7795–7810,
1655 <https://doi.org/10.1175/JCLI-D-22-0312.1>, 2022.

1656 Pepler, A. S., Dowdy, A. J., van Rensch, P., Rudeva, I., Catto, J. L., and Hope, P.: The contributions of fronts, lows
1657 and thunderstorms to southern Australian rainfall, *Clim. Dyn.*, 55, 1489–1505, <https://doi.org/10.1007/s00382-020-05338-8>, 2020.

1659 Pepler, A. S., Dowdy, A. J., and Hope, P.: The differing role of weather systems in southern Australian rainfall
1660 between 1979–1996 and 1997–2015, *Clim. Dyn.*, 56, 2289–2302, <https://doi.org/10.1007/s00382-020-05588-6>,
1661 2021.

1662 Peter, J., Vogel, E., Sharples, W., Bende-Michl, U., Wilson, L., Hope, P., Dowdy, A., Kociuba, G., Srikanthan, S.,
1663 Duong, V. C., Roussis, J., Matic, V., Khan, Z., Oke, A., M., T., Baron-Hay, S., Johnson, F., Mehrotra, R., Sharma,
1664 A., Thatcher, M., Azarvinand, A., Thomas, S., Boschat, G., Donnelly, C., and Argent, R.: Continental-scale bias-
1665 corrected climate and hydrological projections for Australia, *Geosci. Model Dev.*, Accepted,
1666 <https://doi.org/10.5194/gmd-2023-7>, 2023.

1667 Pilgrim, D. and Cordery, I.: Flood runoff, in: *Handbook of Hydrology*, edited by: Maidment, D., McGraw-Hill,
1668 1993.

1669 Power, S. B. and Callaghan, J.: The frequency of major flooding in coastal southeast Australia has significantly
1670 increased since the late 19th century, *J. South. Hemisph. Earth Syst. Sci.*, 66, 2–11, <https://doi.org/10.1071/es16002>,
1671 2016.

1672 Prosdocimi, I. and Kjeldsen, T.: Parametrisation of change-permitting extreme value models and its impact on the
1673 description of change, *Stoch. Environ. Res. Risk Assess.*, 35, 307–324, <https://doi.org/10.1007/s00477-020-01940-8>,
1674 2021.

1675 Quintero, F., Villarini, G., Prein, A. F., Zhang, W., and Krajewski, W. F.: Discharge and floods projected to increase
1676 more than precipitation extremes, *Hydrol. Process.*, 36, e14738, <https://doi.org/10.1002/hyp.14738>, 2022.

1677 Rahman, A., Weinmann, E., and Mein, R. G.: The Use of Probability-Distributed Initial Losses in Design Flood
1678 Estimation, *Australas. J. Water Resour.*, 6, 17–29, <https://doi.org/10.1080/13241583.2002.11465207>, 2002.

1679 Rakhecha, P. R. and Kennedy, M. R.: A generalised technique for the estimation of probable maximum precipitation
1680 in India, *J. Hydrol.*, 78, 345–359, [https://doi.org/10.1016/0022-1694\(85\)90112-X](https://doi.org/10.1016/0022-1694(85)90112-X), 1985.

1681 Rastogi, D., Kao, S., Ashfaq, M., Mei, R., Kabela, E. D., Gangrade, S., Naz, B. S., Preston, B. L., Singh, N., and
1682 Anantharaj, V. G.: Effects of climate change on probable maximum precipitation: A sensitivity study over the
1683 Alabama-Coosa-Tallapoosa River Basin, *J. Geophys. Res. Atmos.*, 122, 4808–4828,
1684 <https://doi.org/10.1002/2016JD026001>, 2017.

1685 Reid, K. J., O’Brien, T. A., King, A. D., and Lane, T. P.: Extreme Water Vapor Transport During the March 2021
1686 Sydney Floods in the Context of Climate Projections, *Geophys. Res. Lett.*, 48, e2021GL095335,
1687 <https://doi.org/10.1029/2021GL095335>, 2021.

1688 Reid, K. J., King, A. D., Lane, T. P., and Hudson, D.: Tropical, Subtropical, and Extratropical Atmospheric Rivers
1689 in the Australian Region, *J. Clim.*, 35, 2697–2708, <https://doi.org/10.1175/JCLI-D-21-0606.1>, 2022.

1690 Robertson, D. E., Chiew, F. H. S., and Potter, N.: Adapting rainfall bias-corrections to improve hydrological
1691 simulations generated from climate model forcings, *J. Hydrol.*, 619, 129322,
1692 <https://doi.org/10.1016/j.jhydrol.2023.129322>, 2023.

1693 Roderick, T. P., Wasko, C., and Sharma, A.: An Improved Covariate for Projecting Future Rainfall Extremes?,
1694 *Water Resour. Res.*, 56, e2019WR026924, <https://doi.org/10.1029/2019WR026924>, 2020.

1695 Rohde, R. A. and Hausfather, Z.: The Berkeley Earth Land/Ocean Temperature Record, *Earth Syst. Sci. Data*, 12,
1696 3469–3479, <https://doi.org/10.5194/essd-12-3469-2020>, 2020.

1697 Rossman, L.: *Storm Water Management Model - User's Manual Version 5.0*, Cincinnati, OH, 285 pp., 2010.

1698 Rouhani, H. and Leconte, R.: Uncertainties of Precipitable Water Calculations for PMP Estimates in Current and
1699 Future Climates, *J. Hydrol. Eng.*, 25, 04019066, [https://doi.org/10.1061/\(ASCE\)HE.1943-5584.0001877](https://doi.org/10.1061/(ASCE)HE.1943-5584.0001877), 2020.

1700 Rousseau, A. N., Klein, I. M., Freudiger, D., Gagnon, P., Frigon, A., and Ratté-Fortin, C.: Development of a
1701 methodology to evaluate probable maximum precipitation (PMP) under changing climate conditions: Application to
1702 southern Quebec, Canada, *J. Hydrol.*, 519, 3094–3109, <https://doi.org/10.1016/j.jhydrol.2014.10.053>, 2014.

1703 Salas, J. D. and Obeysekera, J.: Revisiting the Concepts of Return Period and Risk for Nonstationary Hydrologic
1704 Extreme Events, *J. Hydrol. Eng.*, 19, 554–568, [https://doi.org/http://dx.doi.org/10.1061/\(ASCE\)HE.1943-5584.0000820](https://doi.org/http://dx.doi.org/10.1061/(ASCE)HE.1943-5584.0000820), 2014.

1705 Salas, J. D., Obeysekera, J., and Vogel, R. M.: Techniques for assessing water infrastructure for nonstationary
1706 extreme events: a review, *Hydrol. Sci. J.*, 63, 325–352, <https://doi.org/10.1080/02626667.2018.1426858>, 2018.

1707 Salas, J. D., Anderson, M. L., Papalexiou, S. M., and Frances, F.: PMP and Climate Variability and Change: A
1708 Review, *J. Hydrol. Eng.*, 25, 1–16, [https://doi.org/10.1061/\(asce\)he.1943-5584.0002003](https://doi.org/10.1061/(asce)he.1943-5584.0002003), 2020.

1709 Sarkar, S. and Maity, R.: Increase in probable maximum precipitation in a changing climate over India, *J. Hydrol.*,
1710 585, 124806, <https://doi.org/10.1016/j.jhydrol.2020.124806>, 2020.

1711 Sauter, C., White, C. J., Fowler, H. J., and Westra, S.: Temporally compounding heatwave–heavy rainfall events in
1712 Australia, *Int. J. Climatol.*, 43, 1050–1061, <https://doi.org/10.1002/joc.7872>, 2023.

1713 Schaefer, M.: PMP and Other Extreme Storms: Concepts and Probabilities, in: *Proceedings, Association of State
1714 Dam Safety Officials National Conference*, 1994.

1715 Schlef, K. E., François, B., Robertson, A. W., and Brown, C.: A General Methodology for Climate-Informed
1716 Approaches to Long-Term Flood Projection—Illustrated With the Ohio River Basin, *Water Resour. Res.*, 54, 9321–
1717 9341, <https://doi.org/10.1029/2018WR023209>, 2018.

1718 Schlef, K. E., Kunkel, K. E., Brown, C., Demissie, Y., Lettenmaier, D. P., Wagner, A., Wigmosta, M. S., Karl, T.
1719 R., Easterling, D. R., Wang, K. J., François, B., and Yan, E.: Incorporating non-stationarity from climate change into
1720 rainfall frequency and intensity-duration-frequency (IDF) curves, *J. Hydrol.*, 616, 128757,
1721 <https://doi.org/10.1016/j.jhydrol.2022.128757>, 2023.

1722 Schleiss, M.: How intermittency affects the rate at which rainfall extremes respond to changes in temperature, *Earth
1723 Syst. Dyn.*, 9, 955–968, <https://doi.org/10.5194/esd-9-955-2018>, 2018.

1724 Seneviratne, S. I., Corti, T., Davin, E. L., Hirschi, M., Jaeger, E. B., Lehner, I., Orlowsky, B., and Teuling, A. J.:
1725 Investigating soil moisture-climate interactions in a changing climate: A review, *Earth-Science Rev.*, 99, 125–161,
1726 <https://doi.org/10.1016/j.earscirev.2010.02.004>, 2010.

1727 Seneviratne, S. I., Zhang, X., Adnan, M., Badi, W., Dereczynski, C., Luca, A. Di, Ghosh, S., Iskandar, I., Kossin, J.,
1728 Lewis, S., Otto, F., Pinto, I., Satoh, M., Vicente-Serrano, S. M., Wehner, M., and Zhou, B.: *Weather and Climate
1729 Extreme Events in a Changing Climate*, in: *Climate Change 2021 – The Physical Science Basis*, edited by: Masson-
1730 Delmotte, V., Zhai, P., Pirani, A., Connors, S. L., Péan, C., Berger, S., Caud, N., Chen, Y., Goldfarb, L., Gomis, M.
1731 I., Huang, M., Leitzell, K., Lonnoy, E., Matthews, J. B. R., Maycock, T. K., Waterfield, T., Yelekçi, O., Yu, R., and
1732 Zhou, B., Cambridge University Press, Cambridge, United Kingdom and New York, NY, USA, 1513–1766,
1733 <https://doi.org/10.1017/9781009157896.013>, 2023.

1734 Sharma, A., Hettiarachchi, S., and Wasko, C.: Estimating design hydrologic extremes in a warming climate:
1735 alternatives, uncertainties and the way forward, *Philos. Trans. R. Soc. A Math. Phys. Eng. Sci.*, 379, 20190623,
1736 <https://doi.org/10.1098/rsta.2019.0623>, 2021.

1737 Sheikh, V., Visser, S., and Stroosnijder, L.: A simple model to predict soil moisture: Bridging Event and Continuous
1738 Hydrological (BEACH) modelling, *Environ. Model. Softw.*, 24, 542–556,
1739 <https://doi.org/10.1016/j.envsoft.2008.10.005>, 2009.

1740 Shepherd, T. G., Boyd, E., Calel, R. A., Chapman, S. C., Dessai, S., Dima-West, I. M., Fowler, H. J., James, R.,
1741 Maraun, D., Martius, O., Senior, C. A., Sobel, A. H., Stainforth, D. A., Tett, S. F. B., Trenberth, K. E., van den
1742 Hurk, B. J. J. M., Watkins, N. W., Wilby, R. L., and Zenghelis, D. A.: Storylines: an alternative approach to
1743 representing uncertainty in physical aspects of climate change, *Clim. Change*, 151, 555–571,
1744 <https://doi.org/10.1007/s10584-018-2317-9>, 2018.

1745 Shields, C. A., Kiehl, J. T., and Meehl, G. A.: Future changes in regional precipitation simulated by a half-degree
1746 coupled climate model: Sensitivity to horizontal resolution, *J. Adv. Model. Earth Syst.*, 8, 863–884,
1747 <https://doi.org/10.1002/2015MS000584>, 2016.

1749 Sillmann, J., Kharin, V. V., Zwiers, F. W., Zhang, X., and Bronaugh, D.: Climate extremes indices in the CMIP5
1750 multimodel ensemble: Part 2. Future climate projections, *J. Geophys. Res. Atmos.*, 118, 2473–2493,
1751 <https://doi.org/10.1002/jgrd.50188>, 2013.

1752 Sobel, A. H., Camargo, S. J., Hall, T. M., Lee, C.-Y., Tippett, M. K., and Wing, A. A.: Human influence on tropical
1753 cyclone intensity, *Science* (80-.), 353, 242–246, <https://doi.org/10.1126/science.aaf6574>, 2016.

1754 Srikanthan, S., Azarnivand, A., Bende-Michl, U., Carrara, E., Donnelly, C., Dowdy, A., Duong, V., Hope, P., Khan,
1755 Z., Kociuba, G., Loh, S., Matic, V., Oke, A., Peter, J. R., Roussis, J., Sharples, W., Thomas, S., Turner, M., and
1756 Wilson, L.: National Hydrological Projections - Design and Methodology, 63 pages pp., 2022.

1757 Stedinger, J., Vogel, R., and Foufoula-Georgiou, E.: Frequency analysis of extreme events, in: *Handbook of*
1758 *Hydrology*, edited by: Maidment, D., McGraw-Hill, 1993.

1759 Stedinger, J. R. and Griffis, V. W.: Getting from here to where? Flood frequency analysis and climate, *J. Am. Water*
1760 *Resour. Assoc.*, 47, 506–513, <https://doi.org/10.1111/j.1752-1688.2011.00545.x>, 2011.

1761 Stephens, C. M., Johnson, F. M., and Marshall, L. A.: Implications of future climate change for event-based
1762 hydrologic models, *Adv. Water Resour.*, 119, 95–110, <https://doi.org/10.1016/j.advwatres.2018.07.004>, 2018a.

1763 Stephens, C. M., McVicar, T. R., Johnson, F. M., and Marshall, L. A.: Revisiting Pan Evaporation Trends in
1764 Australia a Decade on, *Geophys. Res. Lett.*, 45, 11,164-11,172, <https://doi.org/10.1029/2018GL079332>, 2018b.

1765 Stephens, D., Nathan, R., Hill, P., and Scorch, M.: Incorporation of snowmelt into joint probability event based
1766 rainfall-runoff modelling, in: *37th Hydrology and Water Resources Symposium 2016: Water, Infrastructure and the*
1767 *Environment*, 532–540, 2016.

1768 Sun, Q., Zhang, X., Zwiers, F., Westra, S., and Alexander, L. V.: A Global, Continental, and Regional Analysis of
1769 Changes in Extreme Precipitation, *J. Clim.*, 34, 243–258, <https://doi.org/10.1175/JCLI-D-19-0892.1>, 2021.

1770 Sunwoo, W. and Choi, M.: Robust Initial Wetness Condition Framework of an Event-Based Rainfall–Runoff Model
1771 Using Remotely Sensed Soil Moisture, *Water*, 9, 77, <https://doi.org/10.3390/w9020077>, 2017.

1772 Tan, X. and Shao, D.: Precipitation trends and teleconnections identified using quantile regressions over Xinjiang,
1773 China, *Int. J. Climatol.*, 37, 1510–1525, <https://doi.org/10.1002/joc.4794>, 2017.

1774 Tauvale, L. and Tsuboki, K.: Characteristics of Tropical Cyclones in the Southwest Pacific, *J. Meteorol. Soc. Japan*.
1775 Ser. II, 97, 711–731, <https://doi.org/10.2151/jmsj.2019-042>, 2019.

1776 Teutschbein, C. and Seibert, J.: Bias correction of regional climate model simulations for hydrological climate-
1777 change impact studies: Review and evaluation of different methods, *J. Hydrol.*, 456–457, 12–29,
1778 <https://doi.org/10.1016/j.jhydrol.2012.05.052>, 2012.

1779 Thompson, C. S. and Tomlinson, A. I.: A guide to probable maximum precipitation in New Zealand, 1995.

1780 Tolhurst, G., Hope, P., Osburn, L., and Rauniyar, S.: Approaches to Understanding Decadal and Long-Term Shifts
1781 in Observed Precipitation Distributions in Victoria, Australia, *J. Appl. Meteorol. Climatol.*, 62, 13–29,
1782 <https://doi.org/10.1175/JAMC-D-22-0031.1>, 2023.

1783 Towler, E., Rajagopalan, B., Gilleland, E., Summers, R. S., Yates, D., and Katz, R. W.: Modeling hydrologic and
1784 water quality extremes in a changing climate: A statistical approach based on extreme value theory, *Water Resour.*
1785 *Res.*, 46, W11504, <https://doi.org/10.1029/2009WR008876>, 2010.

1786 Trambly, Y., Bouvier, C., Martin, C., Didon-Lescot, J. F., Todorovik, D., and Domergue, J. M.: Assessment of
1787 initial soil moisture conditions for event-based rainfall-runoff modelling, *J. Hydrol.*, 387, 176–187,
1788 <https://doi.org/10.1016/j.jhydrol.2010.04.006>, 2010.

1789 Trambly, Y., Amoussou, E., Dorigo, W., and Mahé, G.: Flood risk under future climate in data sparse regions:
1790 Linking extreme value models and flood generating processes, *J. Hydrol.*, 519, 549–558,
1791 <https://doi.org/10.1016/j.jhydrol.2014.07.052>, 2014.

1792 Ukkola, A. M., De Kauwe, M. G., Roderick, M. L., Abramowitz, G., and Pitman, A. J.: Robust Future Changes in
1793 Meteorological Drought in CMIP6 Projections Despite Uncertainty in Precipitation, *Geophys. Res. Lett.*, 47,
1794 e2020GL087820, <https://doi.org/10.1029/2020GL087820>, 2020.

1795 US Army Corps of Engineers: HEC-HMS: Hydrologic Modeling System–Technical reference manua, Davis, CA,
1796 2000.

1797 Vecchi, G. A., Delworth, T. L., Murakami, H., Underwood, S. D., Wittenberg, A. T., Zeng, F., Zhang, W., Baldwin,
1798 J. W., Bhatia, K. T., Cooke, W., He, J., Kapnick, S. B., Knutson, T. R., Villarini, G., van der Wiel, K., Anderson,
1799 W., Balaji, V., Chen, J., Dixon, K. W., Gudgel, R., Harris, L. M., Jia, L., Johnson, N. C., Lin, S.-J., Liu, M., Ng, C.
1800 H. J., Rosati, A., Smith, J. A., and Yang, X.: Tropical cyclone sensitivities to CO2 doubling: roles of atmospheric
1801 resolution, synoptic variability and background climate changes, *Clim. Dyn.*, 53, 5999–6033,
1802 <https://doi.org/10.1007/s00382-019-04913-y>, 2019.

1803 Villarini, G. and Denniston, R. F.: Contribution of tropical cyclones to extreme rainfall in Australia, *Int. J. Climatol.*,
1804 36, 1019–1025, <https://doi.org/10.1002/joc.4393>, 2016.

1805 Villarini, G. and Wasko, C.: Humans, climate and streamflow, *Nat. Clim. Chang.*, 11, 725–726,
1806 <https://doi.org/10.1038/s41558-021-01137-z>, 2021.

1807 Visser, J. B., Wasko, C., Sharma, A., and Nathan, R.: Resolving Inconsistencies in Extreme Precipitation-
1808 Temperature Sensitivities, *Geophys. Res. Lett.*, 47, e2020GL089723, <https://doi.org/10.1029/2020GL089723>, 2020.

1809 Visser, J. B., Wasko, C., Sharma, A., and Nathan, R.: Eliminating the “hook” in Precipitation-Temperature Scaling,
1810 *J. Clim.*, 34, 9535–9549, <https://doi.org/10.1175/JCLI-D-21-0292.1>, 2021.

1811 Visser, J. B., Kim, S., Wasko, C., Nathan, R., and Sharma, A.: The Impact of Climate Change on Operational
1812 Probable Maximum Precipitation Estimates, *Water Resour. Res.*, 58, e2022WR032247,
1813 <https://doi.org/10.1029/2022WR032247>, 2022.

1814 Visser, J. B., Wasko, C., Sharma, A., and Nathan, R.: Changing Storm Temporal Patterns with Increasing
1815 Temperatures across Australia, *J. Clim.*, 36, 6247–6259, <https://doi.org/10.1175/JCLI-D-22-0694.1>, 2023.

1816 Vogel, E., Johnson, F., Marshall, L., Bende-Michl, U., Wilson, L., Peter, J. R., Wasko, C., Srikanthan, S., Sharples,
1817 W., Dowdy, A., Hope, P., Khan, Z., Mehrotra, R., Sharma, A., Matic, V., Oke, A., Turner, M., Thomas, S.,
1818 Donnelly, C., and Duong, V. C.: An evaluation framework for downscaling and bias correction in climate change
1819 impact studies, *J. Hydrol.*, 622, 129693, <https://doi.org/10.1016/j.jhydrol.2023.129693>, 2023.

1820 Vousdoukas, M. I., Mentaschi, L., Voukouvalas, E., Verlaan, M., Jevrejeva, S., Jackson, L. P., and Feyen, L.: Global
1821 probabilistic projections of extreme sea levels show intensification of coastal flood hazard, *Nat. Commun.*, 9, 2360,
1822 <https://doi.org/10.1038/s41467-018-04692-w>, 2018.

1823 Walsh, K., White, C. J., McInnes, K., Holmes, J., Schuster, S., Richter, H., Evans, J. P., Di Luca, A., and Warren, R.
1824 A.: Natural hazards in Australia: storms, wind and hail, *Clim. Change*, 139, 55–67, [https://doi.org/10.1007/s10584-](https://doi.org/10.1007/s10584-016-1737-7)
1825 016-1737-7, 2016.

1826 Wang, J., Church, J. A., Zhang, X., and Chen, X.: Reconciling global mean and regional sea level change in
1827 projections and observations, *Nat. Commun.*, 12, 990, <https://doi.org/10.1038/s41467-021-21265-6>, 2021.

1828 Wang, S., Ma, X., Zhou, S., Wu, L., Wang, H., Tang, Z., Xu, G., Jing, Z., Chen, Z., and Gan, B.: Extreme
1829 atmospheric rivers in a warming climate, *Nat. Commun.*, 14, 3219, <https://doi.org/10.1038/s41467-023-38980-x>,
1830 2023.

1831 Warren, R. A., Jakob, C., Hitchcock, S. M., and White, B. A.: Heavy versus extreme rainfall events in southeast
1832 Australia, *Q. J. R. Meteorol. Soc.*, 147, 3201–3226, <https://doi.org/10.1002/qj.4124>, 2021.

1833 Wasko, C.: Review: Can temperature be used to inform changes to flood extremes with global warming?, *Philos.*
1834 *Trans. R. Soc. A Math. Phys. Eng. Sci.*, 379, 20190551, <https://doi.org/10.1098/rsta.2019.0551>, 2021.

1835 Wasko, C.: Floods differ in a warmer future, *Nat. Clim. Chang.*, 12, 1090–1091, [https://doi.org/10.1038/s41558-](https://doi.org/10.1038/s41558-022-01541-z)
1836 022-01541-z, 2022.

1837 Wasko, C. and Guo, D.: Understanding event runoff coefficient variability across Australia using the hydroEvents R
1838 package, *Hydrol. Process.*, 36, e14563, <https://doi.org/10.1002/hyp.14563>, 2022.

1839 Wasko, C. and Nathan, R.: Influence of changes in rainfall and soil moisture on trends in flooding, *J. Hydrol.*, 575,
1840 432–441, <https://doi.org/10.1016/j.jhydrol.2019.05.054>, 2019.

1841 Wasko, C. and Sharma, A.: Quantile regression for investigating scaling of extreme precipitation with temperature,
1842 *Water Resour. Res.*, 50, 3608–3614, <https://doi.org/10.1002/2013WR015194>, 2014.

1843 Wasko, C. and Sharma, A.: Steeper temporal distribution of rain intensity at higher temperatures within Australian
1844 storms, *Nat. Geosci.*, 8, 527–529, <https://doi.org/10.1038/ngeo2456>, 2015a.

1845 Wasko, C. and Sharma, A.: This is a Student Paper Changed Design Temporal Patterns with Higher Temperatures,
1846 in: 36th Hydrology and Water Resources Symposium: The art and science of water, 1237–1244, 2015b.

1847 Wasko, C. and Sharma, A.: Continuous rainfall generation for a warmer climate using observed temperature
1848 sensitivities, *J. Hydrol.*, 544, 575–590, <https://doi.org/10.1016/j.jhydrol.2016.12.002>, 2017a.

1849 Wasko, C. and Sharma, A.: Global assessment of flood and storm extremes with increased temperatures, *Sci. Rep.*,
1850 7, 7945, <https://doi.org/10.1038/s41598-017-08481-1>, 2017b.

1851 Wasko, C., Sharma, A., and Westra, S.: Reduced spatial extent of extreme storms at higher temperatures, *Geophys.*
1852 *Res. Lett.*, 43, 4026–4032, <https://doi.org/10.1002/2016GL068509>, 2016.

1853 Wasko, C., Lu, W. T., and Mehrotra, R.: Relationship of extreme precipitation, dry-bulb temperature, and dew point
1854 temperature across Australia, *Environ. Res. Lett.*, 13, 074031, <https://doi.org/10.1088/1748-9326/aad135>, 2018.

1855 Wasko, C., Nathan, R., and Peel, M. C.: Changes in Antecedent Soil Moisture Modulate Flood Seasonality in a
1856 Changing Climate, *Water Resour. Res.*, 56, e2019WR026300, <https://doi.org/10.1029/2019WR026300>, 2020.

1857 Wasko, C., Nathan, R., Stein, L., and O’Shea, D.: Evidence of shorter more extreme rainfalls and increased flood
1858 variability under climate change, *J. Hydrol.*, 603, 126994, <https://doi.org/10.1016/j.jhydrol.2021.126994>, 2021a.

1859 Wasko, C., Westra, S., Nathan, R., Orr, H. G., Villarini, G., Villalobos Herrera, R., and Fowler, H. J.: Incorporating
1860 climate change in flood estimation guidance, *Philos. Trans. R. Soc. A Math. Phys. Eng. Sci.*, 379, 20190548,
1861 <https://doi.org/10.1098/rsta.2019.0548>, 2021b.

1862 Wasko, C., Shao, Y., Vogel, E., Wilson, L., Wang, Q. J., Frost, A., and Donnelly, C.: Understanding trends in
1863 hydrologic extremes across Australia, *J. Hydrol.*, 593, 125877, <https://doi.org/10.1016/j.jhydrol.2020.125877>,
1864 2021c.

1865 Wasko, C., Guo, D., Ho, M., Nathan, R., and Vogel, E.: Diverging projections for flood and rainfall frequency
1866 curves, *J. Hydrol.*, 620, 129403, <https://doi.org/10.1016/j.jhydrol.2023.129403>, 2023.

1867 Wehner, M. F., Reed, K. A., Loring, B., Stone, D., and Krishnan, H.: Changes in tropical cyclones under stabilized
1868 1.5 and 2.0 °C global warming scenarios as simulated by the Community Atmospheric Model under the HAPPI
1869 protocols, *Earth Syst. Dyn.*, 9, 187–195, <https://doi.org/10.5194/esd-9-187-2018>, 2018.

1870 Westra, S. and Sisson, S. A.: Detection of non-stationarity in precipitation extremes using a max-stable process
1871 model, *J. Hydrol.*, 406, 119–128, <https://doi.org/10.1016/j.jhydrol.2011.06.014>, 2011.

1872 Westra, S., Alexander, L., and Zwiers, F.: Global increasing trends in annual maximum daily precipitation, *J. Clim.*,
1873 26, 3904–3918, <https://doi.org/10.1175/JCLI-D-12-00502.1>, 2013.

1874 Westra, S., Leonard, M., and Zheng, F.: Chapter 5. Interaction of Coastal and Catchment Flooding, Book 6: Flood
1875 Hydraulics, in: *Australian Rainfall and Runoff - A Guide to Flood Estimation*, edited by: Ball, J., Babister, M.,
1876 Nathan, R., Weinmann, E., Retallick, M., and Testoni, I., Commonwealth of Australia, 2019.

1877 White, N. J., Haigh, I. D., Church, J. A., Koen, T., Watson, C. S., Pritchard, T. R., Watson, P. J., Burgette, R. J.,
1878 McInnes, K. L., You, Z.-J., Zhang, X., and Tregoning, P.: Australian sea levels—Trends, regional variability and
1879 influencing factors, *Earth-Science Rev.*, 136, 155–174, <https://doi.org/10.1016/j.earscirev.2014.05.011>, 2014.

1880 Wilks, D. S.: Multisite generalization of a daily stochastic precipitation generation model, *J. Hydrol.*, 210, 178–191,
1881 [https://doi.org/10.1016/S0022-1694\(98\)00186-3](https://doi.org/10.1016/S0022-1694(98)00186-3), 1998.

1882 Wilson, L., Bende-Michl, U., Sharples, W., Vogel, E., Peter, J., Srikanthan, S., Khan, Z., Matic, V., Oke, A., Turner,
1883 M., Co Duong, V., Loh, S., Baron-Hay, S., Roussis, J., Kociuba, G., Hope, P., Dowdy, A., Donnelly, C., Argent, R.,
1884 Thomas, S., Kitsios, A., and Bellhouse, J.: A national hydrological projections service for Australia, *Clim. Serv.*, 28,
1885 100331, <https://doi.org/10.1016/j.cliser.2022.100331>, 2022.

1886 WMO: *Manual on Estimation of Probable Maximum Precipitation (PMP)*, Geneva, Switzerland, 2009.

1887 Woldemeskel, F. and Sharma, A.: Should flood regimes change in a warming climate? The role of antecedent
1888 moisture conditions, *Geophys. Res. Lett.*, 43, 7556–7563, <https://doi.org/10.1002/2016GL069448>, 2016.

1889 Woldemeskel, F. M., Sharma, A., Mehrotra, R., and Westra, S.: Constraining continuous rainfall simulations for
1890 derived design flood estimation, *J. Hydrol.*, 542, 581–588, <https://doi.org/10.1016/j.jhydrol.2016.09.028>, 2016.

1891 Woodham, R., Brassington, G. B., Robertson, R., and Alves, O.: Propagation characteristics of coastally trapped
1892 waves on the Australian Continental Shelf, *J. Geophys. Res. Ocean.*, 118, 4461–4473,
1893 <https://doi.org/10.1002/jgrc.20317>, 2013.

1894 Wu, W., McInnes, K., O’Grady, J., Hoeke, R., Leonard, M., and Westra, S.: Mapping Dependence Between
1895 Extreme Rainfall and Storm Surge, *J. Geophys. Res. Ocean.*, 123, 2461–2474,
1896 <https://doi.org/10.1002/2017JC013472>, 2018.

1897 Wu, X.-Y., Ye, C., He, W., Chen, J., Xu, L., and Zhang, H.: Atmospheric rivers impacting mainland China and
1898 Australia: climatology and interannual variations, *J. South. Hemisph. Earth Syst. Sci.*, 70, 70–87,
1899 <https://doi.org/10.1071/ES19029>, 2020.

1900 Yamaguchi, M., Chan, J. C. L., Moon, I.-J., Yoshida, K., and Mizuta, R.: Global warming changes tropical cyclone
1901 translation speed, *Nat. Commun.*, 11, 47, <https://doi.org/10.1038/s41467-019-13902-y>, 2020.

1902 Yilmaz, A. G. and Perera, B. J. C.: Extreme Rainfall Nonstationarity Investigation and Intensity – Frequency –
1903 Duration Relationship, *J. Hydrol. Eng.*, 19, 1160–1172, [https://doi.org/10.1061/\(ASCE\)HE.1943-5584.0000878.](https://doi.org/10.1061/(ASCE)HE.1943-5584.0000878.),
1904 2014.

1905 Yu, G., Wright, D. B., Zhu, Z., Smith, C., and Holman, K. D.: Process-based flood frequency analysis in an
1906 agricultural watershed exhibiting nonstationary flood seasonality, *Hydrol. Earth Syst. Sci.*, 23, 2225–2243,
1907 <https://doi.org/10.5194/hess-23-2225-2019>, 2019.

1908 Zalnezhad, A., Rahman, A., Nasiri, N., Haddad, K., Rahman, M. M., Vafakhah, M., Samali, B., and Ahamed, F.:
1909 Artificial Intelligence-Based Regional Flood Frequency Analysis Methods: A Scoping Review, *Water (Switzerland)*,
1910 14, <https://doi.org/10.3390/w14172677>, 2022.

1911 Zhan, W., Buckley, S., Genova, P., Grobler, J., Redenbach, M., and Eskola, K.: Selecting and Processing High
1912 Resolution Climate Projections in Queensland Mine Water Planning and Hydrologic Assessment, in: Hydrology and
1913 Water Resources Symposium, HWRS 2022, 518–533, 2022.

1914 Zhang, J., Gao, S., and Fang, Z.: Investigation of Infiltration Loss in North Central Texas by Retrieving Initial
1915 Abstraction and Constant Loss from Observed Rainfall and Runoff Events, *J. Hydrol. Eng.*, 28, 04023013,
1916 <https://doi.org/10.1061/jhyeff.heeng-5883>, 2023.

1917 Zhang, S., Zhou, L., Zhang, L., Yang, Y., Wei, Z., Zhou, S., Yang, D., Yang, X., Wu, X., Zhang, Y., Li, X., and Dai,
1918 Y.: Reconciling disagreement on global river flood changes in a warming climate, *Nat. Clim. Chang.*, 12, 1160–
1919 1167, <https://doi.org/10.1038/s41558-022-01539-7>, 2022.

1920 Zhang, W., Villarini, G., and Wehner, M.: Contrasting the responses of extreme precipitation to changes in surface
1921 air and dew point temperatures, *Clim. Change*, 154, 257–271, <https://doi.org/10.1007/s10584-019-02415-8>, 2019.

1922 Zhang, X., Alexander, L., Hegerl, G. C., Jones, P., Tank, A. K., Peterson, T. C., Trewin, B., and Zwiers, F. W.:
1923 Indices for monitoring changes in extremes based on daily temperature and precipitation data, *WIREs Clim. Chang.*,
1924 2, 851–870, <https://doi.org/10.1002/wcc.147>, 2011.

1925 Zhang, X. S., Amirthanathan, G. E., Bari, M. A., Laugesen, R. M., Shin, D., Kent, D. M., MacDonald, A. M.,
1926 Turner, M. E., and Tuteja, N. K.: How streamflow has changed across Australia since the 1950s: evidence from the
1927 network of hydrologic reference stations, *Hydrol. Earth Syst. Sci.*, 20, 3947–3965, <https://doi.org/10.5194/hess-20-3947-2016>, 2016.

1929 Zheng, F., Westra, S., and Sisson, S. A.: Quantifying the dependence between extreme rainfall and storm surge in
1930 the coastal zone, *J. Hydrol.*, 505, 172–187, <https://doi.org/10.1016/j.jhydrol.2013.09.054>, 2013.

1931 Zheng, F., Westra, S., and Leonard, M.: Opposing local precipitation extremes, *Nat. Clim. Chang.*, 5, 389–390,
1932 <https://doi.org/10.1038/nclimate2579>, 2015.

1933 Zommers, Z., Marbaix, P., Fischlin, A., Ibrahim, Z. Z., Grant, S., Magnan, A. K., Pörtner, H.-O., Howden, M.,
1934 Calvin, K., Warner, K., Thiery, W., Sebesvari, Z., Davin, E. L., Evans, J. P., Rosenzweig, C., O’Neill, B. C.,
1935 Patwardhan, A., Warren, R., van Aalst, M. K., and Hulbert, M.: Burning embers: towards more transparent and
1936 robust climate-change risk assessments, *Nat. Rev. Earth Environ.*, 1, 516–529, <https://doi.org/10.1038/s43017-020-0088-0>, 2020.

1937
1938